

Effects of seasonal riverine run-off on contaminant accumulation in Arctic littoral amphipods

Emelie Skogsberg



Master thesis in toxicology

Department of Bioscience
Faculty of Mathematics and Natural Science

UNIVERSITY OF OSLO

01.06.2019

©Emelie Skogsberg

2019

Effects of seasonal riverine run-off on contaminant accumulation in Arctic littoral amphipods

Emelie Skogsberg

<http://www.duo.uio.no>

Print: Reprosentralen, Universitetet i Oslo

The present project was carried out in collaboration between University of Oslo (UiO), the University Center in Svalbard (UNIS) and Norwegian Institute for Water Research (NIVA).



Acknowledgments

The work presented in the current thesis was conducted at the Department of Biosciences at the University of Oslo (UiO) and in collaboration with the Department of Arctic Biology at The University Centre in Svalbard (UNIS) and the Norwegian Institute for Water Research (NIVA). It was carried out under the supervision of main supervisor Katrine Borgå (UiO), and co-supervisor Øystein Varpe (UNIS and Akvaplan-niva).

I want to thank my supervisors for excellent and invaluable feedback, suggestions and support during fieldwork, lab work, data processing and writing. I especially want to thank Katrine for being an inspirational woman in science, convincing me to do research in the North and motivating me to finish. Furthermore, she introduced me to the TerrACE project, where I have learnt and experienced more than I ever could have imagined, and for that, I will always be grateful.

I would like to thank logistics at UNIS for helping me find field equipment and making sure I was prepared for fieldwork in the Arctic. I wish to thank Jan Marcin Weslawski for showing me how to collect and identify my amphipods, and giving me helpful advice and answering my many emails. I'm eternally grateful for to all my little amphipod whisperers in the field: Nina, Maeve, Eirik, Emilie, Nathalie, Charlotte, Hannah, Helene, Emilie and Guttorm. Without your invaluable help, I wouldn't have a thesis at all. A special thanks to Nina for being at least as much concerned as I about finding my little creatures and sacrificing her own comfort by venturing out in the cold Arctic with me on many, many occasions. Thank you Eirik, for being the great Svalbardian outdoorsman you are and a kick-ass kayaker. Additionally, I want to thank Guttorm for making fieldwork incredibly fun, taking me on scavenger hunts along Svalbard's coastlines and for always being up for a coffee.

I would like to thank the Research Council of Norway for funding the TerrACE project which enabled me to perform fieldwork and chemical analyses. I want to thank Alfhild Kringstad at NIVA, Sofi Jonsson at Stockholm University and Danny Hitchcock at UiO for all your help, patience and educational instructions during chemical analyses. I am also very grateful to Sverre for showing me the ropes around the environmental chemistry lab at NIVA and for giving me helpful tips and support.

Nina, Malin and Oda, my partners in crime, thank you for your wonderful company and moral support, without you I would never have made it. I also want to thank Erik, my beloved fiancé, for always handling my outbursts of panic with love and stuffing my face with food all hours of the day. Thank you Barrie, who made the utmost mistake in offering his services as a proof reader, for taking the time to correct my thesis and giving me a non-toxicology perspective. I also wish to thank my work colleagues and Elisabeth Lie at NIVA for your kind concern for my wellbeing and reminding me that there is a life after university.

And last, but most certainly not the least, I want to give my sincerest and most heartfelt thanks to Amanda Poste and Maeve McGovern. Amanda, thank you for believing in me, listening to my opinions, your kindness, eagerness to always help, and for letting me be a part of TerrACE. As I set out to become a biologist and later a toxicologist, I never, even in my wildest dreams, thought I would learn or have as much fun as I have while being a part of the TerrACE team, so thank you, Amanda, for this fantastic opportunity. Maeve, where should I begin? Not only did I gain a brilliant friend, but you showed me how wonderful science can be and made me believe that I actually could do this. Thank you Maeve for your immense help with planning and executing fieldwork, support during data treatment and writing, giving invaluable feedback, disentangling ropes when I lost my mind, finding my precious glove and introducing me to peanut butter and bananas and much, much more.

Abstract

Factors influencing seasonal concentrations of persistent organic pollutants and mercury were investigated from April to August 2018 in *Gammarus setosus*, a littoral deposit-feeding amphipod, inhabiting an Arctic fjord heavily impacted by riverine run-off. Diet, identified by a combined fatty acid and stable isotope approach, consisted of settled phytodetritus from the spring bloom in May-July, and various detrital-derived carbon sources in April and August. The contamination and diet results in *G. setosus* suggest that a flux from spring thaw may have contributed to a seasonal peak of less hydrophobic persistent organic pollutants in May/June, which could have become transported to littoral amphipods as they fed on primary production from the pelagic compartment. Despite a seasonal increase in these less hydrophobic compounds in May/June, there was an overall seasonal decrease in concentration for all pollutants in *G. setosus*. The present study suggests that growth dilution and increase of terrestrial organic matter from riverine run-off may have caused this lowered contamination. Additionally, contamination in sediments appeared to be decoupled from contamination in *G. setosus*, most likely a result of selective feeding. During the study period, emissions of stored persistent organic pollutants and mercury from secondary sources appeared not to increase the concentrations in *G. setosus*. However, persistent organic pollutants deposited on seasonal snow cover during the previous winter may be an important contamination source. Riverine run-off and biological factors, such as diet and growth dilution, may all contribute to intra-annual contamination variations in Arctic littoral amphipods.

Abbreviations

Σ	Sum
$\delta^{13}\text{C}$	Stable isotope ratio of carbon
$\delta^{15}\text{N}$	Stable isotope ratio of nitrogen
% TFA	Percentage of total fatty acid
ANOVA	Analysis of variance
BSAF	Biota-sediment accumulation factors
CA	Correspondence analysis
CaCO_3	Calcium carbonate
CCA	Canonical correspondence analysis
CHX	Cyclohexane
CH_3Hg^+	Methyl mercury
C:N	Carbon-to-nitrogen ratio
CRM	Certified reference material
d.w.	Dry weight
DCM	Dichloromethane
FA	Fatty acid
FATM	Fatty acid trophic marker
GC-MS	Gas chromatography-mass spectrometry
GPC	Gel permeation chromatography
HCB	Hexachlorobenzene
HCl	Hydrogen chloride
Hg	Mercury
ISTD	Internal standard
l.w.	Lipid weight
LOD	Limit of detection
\log_{10}	Logarithm with base 10
MeHg	Methyl mercury
MUFA	Monounsaturated fatty acid
N_2	Nitrogen gas
n	Number of samples
NA	Not available
Na_2SO_4	Sodium sulphate

NaCl	Sodium chloride
NIVA	Norwegian Institute for Water Research
NMBU	Norwegian University of Life Sciences
PC1	First principal component
PC2	Second principal component
PCA	Principal component analyses
PCBs	Polychlorinated biphenyls
PeCB	Pentachlorobenzene
POM	Particulate organic matter
POPs	Persistent organic pollutants
PUFA	Polyunsaturated fatty acid
RDA	Redundancy analysis
SD	Standard deviation
SFA	Saturated fatty acid
SI	Stable isotope
SPM	Suspended particulate matter
TOC	Total organic carbon
TotHg	Total mercury
UiO	University of Oslo
UNIS	University Centre in Svalbard
w.w.	Wet weight

Table of contents

1	Introduction.....	1
1.1	Persistent organic pollutants and mercury	1
1.2	Riverine run-off.....	3
1.3	The benthic realm.....	4
1.4	Bioaccumulation	5
1.4.1	Dietary descriptors	5
1.5	Seasonality and Arctic coastal invertebrates.....	7
1.6	Aim and objectives.....	8
2	Materials and methods	10
2.1	Study species.....	10
2.2	Site characterization	10
2.3	Field procedures	12
2.4	Laboratory preparations	14
2.5	Chemical analyses.....	16
2.5.1	Stable isotopes.....	16
2.5.2	Fatty acids	19
2.5.3	Persistent organic pollutants	19
2.5.4	Total mercury	24
2.5.5	Methyl mercury.....	25
2.6	Data treatment and statistical analysis	27
2.6.1	Lipid corrected carbon isotopic values	27
2.6.2	Total organic carbon	27
2.6.3	Wet weight and dry weight	28
2.6.4	Fatty acids	28
2.6.5	Statistical treatment.....	29
3	Results.....	36
3.1	Dietary descriptors	36
3.1.1	$\delta^{13}\text{C}$ values	36
3.1.2	$\delta^{15}\text{N}$ values	37
3.1.3	Fatty acids	39
3.2	Lipids	41
3.3	Contaminant concentrations.....	42
3.3.1	Persistent organic pollutants in sediments	43
3.3.2	Total mercury in sediments.....	46
3.3.3	Persistent organic pollutants in amphipods.....	47
3.3.4	Total mercury in amphipods	50
3.3.5	Methyl mercury in amphipods	51
3.3.6	Contaminant patterns	52
4	Discussion	56
4.1	Carbon sources and lipid content	56
4.1.1	Spatial differences.....	56
4.1.2	Phytoplankton spring bloom	57
4.1.3	Pre- and post-bloom situations.....	58
4.1.4	Turnover times	62
4.2	Sediment contamination.....	63
4.2.1	Persistent organic pollutants	63

4.2.2	Total mercury	65
4.3	Amphipod contamination.....	66
4.3.1	Persistent organic pollutants	67
4.3.2	Mercury	71
4.3.3	Seasonality	73
5	Conclusions.....	74
6	Future studies	75
	References	76
	Appendices	94
	Appendix A: Protocols.....	94
	Terrestrial taxa	94
	Stable isotope analysis	94
	Fatty acid analysis.....	95
	Persistent organic pollutant analysis.....	97
	Methyl mercury analysis.....	98
	Appendix B: Tables.....	99
	Appendix C: Figures	104

1 Introduction

1.1 Persistent organic pollutants and mercury

Pollution by anthropogenically produced persistent organic pollutants (POPs) and the natural element mercury (Hg), is of great environmental concern in the Arctic (AMAP, 2011; Macdonald et al., 2000). POPs, being organic, bioaccumulate in lipid deposits, and biomagnify in polar food webs (Borgå et al., 2004). Methyl mercury (MeHg), an organic form of Hg, undergoes bioaccumulation and biomagnification in aquatic food webs, with higher potency than inorganic Hg (Chen et al., 2014; Kidd et al., 2012; Kim et al., 2012; Lavoie et al., 2013; Ruus et al., 2015). Biomagnification results in high POP and Hg concentrations in top predators which can cause adverse health effects, including hormonal, developmental and reproductive defects (Chan et al., 2003; Letcher et al., 2010; Scheuhammer et al., 2007; Starek-Świechowicz et al., 2017).

Since the 1970s, the production of POPs has levelled off (Breivik et al., 2004), and global bans and regulations have been implemented to hinder further pollution (e.g. the Stockholm Convention; Kaiser et al., 2000). Despite these efforts, POPs are still being detected in the abiotic and biotic systems of the Arctic (Holden & Marsden, 1967; Hung et al., 2016; Rigét et al., 2019), and are still considered to be of ecotoxicological concern (AMAP, 2011; Macdonald et al., 2000). There are a few important sources of local contamination within the Arctic region (e.g. local settlements such as Longyearbyen, Pyramiden, etc.) (Hop et al., 2001; Kallenborn et al., 2012b; Rigét et al., 2019). However, the majority of the contaminants originate from industrial and agricultural emission sources at lower latitudes (AMAP, 2004; Carlsson et al., 2018). Due to their semi-volatile and persistent properties, POPs reach the Arctic via long-range transport through the atmosphere, ocean currents, biota, sea ice and northward-draining river systems (Burkow & Kallenborn, 2000; Macdonald et al., 2000). Long-range transport often results in deposition of these chemicals onto glaciers, snow, ice, permafrost and sediments in polar areas (Bogdal et al., 2010; Hermanson et al., 2005). In fact, POPs were found in snow and ice from glaciers in Svalbard (Garmash et al., 2013; Hermanson et al., 2005). Hence, glaciers and permafrost may serve as land reservoirs for contaminants, which can be remobilised through melting, enter coastal environments and increase exposure to coastal biota (Blais et al., 2001; Bogdal et al., 2010; Carlsson et al., 2012; Kallenborn et al., 2012a). These types of secondary sources (remobilised accumulated

contaminants) could potentially surpass the impact of primary sources and contribute to slower declining POP concentrations in the Arctic (Carlsson et al., 2018; Rigét et al., 2019). Slower declining concentrations have already been observed in certain POPs during the last decade (AMAP, 2016). POPs such as polychlorinated biphenyls (PCBs) and chlorobenzenes including hexachlorobenzene (HCB) and pentachlorobenzene (PeCB), mainly display no or slow declining long-term temporal trends in Arctic biota, with estimated annual average rates of decline of PCBs¹, HCB and PeCB concentrations of 3.7%, 2.6% and 3.8%, respectively (Rigét et al., 2019).

Hg, in contrast to POPs, is a naturally occurring element and is ubiquitous in the earth's crust, the atmosphere and the aquatic environment, and have both natural and anthropogenic emission sources (Pirrone et al., 2010; Sunderland & Mason, 2007). Certain anthropogenic activities, particularly since the industrial revolution, have greatly altered the natural geochemical cycle of Hg (Pirrone et al., 2010; Sunderland & Mason, 2007). Today, the major contribution of Hg release is secondary re-emission of historically deposited Hg stored in aquatic and terrestrial environments (Amos et al., 2013; Pirrone et al., 2010). In 2017, the Minamata Convention on Mercury was sanctioned, which aims to globally regulate anthropogenic releases of Hg (Evers et al., 2016).

Elevated concentrations of mercury are found in the biotic (e.g. pelagic systems; Ruus et al. (2015) and benthic systems; Fox et al. (2014)) and abiotic compartments of the Arctic (e.g. sediments; Beldowski et al. (2015), permafrost; Schuster et al. (2018)). Dietz et al. (2009) found that as much as 92% of the Hg burden in Arctic higher trophic level biota can be attributed to anthropogenic activities. There are limited data on long-term trends of Hg accumulation (83 time series) in Arctic biota compared to POPs (more than 1000 time series) (Rigét et al., 2019), and particularly for Hg in invertebrates (AMAP, 2011). Of the 83 Hg time series', 54% displayed no trends, while 16% exhibited significant increasing trends, whereof the majority of the time series' showing increasing trends involved marine species (AMAP, 2011).

Similar to POPs, few local emission sources of Hg exist within the Arctic region (e.g. settlements and erosion) (Drevnick et al., 2012; Hare et al., 2008; Schuster et al., 2011).

¹ Including Σ_{10} PCB (CB-28, -31, -52, -101, -105, -118, -138, -153, -156 and -180) (Rigét et al., 2019)

Hence, natural and anthropogenic Hg travels to the Arctic via long-range transport with the atmosphere, ocean currents, northward-draining rivers, and biota from lower latitudes (AMAP, 1998, 2005). Atmospheric Hg can become deposited and stored in the Arctic cryosphere (Zdanowicz et al., 2009; Zheng et al., 2009), similar to POP congeners (Blais et al., 2001). Indeed, totHg and MeHg have been detected in ice caps from the Canadian Arctic (St Louis et al., 2005; Zdanowicz et al., 2009; Zheng et al., 2009) and permafrost² (Schuster et al., 2018). Permafrost covers most of the terrestrial areas of the Arctic (ACIA, 2005) and is suggested to contain significant amounts of Hg (Schuster et al., 2018). Thus, deposited atmospheric Hg in abiotic cryospheric compartments may serve as important sources of Hg input to coastal environments during the melt season (Kirk et al., 2012; Zhang et al., 2015).

1.2 Riverine run-off

POP and Hg concentrations measured in the Arctic are known to vary seasonally in the air (Dommergue et al., 2010; Hung et al., 2016; Kirk et al., 2012; St Louis et al., 2005), the water column (Hallanger et al., 2011a; Hargrave et al., 2000) and the pelagic ecosystem (Hallanger et al., 2011a; Hargrave et al., 2000; Ruus et al., 2015). Thus, estuarine benthic ecosystems may likewise experience seasonal variations in contamination, possibly due to riverine-run-off.

During the melt season, Arctic estuaries receive riverine run-off from glaciers and permafrost that contain particulate and dissolved organic and inorganic matter, freshwater, nutrients, and remobilised POPs and Hg (Bring et al., 2016; Carlsson et al., 2012; Leitch et al., 2007; St Louis et al., 2005). For instance, Pan-Arctic riverine run-off from the six major rivers (Ob, Yenisey, Lena, Indigirka, Kolyma and Mackenzie) flowing into the Arctic ocean has been estimated to be an important source of POPs contamination in surface estuarine sediments (Carrizo et al., 2011), where POPs biomagnifies in the food web (Hop et al., 2002). In addition, studies from Switzerland have shown high fluxes of POPs from melting Alpine glaciers to lakes, calling this potential contamination source the “glacier hypothesis” or “delayed release hypothesis” (Bogdal et al., 2009). Research from Svalbard and the Canadian Arctic has detected totHg and MeHg in snowmelt and glacial run-off (Dommergue et al.,

² Permafrost is a compartment containing soil, rock, sediment, or other terrestrial material and ice. Permafrost must have a temperature below 0 °C for two or more consecutive years (ACIA, 2005).

2010; Graydon et al., 2009; Loseto et al., 2004; St Louis et al., 2005; Zdanowicz et al., 2009; Zheng et al., 2009). In addition, fluxes from thawing permafrost have been suggested to contribute significant amounts of Hg to the Arctic aquatic environment (Outridge et al., 2008). Overall, studies have indicated that riverine inputs of Hg could be of importance to the marine system (Hare et al., 2008; Leitch et al., 2007; Outridge et al., 2008), where Hg biomagnifies in the food web (Ruus et al., 2015).

Models of the release of organic contaminants from snowmelt show different seasonal release characteristics, reflecting their physicochemical properties (Meyer & Wania, 2011). Chemicals that strongly adsorb to particulate matter or snow experience peak emission at the end of the melting period, whereas water-soluble congeners experience peak releases early in the melting period (Meyer & Wania, 2011). Seasonal studies of Hg in filtered snowmelt and glacial run-off tended to decline over time as melt progressed (Dommergue et al., 2010; St Louis et al., 2005). Whereas, Hg associated with particulate material indicated some evidence of higher concentrations later in the melting period (St Louis et al., 2005).

1.3 The benthic realm

Upon entering the aquatic environment, pollutants can be transported to the benthic realm due to absorption to sinking suspended particles (marine snow) and absorption in phytoplankton that later sinks as phytodetritus if ungrazed (De Souza Machado et al., 2016; Everaert et al., 2015; Lee & Fisher, 2017; Wania & Daly, 2002). Thus, estuarine sediments function as a sink for contaminants, which may expose benthic biota to high concentrations of these contaminants (Lebeuf & Nunes 2005; Outridge et al., 2008). Benthic invertebrates inhabiting estuaries close to river outlets have shown to accumulate more POPs compared to more marine influenced sites (Hummel et al., 1990; Olenycz et al., 2015). In a recent study from a river estuary in the Baltic Sea, macroinvertebrates directly influenced by run-off had higher concentrations of Hg (Jędruch et al., 2019). Mesocosm experiments have suggested that different geochemical Hg pools and sources contribute differently to MeHg quantity in estuarine amphipods, where terrestrial run-off appears to contribute the most (Jonsson et al., 2014).

1.4 Bioaccumulation

Benthic invertebrates such as amphipods may acquire pollutants by two main routes, water ventilation by gills that take up dissolved contaminants in porewater or overlying water and via ingestion of food/sediment that contain particle-bound contaminants (Boese et al., 1990; Forbes et al., 1998; Lawrence & Mason, 2001; Shaw & Connell, 1987). The relative importance of these pathways depends on the hydrophobicity (usually expressed as octanol-to-water partition coefficient or K_{ow}) of the organic compounds and trophic position of the amphipods (Borgå et al., 2004; Thomann et al., 1992). However, experimental studies have suggested that for many POP congeners (among those included in the current study) and Hg, diet may be the main entry point for benthic organisms (Boese et al., 1990; Lawrence & Mason, 2001). This illustrates the importance of investigating diet in contamination studies.

Arctic benthic organisms have been observed to utilise pelagic production settling to the benthic habitat (Grebmeier et al., 1988; Hobson et al., 1995), such that seasonality in pelagic production is reflected in the organic matter subsidising the benthic habitat and, thus, detected in the benthic fauna. Lipid dynamics in a species can provide further clues about feeding strategy and variability in food supplies. For instance, developing large lipid reserves during productive times, as seen in herbivorous copepods, indicates reliance on a temporary food source (Hagen & Auel, 2001; Legeżyńska et al., 2012; Varpe, 2017). Generally, benthic organisms contain little lipids with small changes seasonally, suggesting a stable food source all year round such as a detrital “food bank” in the sediments (Graeve et al., 1997; Mincks et al., 2008). Many benthic amphipods in Svalbard fjords exhibited low dependence on lipid reserves because of feeding on available food sources throughout the year and therefore did not need large seasonal energy reserves (Legeżyńska et al., 2012).

1.4.1 Dietary descriptors

Stable isotope of carbon ($\delta^{13}\text{C}$) and nitrogen ($\delta^{15}\text{N}$) are used as chemical tracers to track dietary preferences (Fry, 2006). $\delta^{15}\text{N}$ is a useful tool to study trophic status in the food web since $\delta^{15}\text{N}$ typically enriches by 3-4‰ from diet to consumer (Peterson & Fry, 1987). The isotopically heavy nitrogen isotope's retention in the consumer compared to diet is due to excretion of the lighter nitrogen isotope in urine (Peterson & Fry, 1987). However, there are challenges with using $\delta^{15}\text{N}$ as a proxy for trophic status. One such potential challenge is that

starvation periods might increase $\delta^{15}\text{N}$ values in organisms (Doi et al., 2017). There could also be a seasonal change in baseline values of $\delta^{15}\text{N}$ in the system, resulting in a seasonal change of $\delta^{15}\text{N}$ in consumers that do not reflect a change in diet (Woodland et al., 2012).

$\delta^{13}\text{C}$ values, on the other hand, demonstrate little variation when moving through food webs (<1‰) and is used to investigate an organisms primary carbon source (Peterson and Fry 1987). For instance, terrestrial C_4 versus C_3 plants have different photosynthetic pathways yielding average $\delta^{13}\text{C}$ values of -12‰ and -27‰, respectively, allowing successful assessment of the utilisation of these energy sources in consumers (Fry & Sherr, 1989; Peterson & Fry, 1987). $\delta^{13}\text{C}$ signatures in aquatic primary producers show a wide range of isotopic values and the mechanisms controlling fractionation are not understood in great detail (Fry & Sherr, 1989). There are several challenges when interpreting $\delta^{13}\text{C}$ results, such as carbon sources having overlapping signatures and isotopic changes due to bacterial degradation (Fry & Sherr, 1989; Peterson & Fry, 1987). Despite these shortcomings, both stable isotopes $\delta^{13}\text{C}$ and $\delta^{15}\text{N}$ have successfully been applied in determining carbon sources and trophic status in aquatic invertebrates (e.g. Iken et al., 2010; Renaud et al., 2011; Søreide et al., 2006a).

Fatty acids or fatty acid trophic marker (FATM) is another dietary descriptor used in the present study. As stable isotopes, FATM functions as a biochemical tracer for dietary information (Kelly & Scheibling, 2012). This concept of FAs functioning as a trophic marker is based on the notion that certain FAs may be conservatively transferred from prey to consumer, and later detected in the consumer (Dalsgaard et al., 2003). In qualitative investigations of food web interactions using FATM, one can compare FA compositions, amount and/or ratios of FAs found in consumers against what has been discovered in potential prey items.

When interpreting FATM result in consumers, several issues need to be taken into consideration (Budge et al., 2006; Kelly & Scheibling, 2012). Dietary FAs may become modified and selectively retained in the consumer, or FA biosynthesis might take place, resulting in FA profiles that do not reflect diet. Another potential challenge is carbon sources that have overlapping FA profiles (Kelly & Scheibling, 2012). Despite these challenges, FATM has successfully been used in identifying food sources in Antarctic and Arctic benthic

amphipods (Graeve et al., 2001; Legeżyńska et al., 2014), in estuarine systems (Kharlamenko et al., 2001), and in addition, documenting seasonal feeding in Arctic benthic invertebrates (Legeżyńska et al., 2014). Both FATM and stable isotopes have limitations as dietary descriptors, although by combining results, the reliability of the interpretations is improved (Graeve et al., 2001; Legeżyńska et al., 2012; Nyssen et al., 2005).

1.5 Seasonality and Arctic coastal invertebrates

The Arctic experiences strong seasonality driven by the annual variation of incoming irradiance (Varpe, 2017). This seasonality results in seasonal variations in primary production, food availability, feeding strategy and lipid accumulation in biota (Varpe, 2017). Seasonality is also evident in POP availability and bioaccumulation in polar pelagic and sympagic invertebrates and lower trophic level biota (Borgå et al., 2001; Hallanger et al., 2011a; Hallanger et al., 2011b; Hargrave et al., 2000). However, no seasonal trend in bioaccumulation of POPs was found in benthic polar invertebrates (Evenset et al., 2016). In contrast, coastal benthic invertebrates from temperate regions show seasonality in POP bioaccumulation, influenced by factors such as reproduction, diet, and riverine run-off (Hummel et al., 1990; Knickmeyer & Steinhart, 1988; Olenycz et al., 2015). Seasonal studies of Hg accumulation in Arctic benthic marine infauna are scarce. However, studies from temperate regions showed seasonality in Hg accumulation, influenced by diet, growth, ice cover, concentrations and bioavailability in the ambient environment, in coastal benthic invertebrates (Baeyens et al., 1997; Jędruch et al., 2019). Thus, many factors can affect seasonal accumulation in biota that may result in intra-annual variations, and when sampling only one time-point these variations will, most likely, go undetected.

Arctic estuaries contain coastal bodies of water comprised of seawater diluted by freshwater, from river run-off during the melt season, and provide vital habitat for an array of organisms such as marine mammals, migratory birds, fish and pelagic and benthic invertebrates (AMAP, 1998; Crossland et al., 2005). Coastal zones are the planets most productive areas, and the most perturbed regions affected by pollution, overfishing, and habitat destruction (Crossland et al., 2005). Arctic estuaries, relative to lower latitude coastlines, have not been studied sufficiently (McClelland et al., 2012), and importantly, lower trophic level biota in Arctic ecosystems are poorly investigated in contamination studies, especially seasonal studies and in relation to riverine run-off. For Arctic marine benthic invertebrates, only one investigation

of seasonal POPs bioaccumulation exists (Evenset et al., 2016), whereas none have considered seasonality in Hg bioaccumulation. Thus, more attention needs to be attributed to understanding the complex patterns of seasonal uptake and transport of POPs and Hg through coastal benthic food webs (Chouvelon et al., 2018; Evenset et al., 2016). This is essential to predict the fate and effects of currently released and remobilised compounds, especially in a changing Arctic.

1.6 Aim and objectives

The main aim of the present study was to investigate how seasonal terrestrial run-off affects contaminant accumulation in coastal benthic organisms. The influence of riverine run-off on POPs and Hg concentrations was studied in a littoral amphipod, *Gammarus setosus* (Dementieva, 1931), inhabiting the Adventelva river estuary, near Longyearbyen in Spitsbergen, Svalbard. Two locations with different proximity to the two river outlets were sampled monthly from April to August 2018. The period of the study allowed for data collection when the environment was subjected to no riverine inputs (April), and when inputs from terrestrial run-off were present (May to August). The aim was addressed through four objectives, described below, accompanied by their respective hypotheses and expectations:

Objective 1: Investigate dietary descriptors in *G. setosus* from spring to autumn to address diet and trophic status.

G. setosus is characterised as a benthic deposit-feeder³ and omnivorous primary consumer (Legeżyńska et al., 2014). It was therefore hypothesised that *G. setosus* feeds on a mixture of carbon sources, with variable food items depending on the season, however with no spatial difference between the stations. Thus, it was expected that outside of the phytoplankton spring bloom, when primary producers are favoured, macroalgae- and flagellate-derived detritus and bacteria are the dominant food source. As the season progresses, terrestrial material coming with riverine run-off is an important dietary component (Dunton et al., 2012; Wiedmann et al., 2016). Furthermore, *G. setosus* occupies a low trophic status (Legeżyńska et al., 2014).

³ As a deposit-feeder, *G. setosus* may gather food items by ingesting the sediment itself, either in bulk or more selectively (Steele et al., 2008).

Objective 2: Quantify total lipid content in *G. setosus* from spring to autumn to evaluate feeding preferences.

Due to the expectations of continuous food availability for polar benthic amphipods (Legeżyńska et al., 2012, 2014), it was hypothesised that *G. setosus* is not dependent on accumulating lipid reserves. Thus, it was expected that *G. setosus* does not have a seasonal accumulation of lipid reserves.

Objective 3: Quantify the contaminant concentration in Adventelva estuarine sediments from spring to autumn to evaluate if estuarine sediments receive contamination from riverine run-off.

Hypothesising that riverine run-off is an important contamination source to estuarine sediments (e.g. Carrizo et al., 2011; St Louis et al., 2005), it was expected that there are higher concentrations of contaminants in the sediments when influenced by riverine run-off than before. Additionally, water-soluble compounds were expected to peak early in the melting period, and contaminants strongly adsorbed to particulate matter to peak later (Dommergue et al., 2010; Meyer & Wania, 2011; St Louis et al., 2005).

Objective 4: Quantify the contamination concentration in *G. setosus* from spring to autumn to address how seasonality in biological processes (diet: objective 1, and lipid content: objective 2) and environmental factors such as riverine influence (sediments: objective 3) might affect contaminant concentrations.

It was hypothesised that the contaminant concentrations in *G. setosus*, a primary consumer that occupies a low trophic status, is influenced by dietary exposure (Boese et al., 1990; Borgå et al., 2004; Kaag et al., 1997; Lawrence & Mason, 2001). It was further hypothesised that the contaminant concentrations in diet might change seasonally due to inputs from riverine run-off, and thus change the contaminant concentration in *G. setosus* over a season. Additionally, as POPs are lipophilic compounds, lipid dynamics in *G. setosus* over a season might impact POP concentrations.

2 Materials and methods

2.1 Study species

The amphipod *G. setosus*, belonging to the family group Gammaridae, was chosen as the study species. *G. setosus* has a polar distribution and inhabits the littoral zone of Svalbard fjord systems (Wesławski, 1994; Wesławski et al., 2010; Wesławski et al., 1997). The habitat colonised by *G. setosus* consists of mud, sand, gravel, detritus, stones, and plants (Wesławski, 1990; Wesławski et al., 1993). Localities with the most abundant populations of *G. setosus* are found on sheltered beaches under flattened stones (Wesławski et al., 1993). *G. setosus* is euryhaline (Salinity 5-34‰ PSU), eurytopic, and found at a depth between 0-2 meters, with variation in temperatures ranging from -1.8 to +4-8°Celsius (Wesławski, 1990; Wesławski et al., 1997). *G. setosus* belong to some of the most abundant littoral macro-organisms in the fjord systems on Svalbard (Wesławski, 1990; Wesławski et al., 1993). Furthermore, these invertebrates are important prey sources for higher trophic level biota including demersal fish, other macroinvertebrates and migratory birds, and may play key functional roles in detritus cycling, thus providing nutrients to primary producers (Väinölä et al., 2008). *G. setosus* life span extends over 2.5-4 years, which can be estimated by measuring the length of the organism (Wesławski & Legeżyńska, 2002).

2.2 Site characterization

Svalbard is a Norwegian archipelago in the Arctic located between 74° and 81°N, and 10° and 35°E (Hisdal, 1985). On the west coast of Spitsbergen, the Adventelva estuary is positioned at 78°N in the inner part of Adventfjorden, which is part of Isfjorden, Spitsbergen's largest fjord system. Adventfjorden is approximately 8.3 km long and 3.4 km wide and its innermost part is composed of an extensive (0.9 km wide) tidal mudflat formed by two braided rivers; Longyearvelva and Adventelva (Figure 1) (Wesławski et al., 1999). Longyearbyen, the principal town on Spitsbergen, is situated along the shore of Adventfjorden (Figure 1). This settlement has several types of influence on the aquatic environment in the fjord, such as discharge of wastewater from a sewage treatment plant, which is not biologically or chemically treated, old dumping sites, coal mining and human activity such as research and tourism (Wesławski, 2011).

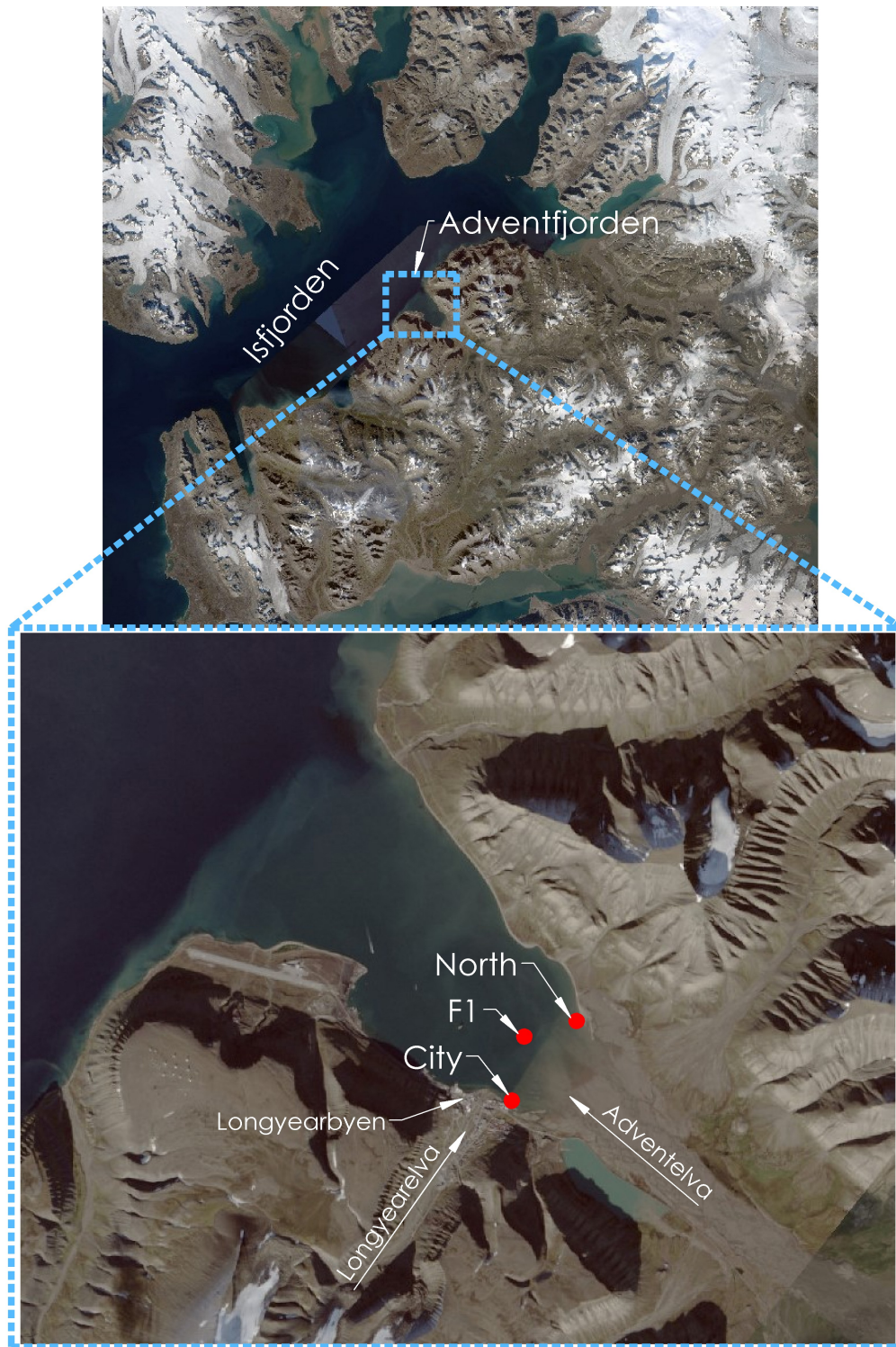


Figure 1. Above: Satellite map of Isfjorden with Adventfjorden and Isfjorden highlighted. Below: Satellite map of Adventfjorden with Longyearbyen, Adventelva, Longyearelva, F1 station, the City and North station highlighted. F1 station was collected in Carrasco (2019), Johansen (2019) and McGovern et al. (in prep). Courtesy of the Norwegian Polar Institute©.

In the Adventelva estuary, two stations (200×150m) were studied; the City station (78°13.465'N 15°40.213'E) and the North station (78°14.455'N 15°43.244'E). They are positioned in the littoral zone on both sides of the Adventelva river outlet (Figure 1). The City

station, situated on the south side of Adventfjorden, is close to Longyearbyen and Longyearelva, while the North station is located on the north side of Adventfjorden (Figure 1). The environment at the City station is impacted by terrestrial run-off from both Longyearelva and Adventelva, and the habitat around the North station is most likely predominantly impacted by Adventelva during the melting season. Both Adventelva and Longyearelva are glacier-fed rivers, with meltwater running from glaciers that have retracted several kilometres from the coast (Zajączkowski & Włodarska-Kowalczyk, 2007). The rivers transport freshwater, glacially eroded material and other terrigenous inorganic and organic matter to Adventfjorden for approximately four months (June to September) when temperatures are above zero degrees (Syvitski et al., 1985; Wesławski et al., 1999; Zajączkowski & Włodarska-Kowalczyk, 2007). However, during the current study, rivers started running in May. Before reaching Adventfjorden, Adventelva travels 35km through Adventdalen (Wesławski et al., 1999), whereas Longyearelva runs through Longyearbyen. During winter and early spring, the stations don't receive any terrigenous material from the rivers, and instead, thick fast ice develops in Adventdalen, on the mudflat, and along the shoreline covering these sites (Wesławski et al., 1999). During the winter of 2017/2018, there was mostly open water in Adventfjorden. Although from January to April, 2018, different sea ice formations were observed; drift ice and fast ice, as well as open water. Fast ice was only observed during March and at the inner parts of the fjord (Norwegian Meteorological Institute, n.d.).

The substrate at the City station is comprised of very muddy sediments and small to large flat stones, with sand, detritus, and other organic material. The North station has similar substrate, but with sandy sediments instead of muddy. Both sites experience a semidiurnal tide exposing the substrate (to different extents depending on how high the low tide is) (Wesławski, 2011; Wesławski et al., 1999; Zajączkowski et al., 2010).

2.3 Field procedures

Sampling was conducted by the student during low-tide (Wesławski et al., 1999; Zajączkowski & Włodarska-Kowalczyk, 2007), monthly between April to August, 2018 (Table 1).

Table 1. Overview of station, collection date and physical parameters from the City and the North station. All samples were collected in 2018.

Station	Collection date	Sediment temperature	Sediment type	River influence
City	15 th April	-2.4°C	Sand	No
	18 th May	2.2°C	Mud	Yes
	15 th June	4.5°C	Mud	Yes
	11 th July	7.3°C	Mud	Yes
	13 th August	7.7°C	Mud	Yes
North	16 th April	-0.6°C	Sand	No
	17 th June	3.0°C	Fine sand	Yes
	12 th July	5.4°C	Fine sand	Yes
	14 th August	7.9°C	Fine sand	Yes

The City station was accessed by foot while the North station was reached by kayaks (and by foot when sea ice was present). During low tide (around 35-15 cm), the appropriate substrate for collecting *G. setosus* is exposed, and there is a two-hour window of opportunity for collecting these organisms, from approximately one hour before to one hour after the lowest low tide. *G. setosus* can be found hidden under stones emerging from the water or burrowed down in sediments beneath the stones (Figure 2). Thus, sampling was accomplished by randomly overturning stones within the station area, and searching for amphipods clinging to the backside or residing in the sediments (Figure 2). Upon uncovering *G. setosus*, the specimens were stored in a water-filled container, and the location was marked. A replicate site was then established with a 10-meter radius from the marked location. Whole specimens of *G. setosus* were pooled in order to obtain enough biomass in each replicate for the necessary chemical analyses in the current study. Following amphipod collection, sediments down to 1.5 cm were gathered with a stainless steel spoon into a pre-combusted 200mL glass container sealed with aluminium foil and a 30mL fluorinated polyethylene vial (Thermo Scientific®). Following sediment collection, another search for amphipods took place, representing the next replicate, by searching outside of the first replicate area. This process was repeated until either four replicates were obtained or the substrate disappeared due to withdrawal of the tidal water. A water sample was collected in a 27.5 L fluorinated polyethylene carboy from the closest water mass. Finally, pictures were taken, and a description of the physical environment and the sediments collected was noted (Table 1). Each sampling effort took two-three days each time point, depending on weather and low-tide heights of the water. The equipment was cleaned inbetween each replicate and sampling site with distilled water (MilliQ water) and 96% ethanol (Sigma-Aldrich, Saint Louis, USA).

An opportunistic search for potential food sources took place within the station area as frequently as possible. During the search, macroalgae, microphytobenthos, terrestrial material

and detritus were collected into polyethylene zip-lock bags (Grippie®). In July, nine terrestrial forbs were collected south of Isdammen (N78°12.1, E15°45.1). Detritus could be an important food source (Legeżyńska et al., 2012, 2014), and were thus collected. However, detritus can consist of different types of plant tissue (e.g. terrestrial leaf litter, aquatic macrophytes, phytoplankton), animal tissue (carrion), dead microbes, faeces (e.g. secondary production faecal pellets) etc. in varying degrees (Moore et al., 2004; Tenore, 1988). Detritus's nutritional and food value differs as it receives different organic matter and becomes modified by physical and biological activity (Tenore, 1988). Thus, detritus is difficult to sample directly and may not be representative.



Figure 2. Left: Picture of how *G. setosus* was found under stones emerged from the water or burrowed down in sediments beneath the stones (photo: Emelie Skogsberg). Right: Display of how the student was searching for *G. setosus* at the North station in April (photo by Nina Knutdzon).

2.4 Laboratory preparations

In the laboratory at UNIS, sediment samples were frozen (-20°C) until transportation to the respective facilities for contaminant and stable isotope (SI) preparation and analysis (Table 2). Samples of potential food sources were cleaned with distilled water (MilliQ water), identified to the lowest possible taxa (all terrestrial plants were pooled) (Gjærevoll et al., 1999; Wesławski, 2011) and frozen (-20°C) until transportation to the proper facility for SI preparation and analysis (see Appendix A for specific terrestrial taxa) (Table 2). Water samples were filtered through a pre-combusted (4 hours at 450°C) Whatman® 25mm GF/F glass filter for SI analysis of the pelagic particulate organic matter (POM) fraction (Table 2). Filters were packed and stored in aluminium foil and frozen (-20°C) until transportation to the proper facility for SI preparation and analysis.

In the laboratory at UNIS, amphipod samples were placed in bigger containers filled with filtered seawater from Adventfjorden and stored in the dark at approximately 4°C for 12-24 hours (Figure 3). This procedure allowed the amphipods to evacuate their gut contents, which prevents this material from influencing results from SI analysis. Following evacuation, amphipods were measured from the tip of the rostrum to the end of the telson to determine the age (Wesławski & Legeżyńska, 2002). Individuals under 10 mm, indicating a juvenile stage (Wesławski & Legeżyńska, 2002), were not used any further in the present study. Nevertheless, variation in the contamination load could still be possible due to age-related accumulation and ontogenetic preferences in diet between 2- and 3-year-old amphipods (Borgå et al., 2004). Therefore, approximately equal amounts of 2- and 3-year-olds were assigned to each analysis every month to minimise possible confounding ontogenetic differences. A random subsample of amphipods from every replicate was used for species identification. Species determination was confirmed using a stereo microscope following (Tzvetkova, 1972) and in communication with professor Jan Marcin Wesławski (Institute of Oceanology Polish Academy of Sciences, Department of Marine Ecology) (Figure 3).



Figure 3. Left: Picture of *G. setosus* (photo: Emelie Skogsberg). Right: Picture of a amphipod sample placed in a container filled with filtered seawater for the organisms to evacuate their stomach contents before being sorted for analysis (photo: Emelie Skogsberg).

Amphipods within the accurate size range and characterized as *G. setosus* were sorted into three different containers destined for 1) SI analysis, total mercury- (totHg) and methyl mercury (MeHg) analysis, 2) fatty acid (FA) analysis and 3) POP analysis, based on mass required for analysis, differences in pre-treatment procedure and where the analysis was to take place (Table 2). Amphipods used for FA analysis were collected in 2mL polypropylene cryogenic vials (VWR®) and frozen (-80°C) until transportation to the proper facility for

analysis. Amphipods intended for SI/totHg/MeHg analysis, and POP analysis were packed in aluminium foil and frozen (-20°C) until transportation to the proper facility for analysis. The number of amphipods allocated to each analysis and the overall weight (Mettler Toledo®, AG204 Deltarange) was noted down (Appendix B, Table B1).

Table 2. Overview of station and analysis information, showing number of replicates of amphipods, sediments and water samples collected for each analysis and type of food source sampled. Letter corresponds to: SI; stable isotope analysis, FA; fatty acid analysis, POP; POP analysis, totHg and MeHg; total and methyl mercury analysis, P; pooled samples, Te; Terrestrial material, De; Detritus, U; *Ulva* spp. (Green macroalgae), Ac; *Acrosiphonia* spp. (Green macroalgae), Pa; *Palmaria palmate* (Red macroalgae), L; *Laminaria digitata* (Brown macroalgae), Mi; Microphytobenthos.

Station	Month	Amphipods		POP	totHg	MeHg	Sediments		TotHg	Potential food sources	Water sample
		SI	FA				SI	POP		SI	
City	April	4	3	3	3	4	P	3	4	U, Pa	1
	May	4	3	3	4	4	P	P	4	U, Pa	1*
	June	4	3	3	4	4	P	P	4		1*
	July	4	3	3	4	4	P	P	4	De, Te	1*
	August	4	3	3	4	4	P	3	4	De, Mi,	1*
North	April	4	3	3	4	4	P	3	4	Ac, L	1
	June	4			4	4	P	P	4		1*
	July	2	2	2	2	2	P	P	2		1*
	August	4	3	3	4	4	P	3	4		1*

*Because of budget limitations these samples were not analysed.

2.5 Chemical analyses

2.5.1 Stable isotopes

Pre-treatment

SI pre-treatment laboratory work was performed by the student in the toxicology laboratory at the University of Oslo (UiO), Norway. The staff at UC Davis Stable Isotope Facility at the University of California (California, USA) conducted the chemical analysis and quantification. When working in the lab at UiO, no wool clothes were worn, and a lab coat and gloves were used at all times in order to avoid adding carbon and nitrogen sources. The tools used were washed with distilled water (MilliQ water), 96% ethanol (Sigma-Aldrich, Saint Louis, USA) and air dried/or dried lightly with disposable paper tissues (Kimwipes®) before and in between samples.

Samples of *G. setosus*, sediment POM, detritus, terrestrial plant material, macroalgae, microphytobenthos, and filters with pelagic POM from water samples were used for SI analysis. Since these matrixes compose of different material, they were prepared differently before the analytic determination, depending on how their specific content could affect the $\delta^{15}\text{N}$ and $\delta^{13}\text{C}$ signatures. Inorganic carbon (CaCO_3) in exoskeleton is enriched in $\delta^{13}\text{C}$,

compared to internal tissues, resulting in a skewed $\delta^{13}\text{C}$ signature (Søreide et al., 2006b). Søreide and Nygård (2012) showed that with carbonate removal, $\delta^{13}\text{C}$ values between exoskeleton, internal tissues and whole specimens had relatively little variation in amphipods. Carbonate removal was necessary for amphipods, sediments and POM-filters to obtain correct $\delta^{13}\text{C}$ values. In addition, lipids are depleted in $\delta^{13}\text{C}$ relative to other tissues (DeNiro & Epstein, 1977), thus depending on the lipid content of the organism, it is recommended to exclude lipids before analysis (Søreide et al., 2006b). Benthic organisms usually contain little lipids (Graeve et al., 1997), and it has been shown that the $\delta^{13}\text{C}$ signatures are reasonably similar between lipid versus lipid-removed benthic samples (Iken et al., 2010). Thus, lipids were not removed in *G. setosus* in the present study.

Certain pre-treatment techniques such as lipid and carbonate removal may affect $\delta^{15}\text{N}$ signatures (Carabel et al., 2006). Findings from research are not consistent regarding exactly how stable isotope signatures are affected by different methods (Carabel et al., 2006; Søreide et al., 2006b). Thus, in an attempt to avoid bias in the current study, for samples requiring carbonate removal, two duplicates were taken from each sample. One duplicate was only freeze-dried and analysed for $\delta^{15}\text{N}$ signature, while the other duplicate was freeze-dried and acidified for carbonate removal and analysed for $\delta^{13}\text{C}$ signature (Carabel et al., 2006; Søreide et al., 2006b).

During pre-treatment, all samples were lyophilised in a freeze drier (Leybold-Heraeus GT2 Freeze Dryer with Leybold Vakuum GmbH vacuum pump, Cologne, Germany). Following freeze-drying, the samples were homogenised to a fine powder with an agate mortar and pestle. However, sediments were homogenized with a stainless-steel spoon, and filters were not homogenized. In addition, all samples, except filters, were weighed before and after freeze-drying to calculate water content. The powder was placed in 5x8mm tin-capsules (Element microanalysis Ltd.) and weighed on a microbalance (Mettler Toledo® MX5), packed together and put in 96-well plate. Filter samples were carefully packed in 8x12mm tin-capsules (Element microanalysis Ltd.) and placed in labelled baggies for shipping.

From the homogenised amphipod samples, a subsample was taken for CaCO_3 removal, by adding 1M hydrochloric acid (HCl) (Sigma-Aldrich, Saint Louis, USA) drop by drop to the powder until it stopped bubbling. When bubbling ceases, this indicates that all inorganic

carbon has evaporated. Following acidification, the amphipod samples were frozen (-20°C), lyophilised in a freeze drier (Leybold-Heraeus GT2 Freeze Dryer with Leybold Vakuum GmbH vacuum pump, Cologne, Germany) and again homogenised with an agate mortar and pestle. These samples were thereafter placed in 5x8mm tin-capsules (Element microanalysis Ltd.) and weighed on a microbalance (Mettler Toledo® MX5), packed together and put in 96-well plate and transported to UC Davis stable isotope facility for chemical analysis. This protocol followed the method mentioned in Søreide and Nygård (2012), however, with adjustments.

Subsamples from the homogenised sediments were treated with 12M HCl (37%) (Sigma-Aldrich, Saint Louis, USA) fumes to remove inorganic carbon, according to Harris et al. (2001). Distilled water (MilliQ water) was added to the subsamples (approximately 300mg), mixed with a vortex and placed in a desiccator with a beaker (150mL) containing 100mL 12M HCl for 48 hours, resulting in a conversion of the inorganic carbon in the sediments being released as CO₂. Following fumigation, the sediment samples were frozen (-20°C), lyophilised in a freeze drier (Leybold-Heraeus GT2 Freeze Dryer with Leybold Vakuum GmbH vacuum pump, Cologne, Germany), and again homogenised. These samples were then placed in 5x8mm tin-capsules (Element microanalysis Ltd.) and weighed on a microbalance (Mettler Toledo® MX5), packed together and put in 96-well plate and sent to UC Davis stable isotope facility for chemical analysis. Sediments were fumigated instead of acid washed to avoid acid-soluble organic carbons to be washed away through rinsing (Harris et al., 2001).

Filters were likewise acid-fumigated in order to remove inorganic carbon. Acidified and lyophilised (Leybold-Heraeus GT2 Freeze Dryer with Leybold Vakuum GmbH vacuum pump, Cologne, Germany) filter samples were carefully packed in 8x12mm tin-capsules (Element microanalysis Ltd.) and placed in baggies before being transported to UC Davis stable isotope facility.

Instrumental analysis, analytic quantification and quality assurance

The instrumental analysis was performed according to Fry (2006), shortly summarized in Appendix A, together with analytic quantification and quality assurance.

From UC Davis Stable isotope facility, the $\delta^{13}\text{C}$ and $\delta^{15}\text{N}$ were quantified in 34 amphipod samples, nine pooled sediment samples, nine potential food sources and two water samples (filters). For samples requiring acidification, $\delta^{13}\text{C}$ values were taken from acidified duplicates, while $\delta^{15}\text{N}$ values were taken from un-acidified duplicates. Further information received from UC Davis stable isotope facility were total carbon and total nitrogen expressed as % of dry weight (d.w.).

2.5.2 Fatty acids

FA analysis of amphipods was conducted by professor Michael T. Arts and his staff at Ryerson University, Canada. The chemical analysis involved three steps: lipid extraction (including lipid determination), derivitization, and quantification using a gas chromatograph (GC), and 42 different FAs were investigated. Lipid extraction followed the method described by Folch et al. (1957). Chemical analysis, instrumental analysis and analytic quantification and quality assurance are described in Appendix A.

Of the 42 FAs quantified in 23 amphipod samples, the four FAs 24:0, 20:1n-11, 19:1n-12, and 15:1n-5 were not found in any samples. The data was reported on a mass fraction (wet weight (w.w.), d.w.), a molar fraction (w.w., d.w.) and a molar and a weight percentage basis. In addition, total lipid content (w.w., d.w.) was reported.

2.5.3 Persistent organic pollutants

Analysis of POP concentrations in amphipods and sediments were conducted at the Norwegian Institute for Water Research (NIVA) in Oslo at the environmental chemistry laboratory, Norway. The student performed extraction and clean-up, whilst the staff at the environmental chemistry laboratory conducted the instrumental analysis and quantification. The method used for the analysis of POPs followed NIVA's internal protocol H 3-4 and H 3-3 for biota and sediments, respectively. All glassware used during preparation were pre-combusted at 650°C, and all tools were washed, cleaned with acetone (J.T. Baker, United States) and rinsed with cyclohexane (J.T. Baker, United States) before use.

Prior to analysis, a range finding procedure was carried out with sediment and amphipod samples by weighing out five systematic smaller amounts in order to determine if the elaborated method and instrument available in the laboratory were able to detect the analytes

in question (Table 3). Furthermore, this range-finding procedure was essential to establish how much mass was required for reliable results. The analytes investigated belong to the groups PCBs and chlorobenzenes (Table 3). Details regarding the internal standard see Appendix B, Table B3.

Table 3. Overview of the nine POP congeners investigated divided into two main groups; PCBs and chlorobenzenes.

Group	Abbreviation	Analyte
PCBs	PCB 28	2,4,4'-Trichlorobiphenyl
	PCB 52	2,2',5,5'-Tetrachlorobiphenyl
	PCB 101	2,2',4,5,5'-Pentachlorobiphenyl
	PCB 118	2,3',4,4',5-Pentachlorobiphenyl
	PCB 138	2,2',3,4,4',5'-Hexachlorobiphenyl
	PCB 153	2,2',4,4',5,5'-Hexachlorobiphenyl
	PCB 180	2,2',3,4,4',5,5'-Heptachlorobiphenyl
	PeCB	Pentachlorobenzene
Chlorobenzenes	Hexachlorobenzene	
	PeCB	Pentachlorobenzene

Preparation procedure for sediments

Organic solvent extraction with sonication

First, sediment samples were lyophilised in a freeze drier (Leybold-Heraeus GT2 Freeze Dryer with Leybold Vakuum GmbH vacuum pump, Cologne, Germany), thoroughly mixed with a stainless steel spoon and sifted through a 5mm mesh size sieve in order to remove stones and foreign inorganic objects. Approximately 10 g (Mettler Toledo®, AG204 Deltarange) of freeze-dried sediment and 40mL of cyclohexane- dichloromethane (Rathburn chemicals Ltd, United Kingdom) (CHX: DCM) (1:1) solvent was transferred to a centrifuge tube together with exactly 20µl internal standard. This solution was thoroughly shaken to mix the solutes, after which they were transferred to an ultrasonic bath for 60 minutes. Sonic waves break intermolecular interactions and disrupt cell membranes, which facilitates extraction. The PCB and chlorobenzene congeners investigated in the current study are lipid soluble. Thus, a lipophilic solvent such as CHX was used to extract them, aided by sonication. Contaminants and other organic molecules (for instance triglycerides) that are lipid-soluble, originating in the sediment, will become solved in the non-polar CHX: DCM solvent during sonication extraction. After sonication, the tubes were spun down in a centrifuge to allow proper phase separation, and the solvent-extract mixture, laying as a supernatant, was removed to zymark tubes. This extraction was done once more, and the solvent-extracts were transferred to the same zymark tube, combining the extracts.

Clean-up with acid treatment and gel permeation chromatography

Three drops of isooctane (Emsure, Germany) were added to the extracts to help prevent desiccation before gentle evaporation by nitrogen gas (N₂) in a TurboVap II®. The extracts were concentrated down to 1mL and transferred quantitatively with cyclohexane to test tubes. Since sediments contain many compounds other than PCBs and chlorobenzenes, the clean-up procedure is performed to remove, ideally, anything that is not the solvent or the analyte, as these compounds can interfere with the following instrumental analysis. PCBs and chlorobenzenes are stable during acid treatment, while most other organic molecules degrade under acid conditions. Hence it works as a suitable clean-up treatment. Concentrated (37%) sulphuric acid (2mL) (Emsure, Germany) was added to the extracts, and the solution was thoroughly vortexed to allow break down of unwanted organic molecules, that otherwise would interfere with the analysis. The acid-extraction solution was left for 30-48 hours. After which the test tubes were spun down in a centrifuge to allow proper phase separation and the acid layer was removed. New concentrated sulphuric acid was added, and the same procedures took place until the acid layer had a clear, transparent colour. After the last acid layer was removed, distilled water (MilliQ water) was added to assure that any acid residues left would be dissolved in the water instead of the organic phase. The test tubes were vortexed and centrifuged, allowing proper phase separation.

Sediments contain sulphur that together with the contaminants become extracted during sonication. Furthermore, sulphur does not break down during acid treatment. Hence another clean-up step is necessary when dealing with sediments. Gel permeation chromatography (GPC) is a type of liquid chromatography method, separating the analytes and the sulphur based on molecular size, with larger molecules being excluded earlier than smaller ones when run through a column. In addition, other interfering compounds that might be left in the extracts are also eliminated (if their molecular size falls outside the analytes fractionation collecting window). Thus, by collecting the extract from the column during a particular size eluding window, sulphur is excluded, while the analytes are retrieved. After acidification, the extracts were transferred from the test tubes to ASE-tubes and gently evaporated with N₂-gas in a TurboVap LV® until almost dryness. Ethyl acetate (Honeywell, Riedel-de Haën, Germany)- cyclohexane (5:1) solvent was added, and the extracts were quantitatively transferred to spinex tubes containing filters and spun down in a centrifuge, twice, to ensure that no particles were remaining in the extracts. Afterwards, they were quantitatively transferred to 2mL glass GPC-vials (Agilent) and gently evaporated with N₂-gas in a Reacti-

Vap® to 0,5mL. Subsequently, the GPC-vials were run through the GPC-machine (Agilent Technologies, 1260 infinity II) (for detailed information about operational settings see Appendix B, B4). In the GPC machine the extracts containing the correct size-fractions enclosing the analytes were collected in ASE-tubes, which were gently evaporated with N₂-gas in a TurboVap LV®, and quantitatively transferred with cyclohexane to 2mL glass GC vials (Agilent). The fluid in the GC-vials was gently N₂ evaporated (Reacti-Vap®) to reduce the volume. The vials were stored in a fridge at 4°C until further processing.

Preparation procedure for amphipods

Homogenization

The amphipods were thawed at room temperature prior to homogenisation with an Ultra Turrax machine (Pro250 homogeniser). As much as possible of amphipod material was retrieved from the machine knives to diminish the loss of material.

Organic solvent extraction with sonication

Between 0.5 and 10 g (Mettler Toledo®, AG204 Deltarange) of homogenised material and 20mL cyclohexane-isopropanol (Rathburn chemicals Ltd, United Kingdom) (1:1) solvent were transferred to a centrifuge tube, together with 50 or 25µl internal standard (depending on the biomass). This solution was thoroughly shaken to mix the solutes, after which they were transferred to an ultrasonic bath for 60 minutes. After sonication, the tubes were spun down in a centrifuge to allow proper phase separation, and the solvent-extract, laying as a supernatant, were removed to new centrifuge tubes. This extraction was performed once more, and the solvent-extracts were combined with the first extracts in the second centrifuge tubes. To the combined extracts, 25mL of 0.5% Sodium Chloride (NaCl) (Emsure, Germany) solution were added, shaken thoroughly and centrifuged, resulting in the extracts laying on top of the NaCl-solution.

Extractable organic matter

Extractable organic matter as a proxy for lipid content was determined gravimetrically. Extracts were transferred from the centrifuge tubes to pre-weighed ASE-tubes and gently evaporated with nitrogen-gas to dryness in a TurboVap LV®. After which the tubes were put in a laboratory oven for an hour at 60°C and afterwards weighed. To ensure stabilisation of the weight, the samples were dried and weighed (Mettler Toledo®, AG204 Deltarange) again until a stable weight (within ± 0.005 g) was reached. Thus, the lipid weight was calculated

from the difference between the ASE-tubes with the dried extracts and the empty ASE-tubes (Equation 1). After weighing the dried extracts, cyclohexane was added, and the sample was transferred quantitatively with cyclohexane to test tubes.

$$\text{Lipid content\%} = (\text{Lipid weight/wet weight}) * 100 \quad (\text{Equation 1})$$

Lipid content % = lipid content in the tissue (%)

Lipid weight = difference between the weight of empty containers and the weight of containers with concentrated extracts (g)

Wet weight = wet weight (g) of the sample prior to extraction

Clean-up with acid treatment

Since tissues, similar to sediments, contain many compounds other than PCBs and chlorobenzenes, the clean-up procedure is performed to remove anything that is not the solvent or the analyte, as these compounds can interfere with the following analysis. Concentrated sulphuric acid (2mL) was added to the extracts, and the solution was shaken several times to assist the acid in accessing as much of the extract as possible to allow break down of unwanted organic molecules. The acid-extraction solution was left for 30-48 hours, after which the test tubes were spun down in a centrifuge to allow proper phase separation and the acid layer was removed. New concentrated sulphuric acid was added, and the same procedures took place until the acid layer had a clear, transparent colour. After the last acid layer was removed distilled water (MilliQ water) was added. The test tubes were shaken and centrifuged, allowing proper phase separation, and the extracts were afterwards transferred to 2mL glass GC-vials (Agilent). The fluid in the GC-vials was gently evaporated (Reacti-Vap®) with N₂-gas to reduce the volume. The vials were stored in a fridge at 4°C until further processing.

Instrumental analysis, analytic quantification and quality assurance

The procedure for instrumental analysis, analytic quantification and quality assurance are described in Appendix A.

From NIVA, nine POP congener concentrations were quantified in 23 amphipod samples and 17 sediment samples (where five sediment samples were pooled samples). The data was reported on a mass fraction (ng/g w.w.) basis, and total lipid content (% w.w.) was included. Recoveries of CRMs (1944, 2974a) used in the POP analysis had on average 60-82% recovery, however, PCB-28 in amphipods had a consistent low recovery average of 45%. The

relative percent difference between duplicate samples from the range finding procedure were 12.6%.

2.5.4 Total mercury

The student conducted the instrumental analysis, quantification and quality assurance measurements of totHg concentration in amphipods and sediments in the toxicology laboratory at UiO, Norway. A direct mercury analyser (DMA-80, Milestone, Inc. Italy) was used, and when operating, minimal sample preparations are required. The preparation steps merely involved lyophilising in a freeze drier (Leybold-Heraeus GT2 Freeze Dryer with Leybold Vakuum GmbH vacuum pump, Cologne, Germany) and homogenisation of the samples using an agate mortar and pestle. Sediments were in addition sifted through a 5mm mesh size sieve in order to remove stones and foreign inorganic objects. After which the samples were weighed (Mettler Toledo®, AG204 Deltarange) into pre-combusted (550-650°C) quartz boats that were subsequently placed in the auto-sampler of the DMA-80.

Prior to analysis, a range finding procedure and precision investigation was carried out. The range finding procedure involved taking five sub-samples from one amphipod and weight into five systematic smaller amounts. The precision investigation involved taking subsamples from three sediment samples and two amphipod samples and splitting them into triplicates, each triplicate weighing the same. Range finding and precision investigations allow determination of what masses were required to give accurate values and how precise the machine was performing (assuming homogenised samples). All tools used were thoroughly washed before and in-between samples with distilled water, 96% ethanol (Sigma-Aldrich, Saint Louis, USA) and 0,1% HCl (Sigma-Aldrich, Saint Louis, USA).

Instrumental analysis

The direct mercury analyser first dried and then decomposed the sample, rendering mercury, together with other components of the sample, volatilised. A carrier gas, oxygen, transported the decomposed sample to a “catalyst furnace”, where interfering compounds, including halogens, were trapped, and all mercury species were reduced to elemental mercury (Hg(0)). Next, as the Hg(0) followed the carrier gas, it became selectively trapped in a gold amalgamator, while other volatilized compounds were flushed away. Selectively trapped mercury was then released, by heating of the amalgamator. Following heating, mercury was carried by oxygen gas past absorbance cells, which were irradiated with light from a single

wavelength atomic absorption spectrophotometry and became quantified (USEPA, 2007). For detailed information about operational settings see Appendix B, Table B6.

Analytic quantification and quality assurance

Quantification of the analytes was accomplished by using an external standard to construct a calibration curve with linear regression. The calibration curve was produced by plotting increasing values of known concentrations of the external standard against the corresponding peak areas calculated from the light absorbance measurements during atomic absorption spectrophotometry. Analyte concentrations were thus determined by comparing the peak areas produced from the samples against the calibration curve.

Quality assurance techniques, such as blanks, duplicates and certified reference material (CRM-DORM-4; National Research Council Canada), were used for every batch run. To investigate the accuracy, certified reference materials (n=2-3) with known concentration were analysed together with the samples. Hence, by comparing known concentrations with concentrations detected from the analytic measurements, one can investigate how close the outcome of the analytic procedure was to the true concentration. Quartz boat blanks (n=2) were run alongside every sample batch to disclosure contaminating of mercury from the boats. While every 5th sample included a duplicate to determine instrumental precision (however variation could also be due to un-homogenised samples). Furthermore, inter-laboratory comparison in totHg quantification between UiO and Norwegian University of Life science (NMBU) was satisfactory (within 15%).

TotHg concentrations in 35 amphipod samples and 34 sediment samples were quantified and reported on a ng/g d.w. basis. Recoveries of CRM DORM-4 were between 88-92%. The relative on average difference in totHg concentrations between duplicate amphipod samples and sediments samples were 4% (range:1-7%) and 27.5% (range:4-46%), respectively.

2.5.5 Methyl mercury

Analysis of MeHg (or CH_3Hg^+) concentration in amphipods was performed at Stockholm University, Sweden, at the Environmental Science and Analytic Chemistry Department. The student conducted the preparation steps and instrumental analysis, and the staff at Stockholm University performed the quantification and quality assurance measurements of CH_3Hg^+ . All glassware used during preparation was pre-combusted at 650°C, and all tools were washed

before use. The procedure for preparation and the consequential analysis of MeHg was based on the method described in Braaten et al. (2014) and Hintelmann and Nguyen (2005), however with minor adjustments.

Amphipod samples were lyophilised in a freeze drier (Leybold-Heraeus GT2 Freeze Dryer with Leybold Vakuum GmbH vacuum pump, Cologne, Germany) and homogenised using an agate mortar and pestle. Following homogenisation, the samples were weighed out (Mettler Toledo®, AG204 Deltarange) into digestion vials (25mL Polypropylene falcon tubes, Fisher Scientific®) and MeHg was extracted via digestion using nitric acid (30%) (Fisher Scientific®). The digestion took place for 16-17 hours at 60°C in a bath. Following extraction, the sample solutions were pipetted into glass vials containing distilled water (MilliQ water), after which the solutions were neutralised with 45% potassium hydroxide (Sigma Aldrich®) and buffered with sodium acetate buffer (Sigma Aldrich®). If necessary, the pH was adjusted by adding the 45% potassium hydroxide or the 30% nitric acid. Next, sodium tetraethyl borate solution (Fisher Scientific®) was added to ethylate CH_3Hg^+ , which evaporates CH_3Hg^+ in the sample. Next, the samples were placed in a Methyl Mercury Analyser machine (2700 Methyl Mercury Auto-Analysis System, Tekran, Canada) that measures the CH_3Hg^+ concentrations in the samples.

Instrumental analysis

In the Methyl Mercury Analyser, samples were purged with nitrogen gas directly in the vials, and the volatile mercury species became trapped. Following absorption, the trapped CH_3Hg^+ became thermally desorbed, and an inert gas carried CH_3Hg^+ to a decomposition column, where organic forms of mercury became transformed to elemental mercury ($\text{Hg}(0)$). $\text{Hg}(0)$ was then transported to a cell with a cold-vapour atomic fluorescence spectrometer (CVAFS) for detection. In the CVAFS, the sample vapours became excited with UV radiation, and the amount of CH_3Hg^+ was measured by the emitted radiation. The 2700 Methyl Mercury analyser is designed and pre-programmed to follow the EPA Method 1630 (USEPA, 1998), and is a fully automated system (for operational settings see Appendix B, Table B7).

Analytic quantification and quality assurance

The procedure for analytic quantification and quality assurance are described in Appendix A.

The MeHg concentrations in 35 amphipod samples were quantified on a ng/g d.w. basis. Recoveries from CRM DORM-4 and spike samples were between 91-112% and 90%, respectively. On average, the relative percent difference in MeHg concentrations between duplicate samples was 24.8% (range: 2-44%).

2.6 Data treatment and statistical analysis

2.6.1 Lipid corrected carbon isotopic values

After calculating C:N atomic ratios in amphipod samples (Equation 2), the C:N values ranged from 3.8 and 6.1, and the carbon isotope values were therefore lipid corrected (Equation 3), to account for possible bias from depleted lipids (Post et al., 2007).

$$C:N = (\text{Weight \% Carbon} / \text{Atomic weight C}) / (\text{Weight \% Nitrogen} / \text{Atomic weight N}) \quad (\text{Equation 2})$$

C:N= carbon to nitrogen atomic ratio
 Weight% Carbon= g carbon/ g sample d.w. (acidified)
 Weight% Nitrogen= g nitrogen/ g sample d.w.
 Atomic weight C= 12.011
 Atomic weight N= 14.007

$$\delta^{13}C_{\text{normalized}} = \delta^{13}C_{\text{untreated}} - 3.32 + 0.99 \times C:N \quad (\text{Equation 3})$$

$\delta^{13}C_{\text{normalized}}$ = Lipid corrected $\delta^{13}C$ values
 $\delta^{13}C_{\text{untreated}}$ = $\delta^{13}C$ values
 C:N= carbon to nitrogen atomic ratio

2.6.2 Total organic carbon

Total organic carbon (TOC) content in sediment samples was determined at the UC Davis stable isotope facility on acidified samples. Acid treatment removes inorganic carbon, permitting calculations of organic carbon normalised contamination concentration in sediments according to equation 4.

$$\text{ConcTOC}_{\text{sediment}} = \text{Conc}_{\text{sediment}} / \text{Fraction}_{\text{TOC}} \quad (\text{Equation 4})$$

ConcTOC_{sediment}= Contaminant concentration in sediments ng/g TOC d.w.
 Fraction_{TOC}= Fraction of TOC in sediments (g organic carbon/ g d.w.)
 Conc_{sediment}= Contaminant concentration in sediments ng/g d.w.

2.6.3 Wet weight and dry weight

When measuring totHg and MeHg concentration in amphipods, lyophilised material was used. Biota was weighed (Mettler Toledo®, AG204 Deltarange) before and after freeze-drying (Leybold-Heraeus GT2 Freeze Dryer with Leybold Vakuum GmbH vacuum pump, Cologne, Germany), thus enabling the opportunity to report contaminant concentration on a w.w. basis as well as d.w. basis. Water content in percent was calculated according to equation 5, and in Appendix B, Table B8 totHg and MeHg are reported on a w.w basis and calculated according to equation 6.

$$\text{Water content \%} = \left(1 - \frac{\text{Sample}_{\text{dry}}}{\text{Sample}_{\text{wet}}}\right) \times 100 \quad (\text{Equation 5})$$

Water content%= water content (%) in the sample

Sample_{dry} (g d.w.) = weight of the sample when dried

Sample_{wet} (g w.w.) = weight of sample prior to freeze-drying

$$\text{Conc}_{\text{wet}} = \text{Conc}_{\text{dry}} \times (1 - (\text{Water content\%/100})) \quad (\text{Equation 6})$$

Conc_{wet}= contaminant concentration in amphipods ng/g w.w.

Water content %= water content (%) in the sample

Conc_{dry}= contaminant concentration in amphipods ng/g d.w.

2.6.4 Fatty acids

Literature values of different FA markers, single, sums or ratios of FAs proportions were used as different indicators of major carbon sources, as is a common practice when studying a complex dataset such as FA compositions (e.g. Budge & Parrish, 1998; Legeżyńska et al., 2014; Søreide et al., 2008) (Table 4 which includes a short explanation of the FA aberration system in the table text). These metrics of major carbon sources were used in correspondence analysis (CA) to aid in interpreting the relative importance of different carbon sources through the season.

Table 4. Overview of summary FA metrics used in the present study together with included FAs, and references. A FA consists of a hydrocarbon chain with a carboxylic acid terminus and a methyl terminus at each end and often containing 14-20 carbons and zero to six double bonds. FAs with no double bonds are known as saturated FAs (SFA), while FAs with one double bond are called monounsaturated FAs (MUFA) and FAs with two or more double bonds are known as polyunsaturated FAs (PUFA) (Budge et al., 2006). The nomenclature to describe different FAs is based on a shorthand system, A:Bn-X. Where A stands for the number of carbon atoms in the molecule, B is the number of double bonds and X represents the location of the first double bond relative to the methyl terminus (Budge et al., 2006). The table is adapted from Legeżyńska et al. (2014) and Kelly and Scheibling (2012).

Summary metrics	FAs included	References
Flagellate metric	\sum C18PUFA and 22:6n-3	(Falk-Petersen et al., 1998)
Flagellate ratio	High 16:0/16:1n-7 ratio (Low 20:5n-3/22:6n-3 ratio)	(Nelson et al., 2001; Reuss & Poulsen, 2002)
Diatom metric	\sum 16:1n-7 and 20:5n-3	(Dalsgaard et al., 2003; Søreide et al., 2008)
Diatom ratio	High 20:5n-3/22:6n-3 ratio (Low 16:0/16:1n-7 ratio)	(Nelson et al., 2001; Reuss & Poulsen, 2002)
Copepod metric	\sum 20:1 and 22:1	(Sargent & Falk-Petersen, 1988)
Macroalgae metric	20:4n-6	Dalsgaard et al. (2003) and references therein
Bacteria metric	\sum 15:0, 17:0 and 17:1	(Findlay et al., 1990; Guckert et al., 1985)
Detritus metric	\sum 18:0 and 18:1n-9	(Mayzaud et al., 2013; Søreide et al., 2008)
Sum of PUFA	Low \sum PUFA (indicating reliance on detritus)	(Søreide et al., 2008)
Terrestrial metric	22:0	Dalsgaard et al. (2003) and references therein
Terr>2.5%	\sum 18:2n-6 and 18:3n-3	(Budge & Parrish, 1998)
18:1n-9*	18:1n-9	

*The FA 18:1-9 have been attributed to indicate starvation, carnivorous feeding and a diet consisting of ciliates/ macroalgae and detritus depending on which organisms are studied, thus this FA might be important to investigate by itself (Graeve et al., 1997; Legeżyńska et al., 2014; Nyssen et al., 2005).

2.6.5 Statistical treatment

All statistical analyses were performed using the statistical software Rstudio (version R version 3.3.1, the R Foundation for Statistical Computing 2016). Statistical treatment was applied to POP congeners in amphipods and sediments on a ng/g w.w. and a ng/g d.w basis, respectively, and totHg and MeHg concentrations in amphipods and totHg concentrations in sediments were analysed on a ng/g d.w. basis. However, when comparing relative contamination of POPs and Hg in amphipods, MeHg and totHg were analysed on a ng/g w.w. basis. Statistical treatment of FAs was on a proportion basis and SI values of nitrogen and carbon (lipid corrected) were treated statically on a per mille (‰) basis.

Outliers were identified by Cooks distance. In the POP analysis in amphipods, sample April1C, and in MeHg analysis in amphipods, sample June1B, were identified as outliers and were not included in the statistical treatment of the data. The sample June1C in totHg analysis in sediment samples was identified as an outlier and excluded. Furthermore, one MeHg data point (April2C) was above the totHg concentration in the same sample, and the biomass used was very low, thus the reliance on this data point was low.

Data below the limit of detection

Limit of detection (LOD) is the lowest concentration of the analyte that can be quantified with reasonable certainty (Cazes, 2004). At NIVA, the LODs were determined as the concentration of the analyte in the blank plus three times the standard deviation. How LOD was determined for FA and MeHg was not given, and for Hg, the detection limit of the instrument was 0.05 ng Hg. Samples with lower concentrations than LODs are called non-detects, and instead of being point measurements, they are reported as being between 0 and LOD (Baccarelli et al., 2005). If non-detects are included in the dataset, they need to be dealt with in a correct manner to avoid alien patterns being incorporated (Helsel, 2010). There are several techniques available to treat non-detects, however there are both advantages and limitations to all of these methods (Baccarelli et al., 2005). In the current study, a distribution-based multiple imputation method was used to produce and substitute non-detects. This method draws values from an assumed underlying parametric distribution, however, it is robust to moderate departures from this assumption and uncertainty is taken into account, due to multiple imputations (Baccarelli et al., 2005). The distribution-based multiple imputation method attempts to fit a parametric distribution to the data, thus preserving the relationship within the original data set. From this fitted distribution curve values for non-detects are drawn and replaced, conditioned to be between 0 and LOD, resulting in a complete dataset (Baccarelli et al., 2005). Since this method is a multiple imputation procedure, it draws substitute numbers multiple times, thereby creating multiple datasets. From these datasets, parameter estimates and covariance are calculated, combined and the total variance of the final estimate is computed (Baccarelli et al., 2005).

In the distribution-based multiple imputation method, an investigation of the beta distribution shape parameter α -values ($\beta=1$) was conducted on how well it fitted the dataset distributions of POP congener concentrations in amphipod samples (imputation set to 1000 times). After choosing an α -value that explained the most variation, this was used to create a parametric distribution. From this parametric beta distribution, values were drawn and used to substitute non-detects from an imputation algorithm, where imputation was set to 1000 times, lastly creating one dataset containing substituted values.

In the present study, there was 78-100% detection of POP congeners in amphipod samples, and all congeners were included in further investigations. Sediment samples did not contain

any non-detects for POPs. For amphipod POP concentrations, 3 out of 271 (1%) were substituted using the distribution-based multiple imputation method (* indicates substituted values in Table 7). The LODs are included in Appendix B, Table B9. Each matrix (amphipods and sediments) had mercury concentrations above LOD in all samples.

Univariate analysis

The datasets were checked for normality and heteroscedasticity, which are assumptions that need to be satisfied for using parametric two-sample t-tests, linear regression models and one-way analysis of variance (ANOVA) (Whitlock & Schluter, 2015). These assumptions were assessed graphically using boxplots, normal q-q plots and diagnostic plots of the residuals. Often, no formal tests (e.g. Shapiro Wilk's test or Levene's test) for checking normality, nor heteroscedasticity were possible in the current study due to small sample sizes ($n=2-8$), which result in these tests having low power⁴. When assumptions were not met, log10 or square root transformation of the data was conducted to reduce the deviations. However, if neither assumptions were met after transformation, and if the distribution of the data did not have similar shapes, comparisons were instead made by studying 95% t-distribution based confidence intervals or only visual trends (Whitlock & Schluter, 2015). If only the heteroscedasticity assumption was not met, a nonparametric test called Welch ANOVA (Welch's F-test) (Welch, 1947) or two-sample Welch's t-test (Welch's t-test) (Welch, 1938) were used when assessing differences between more than two groups or between two groups, respectively (Whitlock & Schluter, 2015). Welch's ANOVA is robust against unequal sample sizes and testing averages between groups (2-5) against an increase in type I error⁵ (Moder, 2010), with the statistical significance level set to $p=0.05$. Nonparametric Games Howell posthoc test was used after Welch's ANOVA, to investigate which of the groups were different from one another. Statistical significance was set to $p=0.05$.

Linear regression models

Linear regression has the same assumptions as ANOVA and t-tests, and therefore datasets were tested for violations of normality and homoscedasticity of variance as described above when met, the strength of linear association was also investigated with Pearson's correlation

⁴ Power is the probability of discarding a false null hypothesis (Whitlock & Schluter, 2015).

⁵ Type I Error is rejecting a true null hypothesis, and a Type II Error is accepting a false null hypothesis (Whitlock & Schluter, 2015).

coefficient. When assumptions were not met, correlations were investigated with the nonparametric Spearman's rank correlation test (Whitlock & Schluter, 2015). When studying correlations, sampling date was transformed to a continuous variable in units of Julian date calendar (AAVSO, 2017). Spearman's rank correlation (ρ), which is based on ranks, measures the strength and direction of a monotonic relationship between the explanatory and response variable. If ρ values are 1 or -1, this indicates perfectly correlated explanatory and response variables, meaning that the explanatory variable explains all the variation in the response variable. The closer ρ is to 0 the less correlated are the variables, and hence, less of the variation in the explanatory variable is explained (Whitlock & Schluter, 2015).

Multiple linear regression models with backwards model selection based on p-values were used to examine whether the explanatory variables could explain the variation in the response variables (log10 transformed) totHg and MeHg (ng/g d.w.) in amphipods. The explanatory variables included; lipid content%, TOC%, station (2 levels; City and North), sediment temperature (°C), $\delta^{13}\text{C}$ (‰), $\delta^{15}\text{N}$ (‰), sediment concentrations of totHg (ng/g d.w.), %TFA where %TFA is percent of total fatty acid of flagellate-, bacteria-, diatom-, macroalgae-, detritus-, terrestrial- and copepod summary metric. In addition, multiple linear regression model with backwards model selection based on p-values was used to examine whether the variation in the response variable (log10 transformed) totHg (ng/g d.w.) in sediments could be explained by the explanatory variables; sediment type (three levels; sand, mud, fine sand), sediment temperature (°C), TOC%, month (5 levels; April, May, June, July and August) and station (2 levels; City and North).

Multivariate statistics

PCA and RDA

Using the vegan package (Oksanen et al., 2017) in R, principal component analysis (PCA) was used to interpret the POP congener dataset visually, and redundancy analysis (RDA) was used for hypothesis-testing by constraining the ordination with explanatory variables (Greenacre & Primicerio, 2013). In PCA and RDA, datasets containing rows (sample units) and columns (response variables) (contingency table) are used to construct an ordination by collapsing the variation of a large multivariate dataset (with n-dimensional rooms) into a low-dimensional space, that, ideally, accounts for most of the variation (show the main structure in the dataset) by means of linear regression (Palmer et al., 2008; Sparks et al., 1999). The axes in the low dimensional space are called principal components (PCs). In fact, PCA and RDA

create as many axes, or rather PCs, as there are response variables, however, they explain different amounts of variation and are orthogonal. The first PC (PC1) explains the maximum amount of variation found in the dataset, and the subsequent PCs explain sequentially smaller variations (Bro & Smilde, 2014). Variation associated with PCs are expressed as eigenvalues, and eigenvalues are fractions of the total variation (also called inertia) explained by the axes.

A PCA is an exploratory (unconstrained) method that only uses response variables to calculate the site scores (sample units) and vector heads (response variables) in the ordination space (Sparks et al., 1999). Explanatory variables can be projected passively on top of the ordination as arrows (continuous variables) or as class centroids (categorical variables) to interpret relationships between explanatory and response variables visually. The vectors and arrows in the ordination space point in the direction of maximum change with that variable, and with the length being proportional to the rate of change. The degree of correlation between the vectors is indicated by the cosine of the angles between the vectors, with smaller cosines indicating a higher correlation. Orthogonal vectors are not correlated. Class centroids are placed passively on top the ordination at their "weighed" average location in the ordination space (Greenacre & Primicerio, 2013; Oksanen et al., 2017). Right angle projection of centroids onto vectors suggest the degree of correlation. PCA is usually displayed as a biplot (site scores and vector) or as a triplot (site scores, vector and arrows) by extracting the two first PCs and plotting them against each other (Sparks et al., 1999).

RDA is a hypothesis testing (constrained) method, where explanatory variables together with response variables are accounted for in multivariate linear regression of the ordination itself (Greenacre & Primicerio, 2013; Palmer et al., 2008). This means that the response inertia (the variance in the model) can be separated into two types, one constrained and one unconstrained inertia. The constrained inertia is linearly related to the explanatory variables, and the unconstrained is unrelated to the explanatory variables. The constrained inertia, thus variance explained by the model, is the variation that decomposes to PC axes (Greenacre & Primicerio, 2013). Put in another way, in an RDA, the axes are constrained by explanatory variables, unlike PCA, and the variation accompanied with each axis are the variation that can be explained by the constraining variables (Palmer et al., 2008). Using AIC (Akaike information criterion) values and p-values from Monte Carlo permutation test (1999) in forward model selection, significant explanatory variables that account for most of the constrained variation can be found, and hence, the best model. Furthermore, by conditioning

explanatory variables of interest, it is possible to exclude the variation coming from that variable in the analysis.

Prior to analysis, the POP congener dataset from the current study was transformed by adding one and taking the logarithm with base 10 (\log_{10}) of the concentration values to fit the assumption of linearity that both PCA and RDA assume. POP congeners in amphipods and sediments were analysed separately. Continuous explanatory variables (not those on a percentage basis) are standardised with the average of the variable. In the PCA and RDA using sediments, explanatory variables; sediment type (three levels; sand, mud, fine sand), sediment temperature ($^{\circ}\text{C}$), TOC%, month (five levels; April, May, June, July and August) and station (2 levels; City and North) were used. TOC% was also used as a conditioning factor. Significant explanatory variables were found using AIC values and permutations test (999) in forward model selection. In the PCA using sediment samples, two main clusters of POP congeners were formed. From these clusters, two POP congeners (PCB-52 and -153) variables were chosen to be used in the PCA and RDA of amphipods as explanatory variables to investigate if the two main POP patterns in sediments could explain POP congener variation in amphipods. In the PCA and RDA using amphipods, explanatory variables; lipid content%, TOC%, month (5 levels; April, May, June, July and August), station (2 levels; City and North), sediment temperature ($^{\circ}\text{C}$), $\delta^{13}\text{C}$ (‰), $\delta^{15}\text{N}$ (‰), sediment concentrations of PCB-52 and -153 (ng/g d.w.), flagellate-, bacteria-, diatom-, macroalgae-, detritus-, terrestrial- and copepod metric (% TFA) were used. Lipid% was also tested as a conditioning factor. Significant explanatory variables were found using AIC values and permutations test (999) in forward model selection. Note that only significant explanatory variables in the RDA were visualised in the PCA.

CA and CCA

Correspondence analysis (CA) and canonical correspondence analysis (CCA) are statistical methods, analogous to PCA and RDA respectively, for interpretation of datasets visually (CA), and for hypothesis-testing by constraining the ordination with explanatory variables (CCA) (Greenacre & Primicerio, 2013). CA and CCA methods, likewise to PCA and RDA, construct an ordination by collapsing the variation of a large multivariate dataset (with n -dimensional rooms) into a low-dimensional space, that, ideally, accounts for most of the variation (show the main structure in the dataset) (Greenacre & Primicerio, 2013). CA and CCA also produce eigenvalues as a measure of how much of the total variance can be

attributed to each axes and explanatory variables are applied as explained above. Important differences are that CA and CCA analyses the differences between relative values, thus suitable for FA compositional data and while PCA and RDA are based on Euclidean distances, CA and CCA are based on Chi-square distances.

Using the *vegan* package (Oksanen et al., 2017) in R, CCA was performed on FA compositional profiles (% TFA) in amphipods and with the explanatory variables month (5 levels; April, May, June, July and August), $\delta^{13}\text{C}$ (‰) and $\delta^{15}\text{N}$ (‰) in amphipods. The significant explanatory variable month was found using AIC values and permutations test (999) in forward model selection. Note that all explanatory variables in the CCA were visualised in the CA.

3 Results

3.1 Dietary descriptors

FATMs and $\delta^{13}\text{C}$ values indicated contributions of pelagic primary and secondary production, bacteria, terrestrial- and macroalgae-derived detrital material in the diet of *G. setosus*. Still, distinct seasonal signals were seen in *G. setosus*, particularly for utilisation of diatom dominating phytodetritus in May-July. $\delta^{15}\text{N}$ values in amphipods decreased from April to August.

3.1.1 $\delta^{13}\text{C}$ values

The $\delta^{13}\text{C}$ values did not differ in amphipods between the stations for each sampling month, thus values from different stations were pooled (Appendix C, Figure C1). The seasonal $\delta^{13}\text{C}$ values ranged from -18.9‰ to -22.0‰ and displayed a concave pattern of higher values in May, June and July and lower values in April and August (Figure 4, Table 5), with higher $\delta^{13}\text{C}$ in amphipods collected in June than in August (Welch ANOVA; $p=0.03$, followed by Games Howell post-hoc test; May-April: $p=0.2$, June-April: $p=0.1$, July-April: $p=0.6$, August-April: $p=0.8$, June-May: $p=1.0$, July-May: $p=0.4$, August-May: $p=0.07$, July-June: $p=0.3$, August-June: $p=0.04$, August-July: $p=0.2$).

Pelagic, river and sediment POM $\delta^{13}\text{C}$ values were intermediate relative to macroalgae and amphipods samples which were more enriched, while terrestrial material and detritus were the most depleted (Figure 4). Red and brown macroalgae $\delta^{13}\text{C}$ values were greater than for green macroalgae and microphytobenthos (Figure 4). In amphipods, $\delta^{13}\text{C}$ values were inbetween red and brown macroalgae and the remaining samples (Figure 4).

Pelagic POM showed a similar seasonal pattern in $\delta^{13}\text{C}$ values as in amphipods, and with higher values in May compared to April (Appendix C, Figure C2). Although, no correlation was found between amphipods and pelagic $\delta^{13}\text{C}$ values (Spearman's rank-order correlation; $p=0.33$, $\rho=0.8$). The seasonal change in $\delta^{13}\text{C}$ values in sediment and river POM were minimal; <1‰ and 1.4‰, receptively (Appendix C, Figure C2). No positive correlations were found between seasonal $\delta^{13}\text{C}$ values between amphipods and river or sediment POM,

indicating no relationship (Spearman's rank-order correlation; river POM: $p=0.0012$, $\rho=-0.67$, sediment POM: $p=0.45$, $\rho=-0.5$).

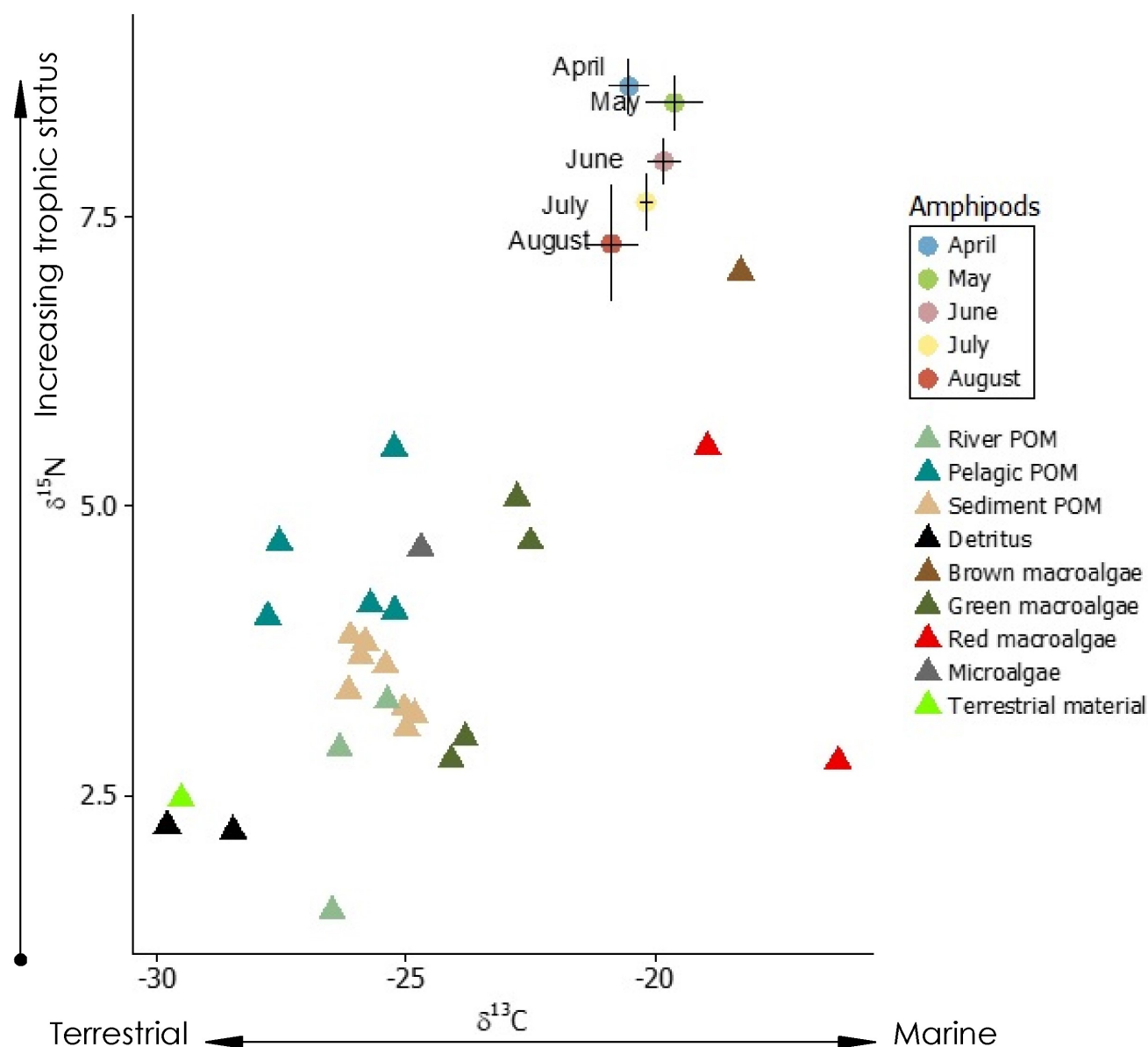


Figure 4. Stable isotope biplot displaying signatures of $\delta^{13}\text{C}$ versus $\delta^{15}\text{N}$ values in amphipods (April/June/August; $n=8$, July; $n=6$, May; $n=4$), sediment POM (April/June/August; $n=2$, July/August; $n=1$), pelagic POM (April; $n=2$, May/June/August; $n=1$), river POM (May/June/August; $n=1$) and potential food sources ($n=1$) to the amphipods. Circles represent the average value of $\delta^{13}\text{C}$ and $\delta^{15}\text{N}$ signatures and the error bars represent 95% confidence intervals in amphipod samples.

3.1.2 $\delta^{15}\text{N}$ values

The $\delta^{15}\text{N}$ values in amphipods did not differ between stations from April to July, however, $\delta^{15}\text{N}$ from the City was higher than North in August (Appendix C, Figure C1). Thus, $\delta^{15}\text{N}$ values in amphipods from different stations were pooled for the months April to July.

However, to maintain consistency, August samples were likewise pooled. The seasonal $\delta^{15}\text{N}$ pattern showed decreasing values from April to August (Figure 4, Table 5) (Spearman's rank-order correlation: Season; $p=2.4\text{e}^{-10}$, $\rho=-0.85$).

Table 5. Overview of $\delta^{13}\text{C}$ and $\delta^{15}\text{N}$ values (‰) in amphipods, sediment POM, pelagic POM, river POM, potential food sources and total lipid content (% w.w.) measured in amphipods during FA analysis. Number of replicates are indicated in parentheses. Asterisk (*) indicates values from McGovern et al. (in prep). Number Asterisk (**) indicates samples collected from station F1 (Figure 1) (McGovern et al., in prep).

Amphipods Month	$\delta^{13}\text{C}$ (‰) average \pm sd	$\delta^{15}\text{N}$ (‰) average \pm sd	lipid content (% w.w.) average \pm sd
April	-20.5 \pm 0.6 (8)	8.6 \pm 0.4 (8)	2.2 \pm 0.4 (6)
May	-19.6 \pm 0.6 (4)	8.5 \pm 0.2 (4)	3.3 \pm 0.6 (3)
June	-19.8 \pm 0.5 (8)	8.0 \pm 0.3 (8)	3.2 \pm 0.6 (3)
July	-20.2 \pm 0.1 (6)	7.6 \pm 0.3 (6)	3.8 \pm 0.9 (5)
August	-20.8 \pm 0.8 (8)	7.3 \pm 0.2 (8)	2.4 \pm 0.6 (6)
Sediment POM Month	$\delta^{13}\text{C}$ (‰) average \pm sd	$\delta^{15}\text{N}$ (‰) average \pm sd	
April	-25.8 \pm 0.5 (2)	3.5 \pm 0.2 (2)	
May	-25.8 (1)	3.8 (1)	
June	-25.6 \pm 0.8 (2)	3.6 \pm 0.4 (2)	
July	-24.8 (1)	3.2 (1)	
August	-25.5 \pm 0.6 (2)	3.4 \pm 0.4 (2)	
River POM*			
Month	$\delta^{13}\text{C}$ (‰)	$\delta^{15}\text{N}$ (‰)	
May	-26.5 (1)	1.5 (1)	
June	-25.8 (1)	2.9 (1)	
August	-25.4 (1)	3.3 (1)	
Pelagic POM			
Month	$\delta^{13}\text{C}$ (‰) average \pm sd	$\delta^{15}\text{N}$ (‰) average \pm sd	
April	-25.5 \pm 0.1 (2)	4.2 \pm 0.1 (2)	
May**	-22.7 (1)	5.5 (1)	
June**	-25.7 (1)	4.7 (1)	
August**	-25.2 (1)	4.1 (1)	
Potential food sources			
Samples	$\delta^{13}\text{C}$ (‰)	$\delta^{15}\text{N}$ (‰)	Month
Red macroalgae (<i>Palmaria palmate</i>)	-19.0 (1)	5.5 (1)	April
Red macroalgae (<i>Palmaria palmate</i>)	-16.3 (1)	2.8 (1)	May
Green macroalgae (<i>Ulva</i> spp.)	-22.5 (1)	4.7 (1)	April
Green macroalgae (<i>Acrosiphonia</i> spp.)	-23.8 (1)	3.0 (1)	April
Green macroalgae (<i>Ulva</i> spp.)	-24.1 (1)	2.8 (1)	April
Green macroalgae (<i>Ulva</i> spp.)	-22.8 (1)	5.1 (1)	May
Brown macroalgae (<i>Laminaria digitata</i>)	-18.3 (1)	7.0 (1)	April
Detritus	-28.5 (1)	2.2 (1)	July
Detritus	-29.8 (1)	2.2 (1)	August
Terrestrial material	-29.5 (1)	2.5 (1)	July
Microalgae (Microphytobenthos)	-24.7 (1)	4.6 (1)	August

$\delta^{15}\text{N}$ values in amphipods ranged between 6.6‰ to 9.1‰ and were higher than all potential food sources which showed a large variation in $\delta^{15}\text{N}$ values, from 7.0‰ in brown macroalgae in April to 2.2‰ in detritus in August (Figure 4, Table 5). Brown and red

macroalgae collected in April had $\delta^{15}\text{N}$ values ranging from 5.5-7.0‰, being closer to amphipods (Figure 4, Table 5). The same species of red macroalgae (*Palmaria palmate*) was collected in both May and April and had a low $\delta^{15}\text{N}$ of 2.8‰ in May. Pelagic and sediment POM samples displayed a general decreasing pattern of $\delta^{15}\text{N}$ values as the season progressed, however, the values changed very little, 1.4‰ and 0.8‰ for pelagic and sediment POM, respectively (Appendix C, Figure C2). Positive correlations were found between seasonal $\delta^{15}\text{N}$ values in amphipods and pelagic and sediment POM (Spearman's rank-order correlation; pelagic POM: $p=0.05$, $\rho=0.36$, sediment POM: $p=0.002$, $\rho=0.54$).

3.1.3 Fatty acids

Overall, 38 FAs were quantified above LOD in the amphipod samples. The dominating FAs found in *G. setosus* throughout the season were 16:0, 16:1n-7c, 18:1n-9c, 20:5n-3 and 22:6n-3 (Figure 5, Appendix B, Table B10). Together these FAs constituted an average of almost 70% of the total fatty acids (Appendix B, Table B10). The multivariate correspondence analysis of the amphipod FA profiles (% TFA) extracted two axes (CA1 and CA2), which accounted for 69.8% of the total variation in the data set (Figure 5). Modell selection using canonical correspondence analysis with month, $\delta^{15}\text{N}$ and $\delta^{13}\text{C}$ as explanatory variables showed that month significantly explained 64.2% of the total constrained variation in the model (CCA, permutation tests 999, $p=0.001$).

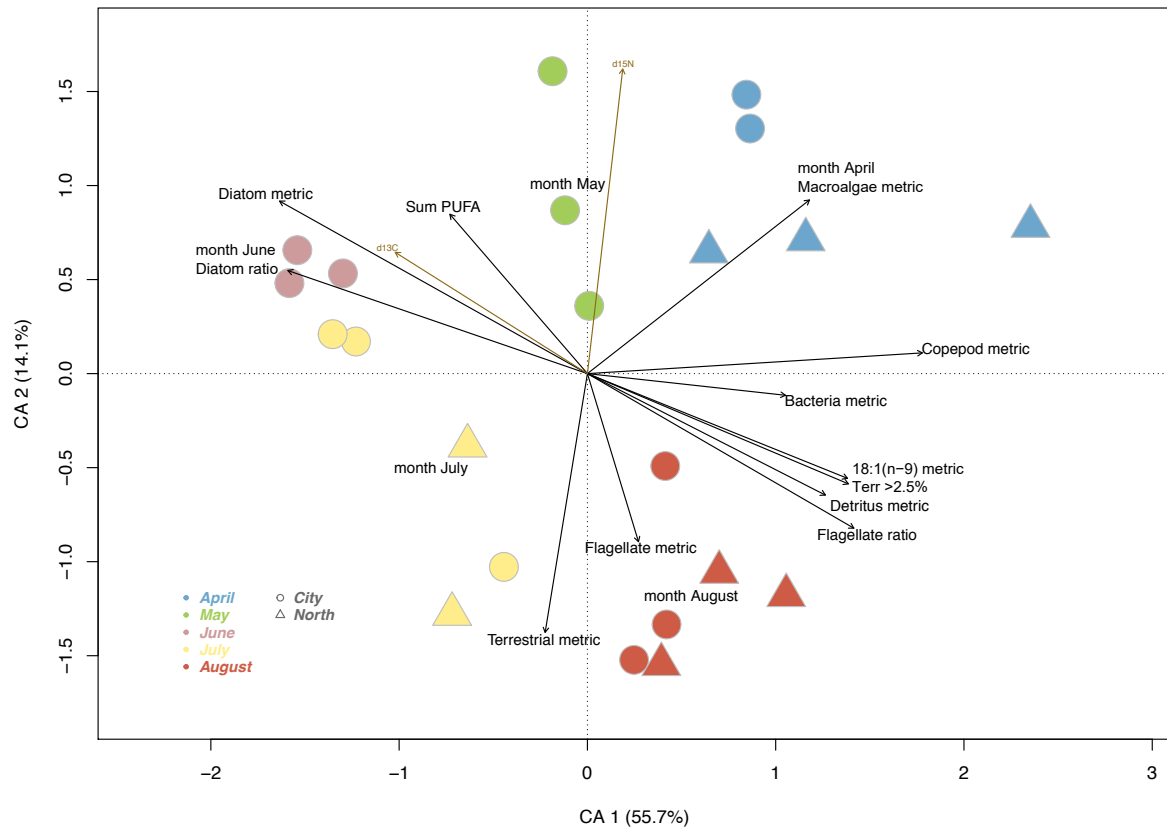


Figure 5. Correspondence analysis plot of correlations between FA composition (% TFA) in amphipod samples (n=22). The site scores represent individual amphipod samples. The significant categorical variable month is placed passively on top of the ordination as a black centroid and the summation FA metrics are visible as black arrows. Meanwhile, insignificant $\delta^{15}\text{N}$ and $\delta^{13}\text{C}$ are placed passively on top of the ordination as brown arrows. The shape and colour of the points represent station and month, respectively. Note that there were no amphipod samples collected in May or June from the North station. The variance explained attributed to each CA axis is given in % on both axis in the figure. An outlier (April1b), identified by Cooks distance, was excluded.

The pattern of FATM inferred from CA showed a seasonal shift in dietary components where April and August separated from May, June and July samples due to higher contributions of copepod (Σ 20:1 and 22:1 MUFAs), bacteria (Σ 15:0, 17:0 and 17:1), flagellate (Σ C18PUFA and 22:6n-3), 18:1n-9 FA, terr>2.5% (Σ 18:2n-6 and 18:3n-3) and detritus (Σ 18:0 + 18:1n-9) summary metrics in April and August (Figure 5 and 6, Appendix C, Figure C3). Amphipods from April and August exhibited differences such as higher reliance on macroalgae in April and a slightly higher contribution of detritus (high detritus metric and low sum PUFA) in August (Figure 5 and 6, Appendix C, Figure C3).

In May, June and July, amphipods had a higher relative contribution of diatoms as a dietary signal, with June amphipods being highest (diatom metric; Σ 16:1n-7, C16PUFA and

20:5n-3) (Figure 5 and 6, Appendix C, Figure C3). The terrestrial FA (22:0) was higher in July and August than in April, May and June. Stable isotope values for carbon were highest in June and correlated with the diatom metric, whereas $\delta^{15}\text{N}$ were highest in amphipods in April and May (Figure 5).

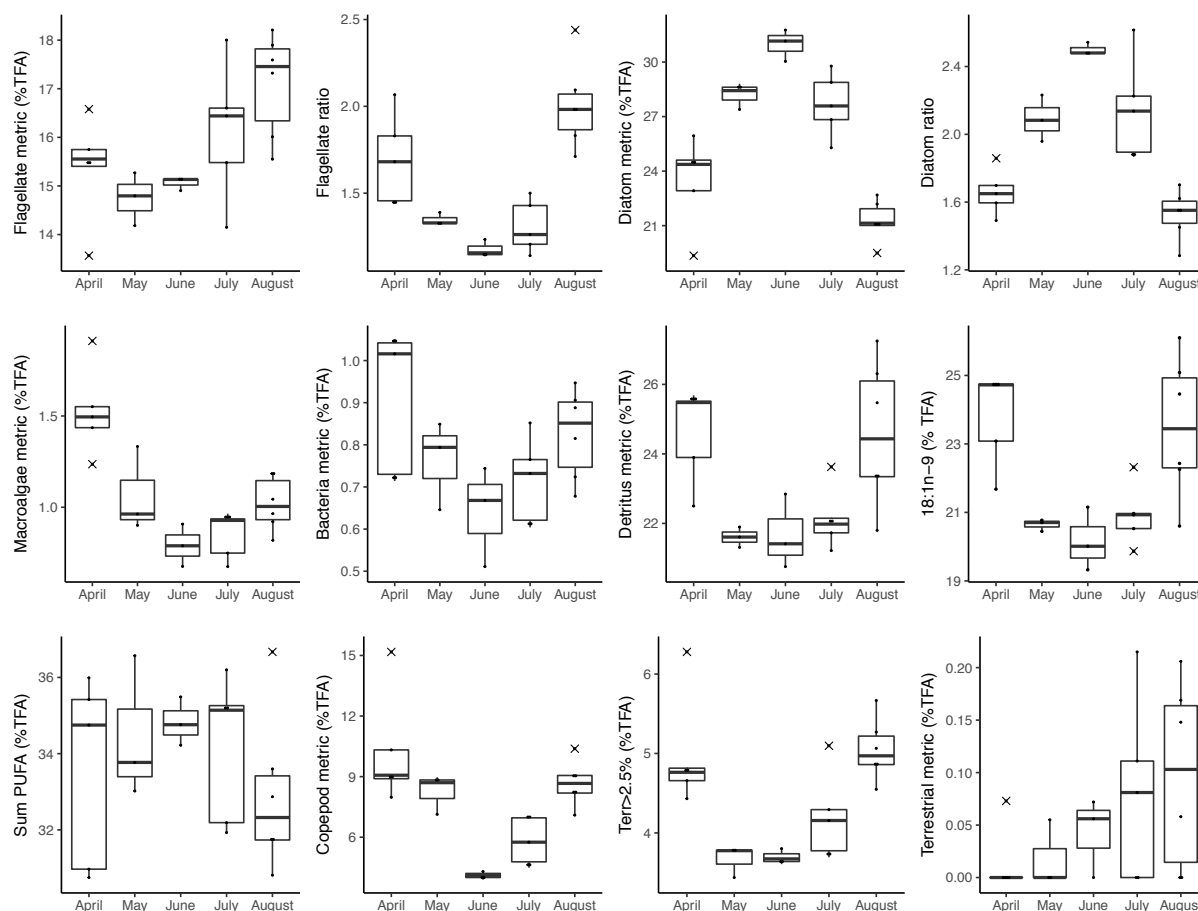


Figure 6. Boxplots of seasonal FA summary metrics (% TFA) in amphipods. Top row from left to right; Seasonal changes in the flagellate summary metrics (% TFA), the flagellate ratio, the diatom summary metrics (% TFA) and the diatom ration. Middle row from left to right; Seasonal changes in the macroalgae summary metrics (% TFA), bacteria summary metrics (% TFA), the detritus summary metrics (% TFA) and the 18:1n-9 FA (% TFA). Bottom row from left to right; Seasonal changes in the sum PUFA (% TFA), copepod summary metrics (% TFA), the Terr>2.5% (% TFA) and the terrestrial summary metric (% TFA). August; n=6, April/July; n=5, May/June; n=3. The acronym %TFA stands for percent of total fatty acid. Data presented as median (line drawn in the middle of the box), quartiles (upper and lower lines of the box), 10-90 percentiles (whiskers) and influential data points (indicated as a cross). An outlier, (April1b), identified by Cooks distance, was excluded.

3.2 Lipids

Total lipid content (% w.w.) did not differ in amphipods between the stations for each sampling month, thus values from different stations were pooled (Welch's t-test; April: p= 0.2, July: p= 0.45, August: p= 0.94) (amphipods in May and June were only collected from

the City station). The seasonal pattern of total lipid content was lowest in April and August and higher in May–July (Figure 7), however no differences in lipid content were found between the months (Games Howell post-hoc test; May-April: $p=0.21$, June-April: $p=0.21$, July-April: $p=0.07$, August-April: $p=0.9$, June-May: $p=1.0$, July-May: $p=0.9$, August-May: $p=0.3$, July-June: $p=0.8$, August-June: $p=0.3$, August-July: $p=0.1$).

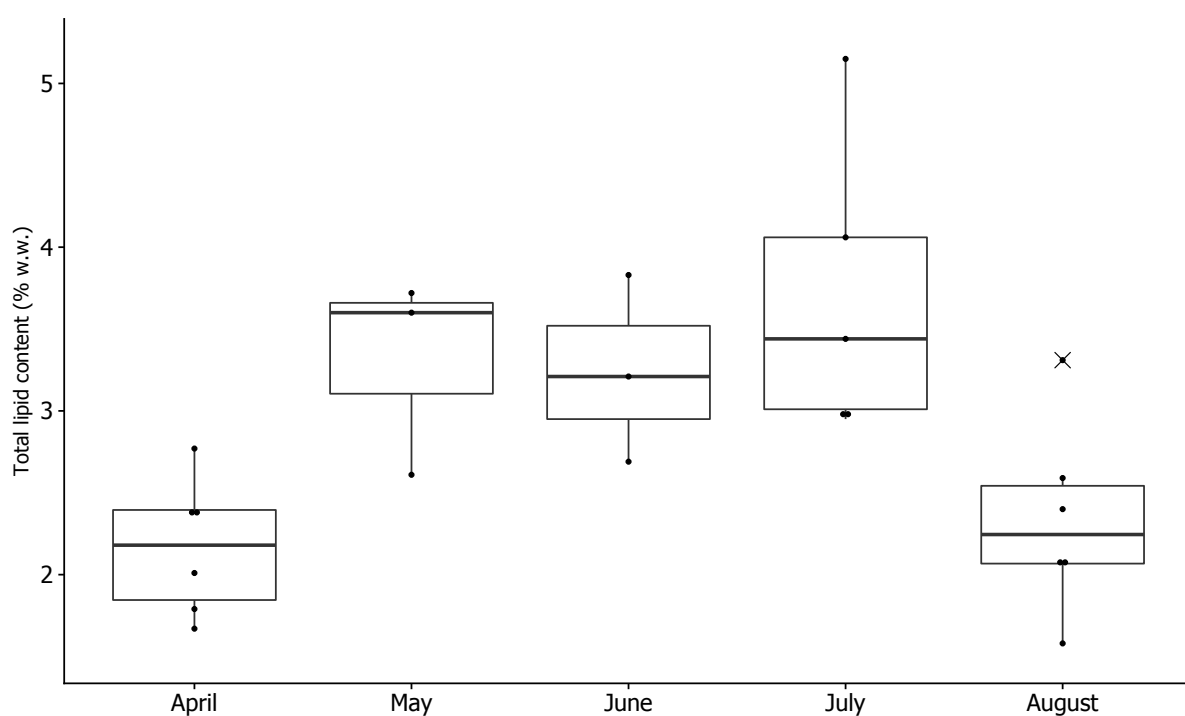


Figure 7. Boxplot of total lipid content (% w.w.) in amphipods between months. April/August; $n=6$, July; $n=5$, May/June; $n=3$. Data presented as median (line drawn in the middle of the box), quartiles (upper and lower lines of the box), 10-90 percentiles (whiskers) and influential data points (indicated as a cross).

3.3 Contaminant concentrations

In sediment samples, HCB was the dominating congener (17-41%) among the POPs, with an average concentration of 69 pg/g d.w., followed by PCB-52 (8-24%) and PCB-153 (4-18%), which had an average concentration of 42 and 37 pg/g d.w., respectively. The overall contamination burden at the City station increased seasonally, while it decreased at the North station. TotHg concentrations in sediments were, on average, 130 times higher than the sum of POPs, and changed both temporally and spatially, appearing to follow TOC%.

Among the POP congeners in amphipod samples, HCB was the overall dominating compound (25-51%) with an average concentration of 258 pg/g w.w., followed by PCB-153 (17-28%)

which had an average value of 132 pg/g w.w.. HCB concentration measured highest in amphipods collected in May and June, while PCB-153 was highest in April. The overall contamination burden decreased seasonally at both the City and North station. TotHg and MeHg concentrations in amphipods, were, on average, eight times higher than the sum of POPs, and overall exhibited a seasonal decrease at both stations.

3.3.1 Persistent organic pollutants in sediments

The first two principal components (PC1 and PC2) from the multivariate principal component analysis on POP concentrations (ng/g d.w.) in sediment samples accounted for 95% of the total variation in the data set (Figure 8). Modell selection using redundancy analysis with sediment type, sediment temperature, TOC%, month and station as explanatory variables, resulted in two significant explanatory variables; station and sediment type. The best model explained 58.14% of the total constrained variation in the model (RDA, permutation tests 999, $p=0.011$). The significant variables station and sediment type explained 24.8% and 2.3% of the constrained variation, respectively.

Two main “clusters” of congeners were found among the response loadings, in which cluster 1 consisted of PCB-180, -153, -138, -101 and PeCB and cluster 2 consisted of PCB-118, -28, -52 and HCB (Figure 8). Cluster 1 congeners increased in concentrations along PC1, showing higher concentrations in sediments from City compared to North, in all months (Table 6). Furthermore, the difference in cluster 1 congeners between the stations increased as the season progressed, with the contamination concentration gradually increasing in City samples, and gradually decreasing at North station resulting in a large difference in August (Σ Cluster1 City; 285 pg/g d.w., North; 38.0 pg/g d.w.) (Figure 8, Table 6). In sediments from April, the difference between City and North in cluster 1 congeners (Σ Cluster1) was small (Figure 8, Table 6).

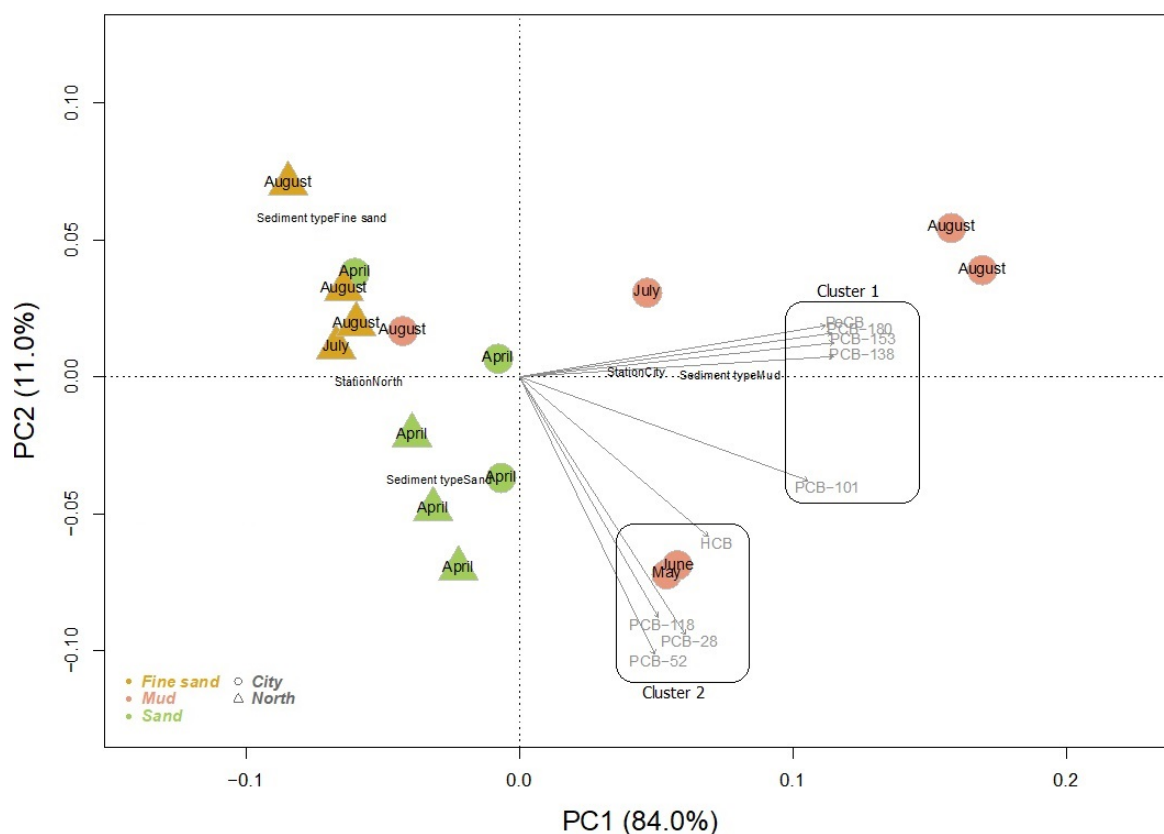


Figure 8. Principal component analysis triplot of correlations between log10 transformed POP concentrations (ng/g d.w.) (grey response loadings/vectors) in sediment samples (n=16) with significant categorical explanatory variables placed passively on top of the ordination as black centroids. The site scores represent individual sediment samples, with shape and colour representing station and type of sediment, respectively. Note that from the North station there were no sediment samples collected in May or June. The variance explained attributed to each PC axis is given in % on both axis in the figure.

Cluster 2 congeners increased in concentrations along decreasing PC2, highlighting different seasonal patterns in sediments between stations (Figure 8). Highest concentrations of cluster 2 compounds were found in sediments collected in May and June from the City station (no North samples from May and June) (Σ Cluster 2; 207 and 200 pg/g d.w respectively). Sediments from North decreased gradually as the season progressed with the lowest cluster 2 concentrations found in August (Figure 8, Table 6).

Sediments from City station in May to August were described as muddy and showed higher POP concentration than fine sand from the North station or sand sediments in April. Lower POP concentrations were found in fine sand (July and August from the North station) compared to sandy sediments (Figure 8, Table 6). Thus, the relationship between these

explanatory levels can be summarised accordingly; Mud (Σ POPs 390 pg/g d.w.) > sand (Σ POPs 230 pg/g d.w.) > fine sand (Σ POPs 130 pg/g d.w.) (Table 6).

Table 6. Overview of POP (pg/g d.w.) concentrations, totHg (ng/g d.w.) concentrations and TOC (%) in sediment samples. Letter A-D indicates replicate. Note that not all replicates were analysed for all analyses, and these are shown as empty boxes in the table below. TOC% has been calculated from SI analysis on pooled samples of sediments.

Station	Month and replicate	PeCB pg/g d.w.	HCb pg/g d.w.	PCB- 28 pg/g d.w.	PCB- 52 pg/g d.w.	PCB- 101 pg/g d.w.	PCB- 118 pg/g d.w.	PCB- 138 pg/g d.w.	PCB- 153 pg/g d.w.	PCB- 180 pg/g d.w.	totHg ng/g d.w.	TOC %
City	April											
	A										44.7	
	B	29.2	65.0	12.5	35.4	25.4	11.3	23.6	31.3	14.2	33.1	
	C	14.3	53.5	6.90	20.4	11.7	5.70	8.90	10.7	4.50	34.5	
	D	20.2	77.3	16.7	47.5	28.7	14.9	24.7	30.6	13.3	28.4	
	Pooled											1.14
	May											
	A										35.9	
	B										455	
	C										42.9	
	D										39.5	
	Pooled	46.0	106	24.7	60.8	39.1	15.5	36.5	50.0	27.5		1.53
	June											
	A										75.9	
	B										57.9	
	C										62.0	
	D										57.9	
	Pooled	40.9	90.2	24.8	66.1	42.5	18.5	42.8	52.4	32.5		1.92
	July											
	A										48.0	
	B										31.1	
	C										41.1	
	D										40.7	
	Pooled	50.8	70.5	15.4	32.7	28.4	8.01	41.0	56.0	29.5		1.66
	August											
	A										37.0	
	B	25.3	77.3	7.50	22.0	13.9	6.01	10.2	12.9	6.10	33.1	
	C	97.3	82.5	17.5	43.4	52.5	12.6	76.2	112	60.1	34.4	
	D	72.3	62.6	16.6	39.5	55.5	16.5	84.4	111	67.0	35.9	
	Pooled											1.27
North	April											
	A	15.1	55.1	15.7	44.6	27.5	15.4	14.5	16.8	4.50	31.5	
	B	12.3	51.2	21.3	58.1	33.1	19.5	18.0	20.2	5.01	28.7	
	C										37.1	
	D	15.2	62.1	23.6	63.5	36.3	21.1	19.8	21.1	5.80	31.0	
	Pooled											0.87
	June											
	A										25.5	
	B										26.2	
	C										23.9	
	D										23.4	
	Pooled											0.60
	July											
	B										25.6	
	D										20.9	
	Pooled	11.8	43.6	13.3	34.7	16.8	7.20	5.40	6.40	1.10		0.41
	August											
	A	15.6	59.8	9.60	24.8	14.4	6.50	7.20	8.60	2.50	25.8	
	B										30.6	
	C	11.6	53.7	7.90	19.7	15.3	8.50	7.60	8.90	2.01	22.1	
	D	6.90	35.6	4.70	10.5	6.90	3.40	3.30	4.01	1.10	28.3	
	Pooled											1.46

3.3.2 Total mercury in sediments

Backwards model selection using a linear regression model on totHg concentrations in sediments and with sediment type, sediment temperatures, TOC%, month, and station as explanatory variables, resulted in two significant explanatory variables; TOC% and station. The best model explained 62.6% of the total variation in the totHg concentration data set (lm; $R^2 = 0.62$, $p = 3.9 \times 10^{-7}$). The significant variables TOC% and station explained 54.6% and 8.0% of the variation in the model, respectively.

TotHg concentrations measured in sediments ranged from 22.1 to 75.8 ng/g d.w. (Table 6). There was a higher concentration of totHg in sediments from City than North, with average values of 42.2 and 27.2 ng/g d.w., respectively (Welch's t-test; $p\text{-value} = 3.5 \times 10^{-5}$). Furthermore, there was a positive relationship between TOC% and totHg concentrations in sediments from the City station, with higher concentrations of totHg with higher levels of TOC% (Spearman's rank-order correlation; $p=0.002$, $\rho=0.7$) (Figure 9). However, this correlation was not seen between TOC % and totHg in sediments from the North station (Spearman's rank-order correlation; $p=0.1$, $\rho=0.4$). At the North station, there was a concave pattern, with the highest totHg concentration around 0.87% TOC (Figure 9). However, when comparing how TOC% and totHg concentration change seasonally, there appears to be a similar pattern of change. Although in April TOC% values were lower than August, the concentration of total mercury was higher in April than in August, resulting in low a correlation (Figure 9).

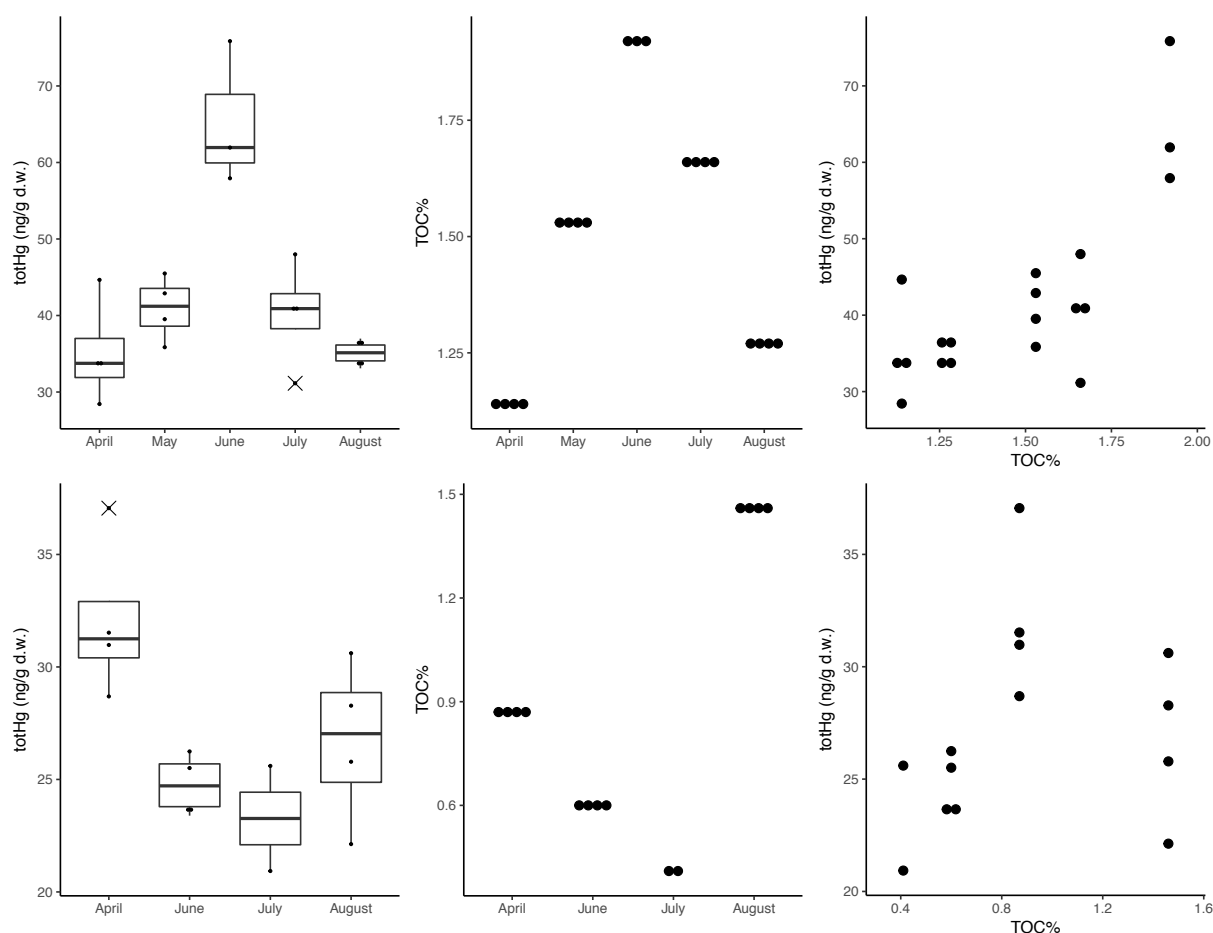


Figure 9. Above left: Boxplot of how total mercury concentrations (ng/g d.w.) in sediments from the City station changed with the season. Above middle: Plot of how TOC% in sediments from the City station changed with the season. Above right: Plot of the relationship between TOC% and total mercury concentrations (ng/g d.w.) in sediments from the City station. City: April/May/July/August; n=4, June; n=3. TOC%: City; n=18. Below left: Boxplot of how total mercury concentrations (ng/g d.w.) in sediments from the North station changed with the season. Below middle: Plot of how TOC% in sediments from the North station changed with the season. Below right: Plot of the relationship between TOC% and total mercury concentrations (ng/g d.w.) in sediments from the North station. North: April/June/August; n=4, July; n=2. TOC%: North; n=14. Note that the Y-axes are on different scales. In boxplots; data presented as median (line drawn in the middle of the box), quartiles (upper and lower lines of the box), 10-90 percentiles (whiskers) and influential data points (indicated as a cross). An outlier, June1C, identified by Cooks distance, was excluded.

3.3.3 Persistent organic pollutants in amphipods

The first two principal components (PC1 and PC2) from the multivariate principal component analysis on POP concentrations (ng/g w.w.) in amphipod samples account for 97.4% of the total variation in the data set (Figure 9). Modell selection using redundancy analysis with lipid content%, TOC%, station, sediment temperature, $\delta^{13}\text{C}$, $\delta^{15}\text{N}$, sediment concentrations of PCB-52 and PCB-153, flagellate-, bacteria-, diatom-, macroalgae-, detritus-, terrestrial- and copepod summary metric as explanatory variables, resulted in three significant variables; sediment concentrations of PCB-52, diatom and copepod summary metric. The best model

explained 60.0% of the total constrained variation in the model (RDA, permutation tests 999, $p = 0.001$). The significant variables sediment PCB-52, diatom and copepod summary metric explained 19.3%, 10.4% and 5.1% of the constrained variation, respectively.

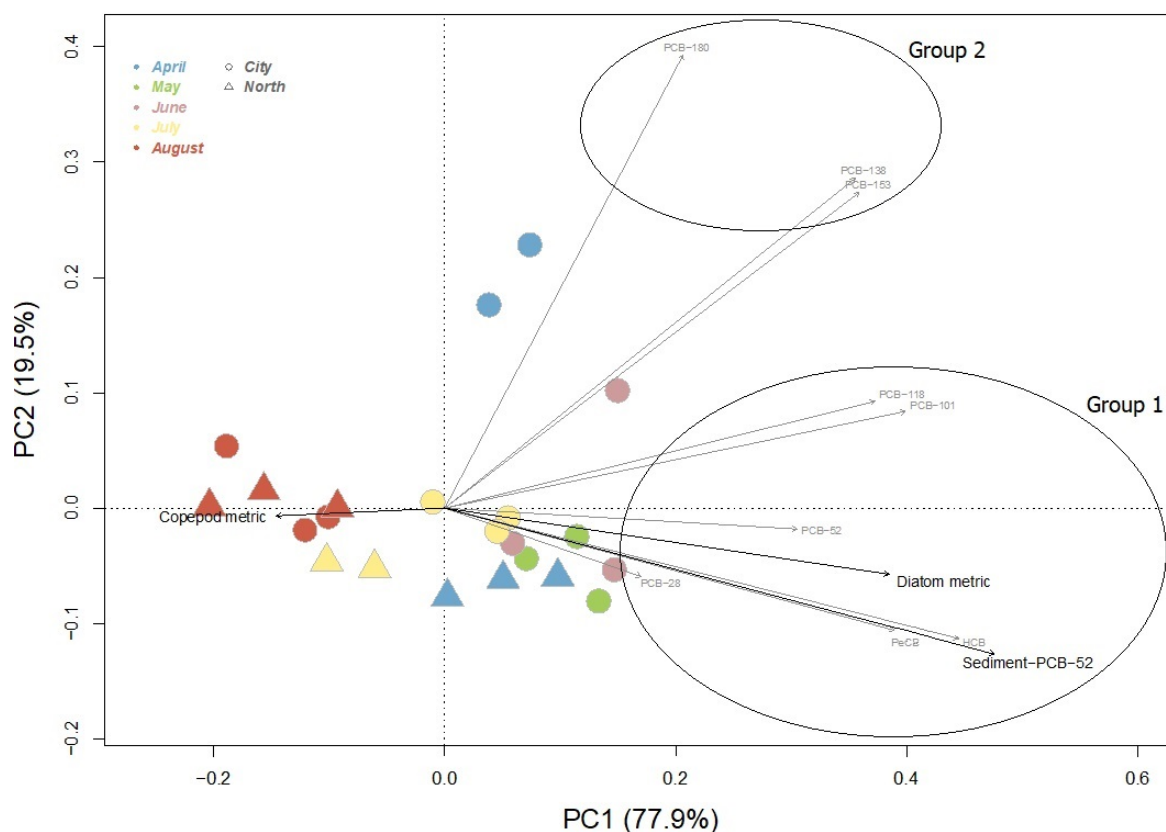


Figure 10. Principal component analysis triplot of correlations between log10 transformed POP concentrations (ng/g w.w.) (visible as grey response loadings/vectors) in amphipod samples ($n=22$) with significant continuous explanatory variables passively placed on top of the ordination as black vectors. The site scores represent individual amphipod samples, with shape and colour representing station and month, respectively. Note that from the North station there were no amphipod samples collected in May or June. The variance explained attributed to each PC axis is given in % on both axis in the figure. An outlier (April 1C), identified by Cooks distance, was excluded.

Two main groups of congeners were found among the response loadings, in which group 1 consisted of PCB-118, -101, -52, -28, HCB and PeCB and group 2 consisted of PCB-180, -153, and -138 (Figure 10). In the ordination, PCB-138 and -153 correlate with both group 1 and PCB-180, however by assessing the actual concentrations, they were similar to PCB-180 not group 1 congeners (Table 7). Group 1 compounds increased along PC1 and showed highest concentrations in amphipods from City in May and June (Σ group1 580 and 570 pg/g w.w., respectively) and correlated positively with the diatom summary metric and cluster 1 congeners in sediments and negatively with the copepod summary metric (Figure 10). Amphipods from the North station showed a decreasing trend of group 1 congeners; April (Σ

group1 490 pg/g w.w.)> July (Σ group1 250 pg/g w.w.)> August (Σ group1 120 pg/g w.w.)
(no samples in May and June from the North station) (Table 7).

Table 7. Overview over POP concentrations (pg/g w.w.), Hg concentrations (ng/g d.w.) and lipid content (%) in amphipods. Letter A-D indicate replicate. Li correspond to lipid content measured from POP analysis. Note that not all replicates (A-D) had enough biomass for all types of analyses, and these are shown as empty boxes in the table below. Asterisk (*) indicates values that have been generated to replace values below LOD.

Station	Month and replicate	PeCB	HCB	PCB-28	PCB-52	PCB-101	PCB-118	PCB-138	PCB-153	PCB-180	tot - Hg	Me-Hg	Li
		pg/g w.w.	pg/g w.w.	pg/g w.w.	pg/g w.w.	pg/g w.w.	pg/g w.w.	pg/g w.w.	pg/g w.w.	pg/g w.w.	ng/g d.w.	ng/g d.w.	%
City	April												
	A										26.2	18.3	
	B	13.1	259.0	9.3	22.9	41.9	26.4	153	252	232	20.6	21.7	1.6
	C	18.8	231.5	11.3	31.0	412	132	1839	2478	1354	21.6	11.4	1.2
	D	18.5	225.5	12.4	25.8	44.1	42.6	138	235	154		15.2	0.9
	May												
	A	42.4	485.6	11.3	26.5	43.8	36.1	80.8	132	43.7	19.5	7.10	1.9
	B	36.1	369.2	9.5	18.2	42.1	30.6	81.4	138	31.8	23.2	5.10	1.5
	C										20.8	2.10	
	D	53.1	417.0	11.9	20.7	46.3	35.7	103	179	41.6	22.0	4.00	7.0
	June												
	A	46.4	494.7	11.1	25.0	35.6	23.0	82.0	156	66.7	22.1	14.3	2.3
	B	57.1	403.7	11.9	28.3	42.8	43.3	136	279	120	21.0	0.70	2.2
	C										19.5	3.30	
	D	40.3	343.1	9.4	22.5	44.4	30.7	76.6	149	30.5	22.4	5.80	1.8
	July												
	A										19.3	4.10	
	B	28.1	324.9	11.1	19.5	38.2	36.8	84.2	175	27.7	24.0	2.80	2.3
	C	30.0	322	10.4	21.5	39.6	22.1	73.6	147	36.5	20.6	9.40	2.4
	D	18.3	234	10.2	22.2	47.3	26.9	71.4	141	27.6	20.3	1.90	2.0
	August												
	A										16.6	2.10	
	B	16.6	9.30*	5.60	12.0	19.8	15.6	38.6	78.1	20.2	20.0	9.70	2.0
	C	17.7	135	6.11	16.4	18.4	15.7	36.3	77.1	21.0	18.2	2.40	2.4
	D	15.9	117	6.90	15.2	17.0	15.3	32.1	57.2	12.9	16.0	1.80	2.6
North	April												
	A	25.9	347.6	57.9	38.7	36.3	35.7	61.6	124	19.7	22.8	19.4	1.5
	B	30.6	297.1	7.0	13.1	21.5	21.6	42.3	81.3	14.8	27.2	22.4	1.3
	C										30.1	39.1	
	D	41.9	413.3	13.3	32.7	37.6	37.4	77.5	153	24.8	21.5	19.4	2.0
	June												
	A										18.8	3.20	
	B										22.0	8.20	
	C										24.4	5.60	
	D										20.7	15.5	
	July												
	B	15.9	205	4.40	16.1	15.2	17.1	29.8	71.5	10.8	25.4	11.7	2.0
	D	9.90	152	4.60	31.9*	20.4	10.3	21.6	51.3	7.70	24.9	14.3	2.5
	August												
	A	12.9	140	4.02	14.2	19.0	19.5	42.5	90.0	21.3	18.3	3.30	2.2
	B										15.8	5.10	
	C	7.10	62.4	3.20	7.80*	10.2	19.2	28.0	70.8	15.1	18.5	2.80	1.4
	D	3.01	19.3	1.10	4.00	5.10	10.0	15.1	33.8	5.40	15.8	1.50	1.4

Investigation of how predictive sediment concentrations of POPs were for amphipod concentrations of group 1 congeners, showed that only PCB-52 and -118 were correlated

(Spearman's rank-order correlation; PCB-118: $p=0.02$ $\rho=0.6$, -101: $p=0.3$ $\rho=0.3$, -52: $p=0.05$ $\rho=0.5$, -28: $p=0.5$ $\rho=0.2$, HCB: $p=0.2$ $\rho=0.4$, PeCB: $p=0.5$ $\rho=0.2$).

Group 2 congeners exhibited higher concentrations in amphipods from City compared to North, in all months (Table 7). This spatial difference between the stations became gradually reduced as the season progressed (Figure 10), opposite of sediments. In April, the sum of group 2 compounds (Σ Group2) was 580 and 190 pg/g w.w. at the City and the North station, respectively (Table 7). In August, however, the difference was negligible, with Σ Group2 were 120 and 110 pg/g w.w. at the City and the North station, respectively (Table 7).

3.3.4 Total mercury in amphipods

Backwards model selection using a linear regression model on totHg in amphipods and with station, sediment temperatures, TOC%, $\delta^{13}\text{C}$, $\delta^{15}\text{N}$, sediment concentrations of total mercury, concentrations of MeHg in amphipods, fatty acid flagellate-, bacteria-, diatom-, macroalgae-, detritus- terrestrial- and copepod summary metric as explanatory variables, resulted in two significant explanatory variables; diatom summary metric and MeHg concentrations in amphipods. The best model explained 60.6% of the total variation in the totHg concentration data set (lm, $R^2 = 0.6$, $p = 0.000143$). Diatom contribution in diet and MeHg concentrations in amphipods explained 29.3% and 31.3% of the variation in the model, respectively. There were positive correlations between totHg concentrations (ng/g d.w.) and diatom summary metric and MeHg concentrations in amphipods (Figure 11) (Spearman's rank-order correlation; MeHg (ng/g d.w.): $p=0.001$, $\rho=0.57$, diatom summary metric (% TFA): $p=0.034$ $\rho=0.45$).

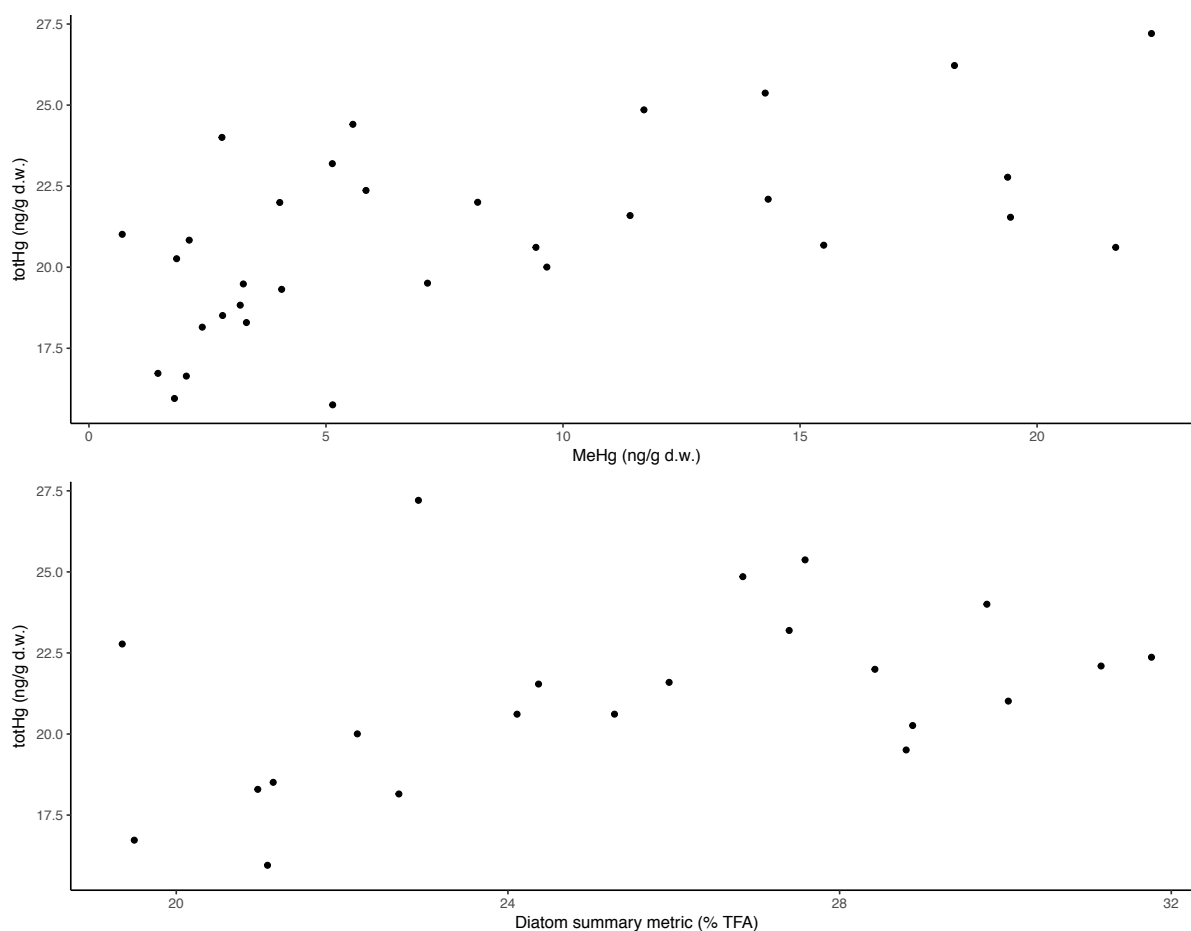


Figure 11. Above: Plot of the relationship between MeHg and totHg concentrations (ng/g d.w.) in amphipods. Below: Plot of the relationship between the diatom summary metric (%TFA) and totHg concentrations (ng/g d.w.) in amphipods. (n=32). The acronym %TFA stands for percent of total fatty acid.

3.3.5 Methyl mercury in amphipods

Backwards model selection using a linear regression model on MeHg concentrations in amphipods and with station, sediment temperatures, TOC%, $\delta^{13}\text{C}$, $\delta^{15}\text{N}$, sediment concentrations of total mercury, fatty acid flagellate-, bacteria-, diatom-, macroalgae-, detritus- terrestrial- and copepod summary metric as explanatory variables, resulted in one significant explanatory variable; TOC%. The best model explained 25.3% of the total variation in the MeHg concentration data set (lm, $R^2=0.25$, $p=0.006$) (Figure 12). Thus, as TOC% in sediments increased MeHg concentrations in amphipods decreased.

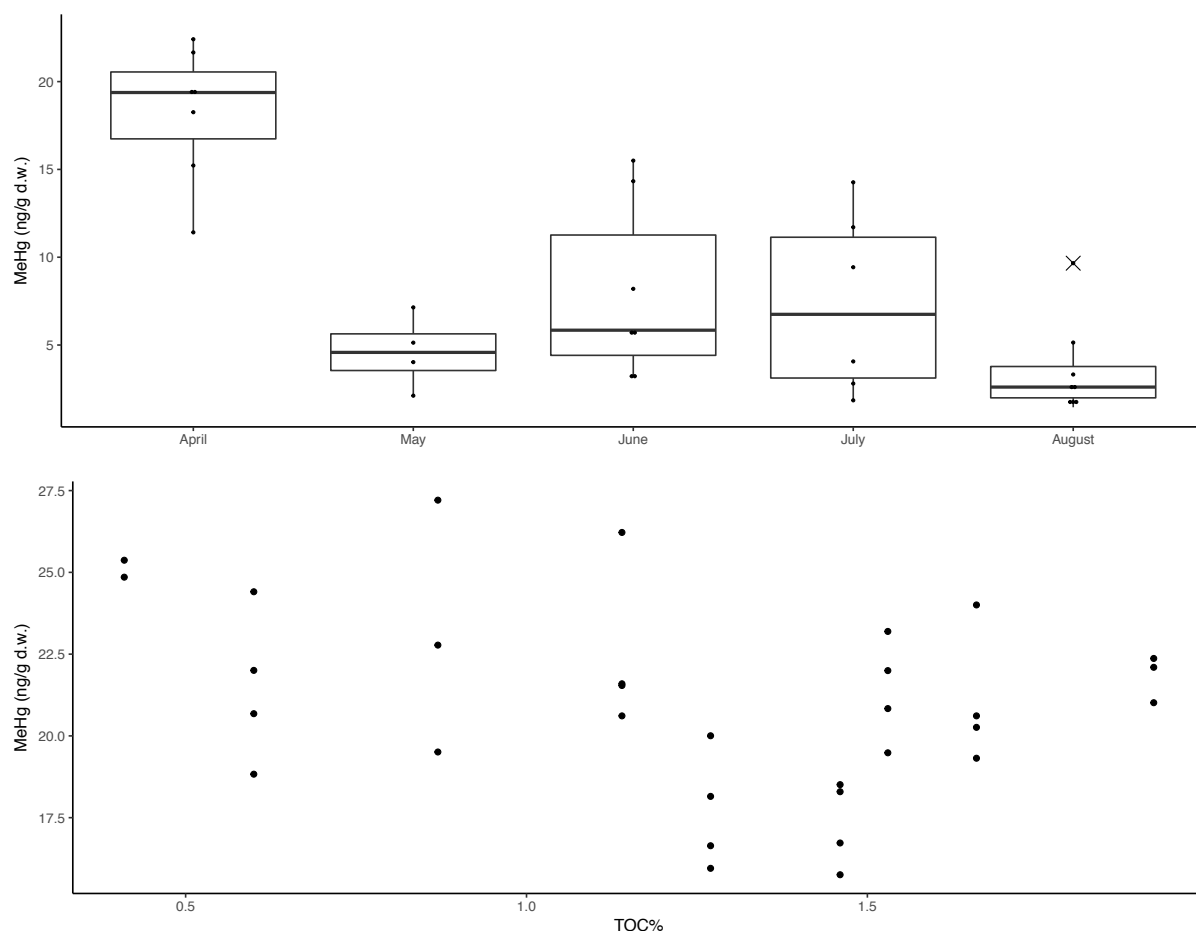


Figure 12. Above: Boxplot of how MeHg concentrations (ng/g d.w.) in amphipods change over the season. June/August; n=8, April; n=7, July; n=6, May; n=4. Below: Plot of the relationship between TOC% and MeHg concentrations (ng/g d.w.) in amphipods (n=32). In boxplots; data presented as median (line drawn in the middle of the box), quartiles (upper and lower lines of the box), 10-90 percentiles (whiskers) and influential data points (indicated as a cross). An outlier, June1C, identified by Cooks distance, was excluded

3.3.6 Contaminant patterns

The relative contaminant pattern in amphipods and sediments were dominated by totHg in all months and at both stations, ranging from an average proportion of 84% to 95% in amphipods and 98% to 99% in sediment samples (Table 6 and 7).

Among the separate POP congeners in sediments, the relative proportion pattern changed spatially and seasonally (Figure 13). At the City station, the relative proportion of PCB-180, -153, -138 and PeCB increased gradually as the season progressed, while PCB-52, -28 and HCB decrease slightly, with PCB-101 being variable. However, at the North station, the relative proportion of PeCB and HCB increased as the season progressed, while PCB-180, -153, -138 -118, -101, -52 and -28 decreased, albeit with some variation in July.

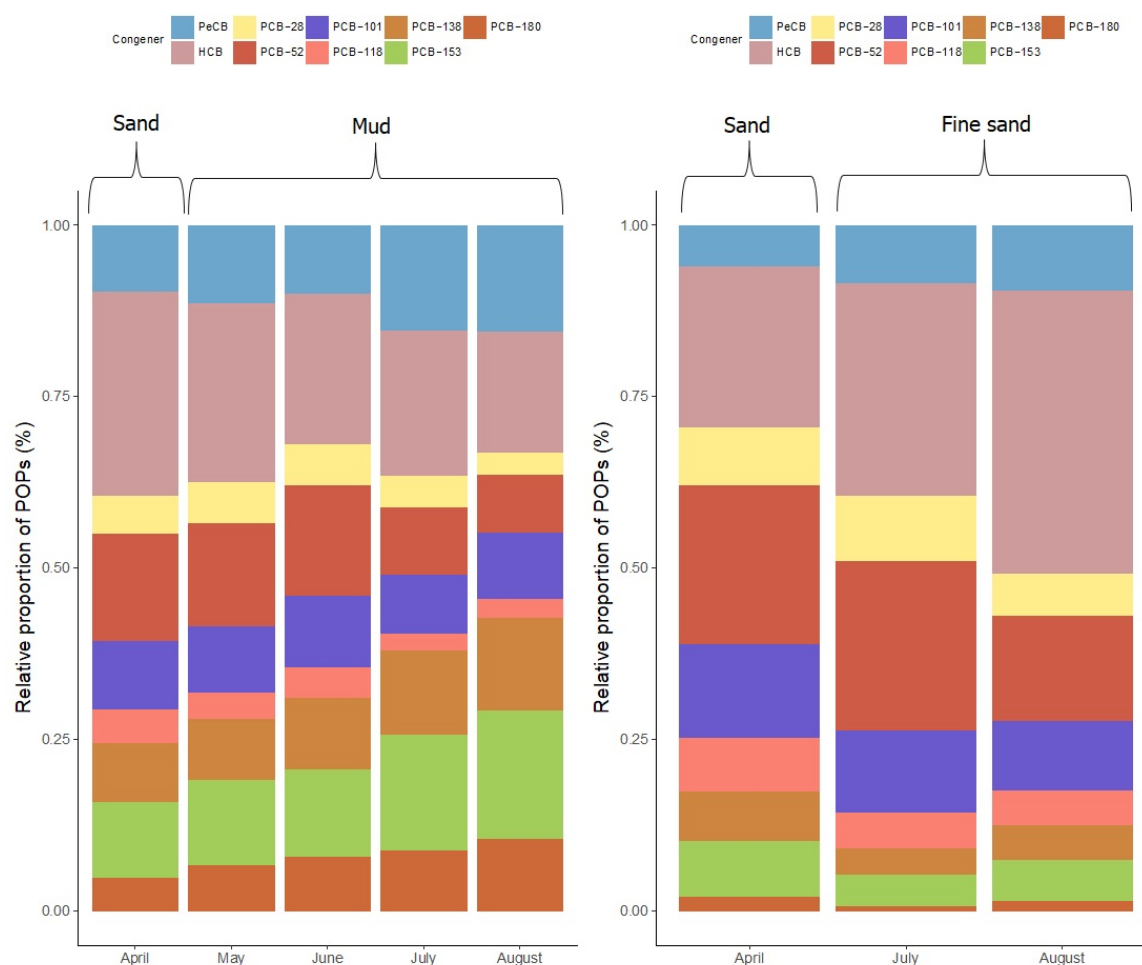


Figure 13. Left: Bar plot of average relative proportions of POP congeners (PeCB, HCB, PCB-28, -52, -101, -118, -138, -153, -180) in sediments from the City station. City: April/August; n=3 and May/June/July; n=1 (analysed as pooled samples). Right: Bar plot of average relative proportions of POP congeners (PeCB, HCB, PCB-28, -52, -101, -118, -138, -153, -180) in sediments from the North station. North: April/August; n=3 and May/June/July; n=1 (analysed as pooled samples).

In amphipods, the relative contribution of each POP congener changed seasonally and by station, as in the sediments, however, the patterns differed (Figure 14). Overall, lower chlorinated POPs, particularly HCB, appeared to dominate the overall relative POP contaminant burden in amphipods. However, in April at the City station and August at the North station, amphipods were dominated by higher chlorinated POPs.

The relative contribution of PeCB and HCB were highest in May at the City station, and then gradually decreased as the season progressed. The opposite pattern was seen in PCB-153 at the City station. The relative contribution of PCB-180, -138, -118, -101, -52 and -28 were seasonally variable (Figure 14). At the North station, April and July samples had similar patterns of relative contribution for most of the POP congeners. However, in August, there

was an increase in the relative contribution of PCB-180, -153, -138 and -118 and a decrease in HCB contribution (Figure 14).

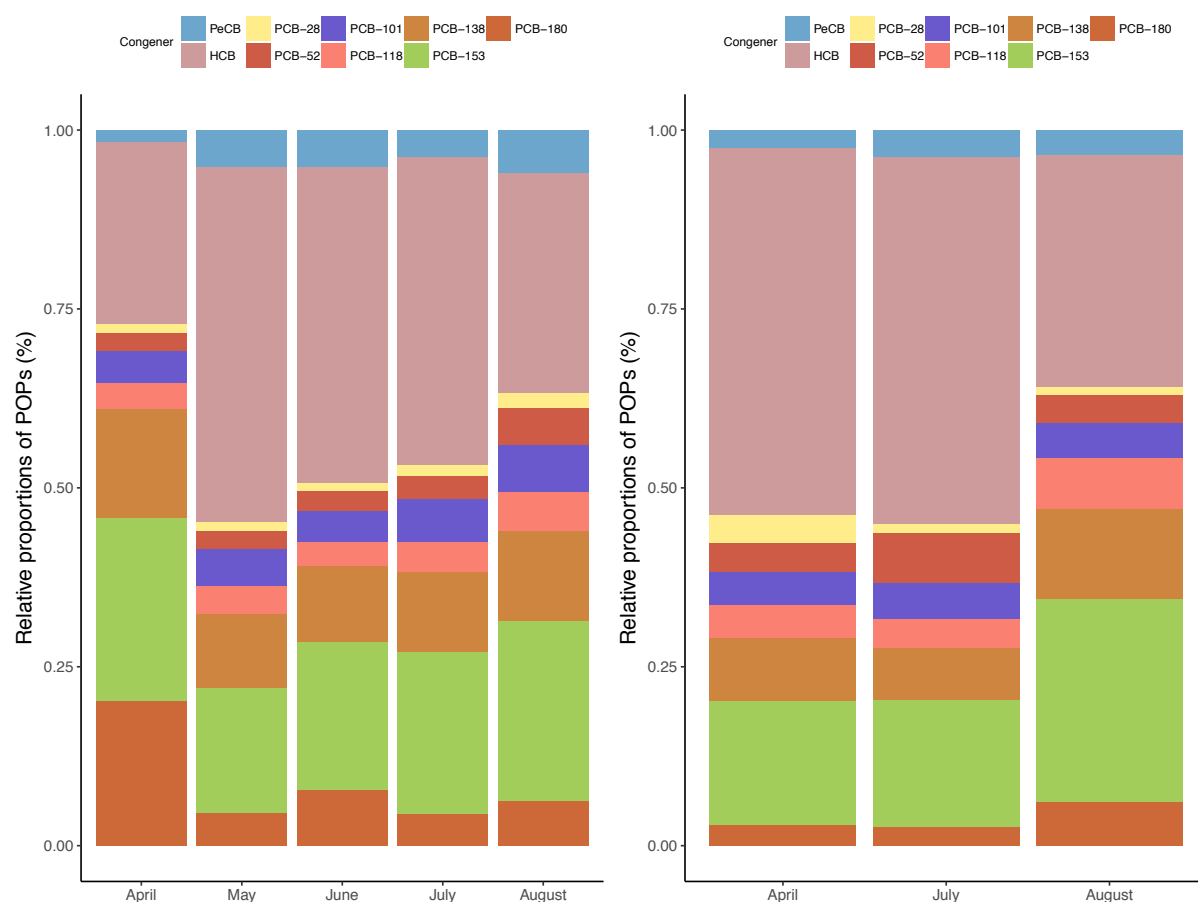


Figure 14. Left: Bar plot of average relative proportions of POP congeners (PeCB, HCB, PCB-28, -52, -101, -118, -138, -153, -180) in amphipods from the City station. City: May/June/July/August; n=3, April; n=2. Right: Bar plot of average relative proportions of POP congeners (PeCB, HCB, PCB-28, -52, -101, -118, -138, -153, -180) in amphipods from the North station. North: April/August; n=3, July; n=2. An outlier, April1C, identified by Cooks distance, was excluded.

In amphipods, the % MeHg of totHg changed seasonally (Figure 15). The highest relative contribution of MeHg was found in April at both locations (City; 66% and North; 80%). Generally, as the season progressed, MeHg contribution in amphipods decreased, however with a slight increase in June/July (Figure 15).

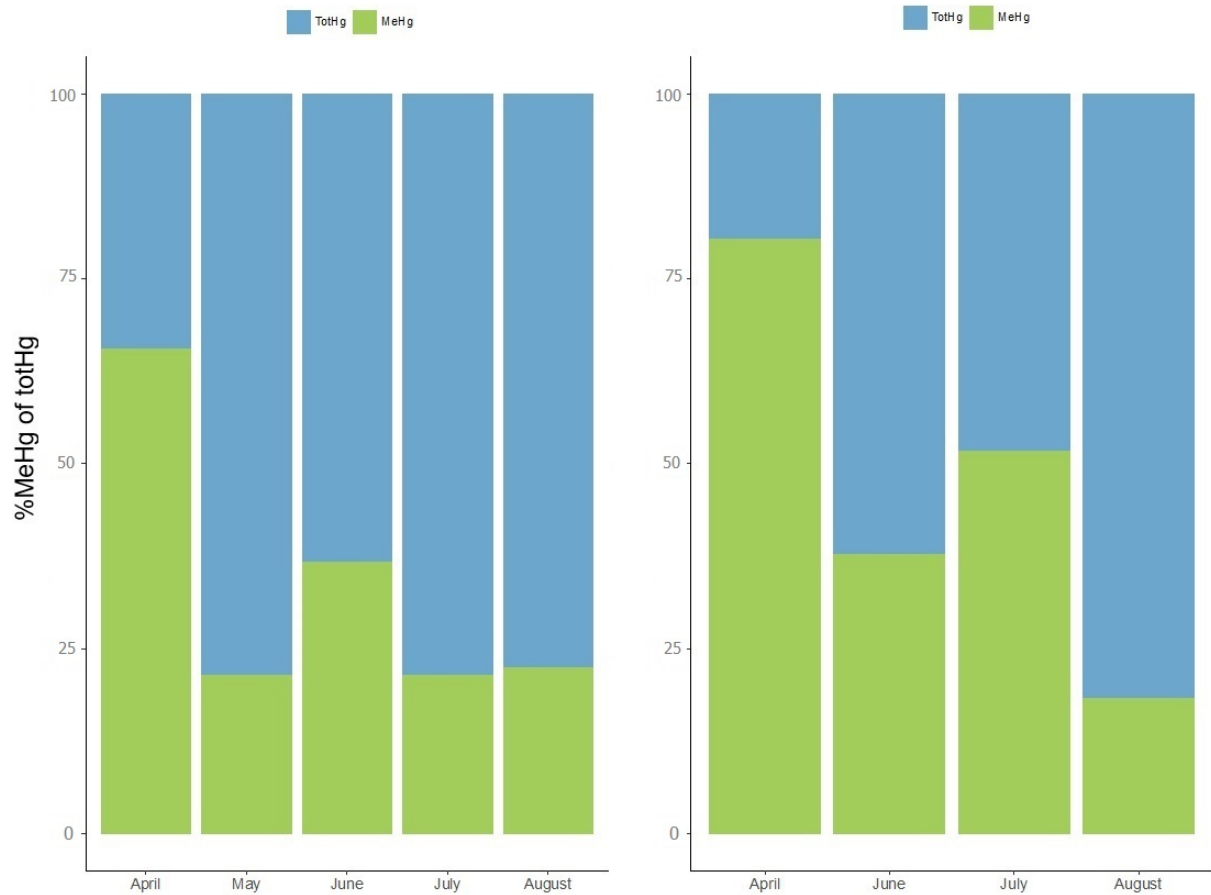


Figure 15. Left: Bar plot of %MeHg of totHg in amphipods from the City station. City-totHg: April/May/June/July/August; n=4. City-MeHg: April/July/August; n=4, May/June; n=3. Right: Bar plot of %MeHg of totHg in amphipods from the North station. North-totHg: June/August; n=4, April; n=3, July; n=2. North-MeHg: April/June/August: n=4, July: n=2. An outlier, June1b from methyl mercury samples, identified by Cooks distance, was excluded

4 Discussion

The present study aims to investigate the influence of diet, lipid dynamics and riverine run-off on contamination in *G. setosus* from spring to autumn. In the current study, *G. setosus* appears to be supported by a detrital “food bank” in the sediments, whereof they feed on a variety of carbon sources. Furthermore, during spring and summer, *G. setosus* seem to feed predominantly on sedimenting diatom dominated phytoplankton material. Riverine run-off seems to affect both POPs and Hg contamination in Adventfjorden estuarine sediments, with a possible localised anthropogenic contamination of higher chlorinated POPs from Longyearbyen. The drivers behind the seasonal changes in sediment contamination differ between Hg and POPs. *G. setosus* appears to feed selectively in sediments, thus contaminant concentrations in bulk sediment samples and amphipods may be decoupled. Settling phytodetritus seems to be an important contaminant source for less chlorinated POPs in *G. setosus*, and growth dilution and riverine- derived organic matter may cause a seasonal decrease in concentrations of POPs and Hg.

4.1 Carbon sources and lipid content

The dominating FAs found in *G. setosus* are highly comparable with FA profiles detected in *G. setosus* and other amphipods collected at Hornsund, Svalbard (Legeżyńska et al., 2014). High levels of 20:5n-3, 22:6n-3 and 16:0 are distinctive in benthic organisms, where they predominate in membrane lipids (phospholipids) (Graeve et al., 1997; Legeżyńska et al., 2012).

4.1.1 Spatial differences

The dietary indicators from $\delta^{13}\text{C}$ and $\delta^{15}\text{N}$ values and fatty acids profiles in amphipods indicate that similar food items are assimilated at the North and City station, which is in line with the expectations of the current study. The North and City station are separated by approximately 2.5 kilometres and experience similar physical environments (close to tidal flat and impacted by riverine run-off), thus it was not expected that potential food sources such as phytoplankton bloom or detritus would differ between the stations. Indeed, assimilation of similar food sources by benthos inhabiting distinctive locations have been observed in Kongsfjorden (Renaud et al., 2011). Nonetheless, $\delta^{15}\text{N}$ values in *G. setosus* differ between stations in August, with values from the City station being 1‰ higher than the North station.

This difference could not ecologically explained with FA signatures. However, $\delta^{15}\text{N}$ values in sediments show a similar pattern, which could explain higher values in amphipods. Despite a small difference in $\delta^{15}\text{N}$ values in August, which might be a result of differences in local abiotic, baseline values, the diet between both locations appears to be similar.

4.1.2 Phytoplankton spring bloom

G. setosus display the highest average value of $\delta^{13}\text{C}$ in May. This coincides with an enrichment in the pelagic POM $\delta^{13}\text{C}$ in Adventfjorden, low chlorophyll a and nutrient concentrations, suggesting that a phytoplankton spring bloom had just taken place (McGovern et al., in prep). Typically, the pelagic spring production, occurring in April-May, is dominated by diatoms and if ungrazed, may cause large biomass fluxes to the benthic community (Eilertsen & Frantzen, 2007; Grebmeier et al., 1988; Hegseth, 1998; Thompson et al., 2008). Indeed, seasonal phytoplankton flux has been observed in Adventfjorden, which can subsidise the benthic habitat with nutritious carbon sources (Wiedmann et al., 2016; Zajaczkowski et al., 2010). The diatom ratio and diatom summary metric in *G. setosus* is highest in May, June and July, whereas the flagellate ratio and summary metric is inverse to that of the diatom markers. Thus, these FATM patterns and enrichment in $\delta^{13}\text{C}$ values may reflect a large consumption of diatoms and low consumption of flagellates during this period, most likely as a result of settling diatom dominated bloom material. These findings are in line with the expectation of the current study and previous studies on polar benthic amphipods, where pelagic primary producers appear to be a major carbon source (Legeżyńska et al., 2012, 2014). In fact, in one study, roughly 40% of the gut volume of *G. setosus* in July were diatoms (Legeżyńska et al., 2012).

In May, June and July, *G. setosus* is isotopically enriched in $\delta^{13}\text{C}$ relative to pelagic POM (McGovern et al., in prep). Enriched $\delta^{13}\text{C}$ values in benthic fauna have been attributed to a diet consisting of microbially reworked organic matter (reworked detritus) (e.g. McTigue et al., 2015; McTigue & Dunton, 2014), whereby microbial processes often result in isotopically enriched organic matter (Macko et al., 1987). Typically, $\delta^{13}\text{C}$ values of POM are used as a proxy for a phytoplankton signal, as it is expected that the majority of the material is derived from phytoplankton (Michener & Lajtha, 2007). However, the pelagic POM samples from the F1 station in Adventfjorden close to the river outlets (Figure 1), do not represent a “clear”

marine phytoplankton signal. A marine POM sample would better represent a phytoplankton signal. McGovern et al. (in prep) report marine POM $\delta^{13}\text{C}$ values (not lipid corrected) from outer Adventfjorden and these values are still more depleted than non-lipid-corrected $\delta^{13}\text{C}$ values in *G. setosus*, suggesting assimilation of bacterial reworked phytodetritus.

Alternatively, enrichment could hypothetically be due to other unacknowledged end members contributing to the diet, such as ice-algae or macroalgae (Harris et al., 2018; Iken et al., 2010; Renaud et al., 2015). However, macroalgae contributed little in gut content analysis of *G. setosus* in July in Hornsund (Legeżyńska et al., 2012) and the macroalgae summary metric patterns from the current study decrease during this period, suggesting that its role as a carbon source was probably minimal during this time. Additionally, there was mainly open water in Adventfjorden during the winter of 2017/2018, and most likely ice-algae was not present (Wiedmann et al., 2016; Zajączkowski et al., 2010). Therefore, macroalgae and ice algae are unlikely important carbon sources in this study, and the isotopic enrichment found here is likely due to reworked phytodetritus.

4.1.3 Pre- and post-bloom situations

The MUFA 18:1n-9 and detritus

High relative concentration of the MUFA 18:1n-9 in *G. setosus*, generally an indication of carnivorous feeding (Graeve et al., 1997; Nyssen et al., 2005; Sargent & Falk-Petersen, 1981), have instead been attributed to a diet mainly consisting of flagellates/ciliates accompanying settled organic matter and/or macroalgae-derived detritus (Legeżyńska et al., 2014). Flagellates, ciliates and macroalgae are known to be rich in the MUFA 18:1n-9 (Kelly & Scheibling, 2012; Peters et al., 2006). This is in line with patterns of seasonal change in FATM in *G. setosus* in the current study, as the highest seasonal values of 18:1n-9 coincide with the highest values of macroalgae, flagellate, bacteria and detritus summary metrics in April and August. High relative concentration of the bacteria metric in samples may indicate reliance on bacteria and/or detritus and low relative concentration of PUFA with high relative concentration of the detritus metric may further indicate provision of detritus (Søreide et al., 2008). These FATM patterns together with higher relative concentrations of macroalgae and flagellates, suggest that macroalgae- and flagellate-derived detritus may be contributing to the amphipods diet before and after the spring bloom. Thus, in *G. setosus* high relative

concentration of 18:1n-9 do not appear to indicate carnivorous feeding (Legeżyńska et al., 2014).

Low $\delta^{15}\text{N}$ values in *G. setosus* provide further support that *G. setosus* does not display high values of carnivorous markers with high relative concentration of the MUFA 18:1n-9. Recognised carnivorous amphipods *Anonyx nugax* and *A. sarsi*, having similar proportions of 18:1n-9 (23-22%) as *G. setosus*, have $\delta^{15}\text{N}$ values of 10-11‰ (Legeżyńska et al., 2012), while *G. setosus* have average values of 8.7-6.6‰. Furthermore, $\delta^{15}\text{N}$ values and the MUFA 18:1n-9 do not display the same seasonal pattern. These findings are in line with the expectation of the current study and previous studies on polar benthic amphipods, where *G. setosus* occupies a low trophic status (Legeżyńska et al., 2012, 2014).

Macroalgae, flagellates and faecal pellets

In near-shore Arctic food-webs, macroalgae-derived detritus is an important carbon source (Renaud et al., 2015) and have been found in the gut of *G. setosus* (Legeżyńska et al., 2012). A diet subsidised with macroalgae detritus, together with other depleted sources, could also explain the intermediate $\delta^{13}\text{C}$ signatures in *G. setosus*.

After the spring phytoplankton bloom, the pelagic production typically shifts towards being dominated by flagellates and herbivorous zooplankton (Leu et al., 2011; Søreide et al., 2008; Zajączkowski et al., 2010), and may, therefore, become more available as food items for *G. setosus* as these settle to the seafloor. Gut content analysis of *G. setosus* from Hornsund collected in July showed that dinoflagellates and protist cysts comprised of approximately 50% of the gut volume (Legeżyńska et al., 2012). Besides flagellate markers being higher during off-bloom periods, so was the copepod marker in the present study. However, carnivorous feeding on *Calanus* copepod zooplankton seems doubtful due to $\delta^{15}\text{N}$ values in *G. setosus* being lower or similar to those measured in polar copepods (Søreide et al., 2008). Thus, a plausible explanation could instead be a diet containing settled copepod faecal pellets, as the MUFAs 20:1 and 22:1 have been shown to effectively become transferred with zooplankton faecal pellets (Mayzaud et al., 2007). Despite the lack of photosynthetic production during the polar night, some production still persists in the water column and may comprise of heterotopic microbes, such as flagellates (Berge et al., 2015; Wiktor, 1999), and certain zooplankton taxa (Berge et al., 2009; Berge et al., 2015; Forest et al., 2011). Indeed,

fluxes of sinking organic material in Conception Bay, Newfoundland, Canada, was dominated by zooplankton faecal pellets before and after the spring bloom (Thompson et al., 2008) and flux measurements from Adventfjorden suggest sinking of flagellates and zooplankton faecal pellets outside of the spring bloom (Wiedmann et al., 2016; Zajaczkowski et al., 2010). Therefore, flagellates and *Calanus* faecal pellets settling to the seafloor, and macroalgae-derived detritus, may provide important food sources to *G. setosus* outside of the spring-bloom dominated by diatoms, as hypothesised in the present study.

Terrestrial material

Terrestrial material, as indicated by the terrestrial and terr>2.5% summary metric, appears to be utilised both before and particularly after assimilation of the diatom spring bloom, when the riverine run-off is highly influencing the environment (McGovern et al., in prep). In addition, $\delta^{13}\text{C}$ values in *G. setosus* are more depleted during these periods, which could reflect a higher reliance on terrestrially-derived organic matter, which is in line with the expectations from the current study. Recent work has illustrated that terrestrially-derived organic matter is assimilated in estuarine environments by various fauna such as benthic crustaceans, including mysids and amphipods (Dunton et al., 2012; Dunton et al., 2006; Harris et al., 2018). Furthermore, *G. setosus* can consume peat detritus (Dunton et al., 2012; Schell, 1983) and organic matter in sediments from Adventfjorden can contain up to 82-83% terrestrial-derived organic matter (Koziorowska et al., 2016). Thus, terrestrial-derived organic matter is in the environment, and may be an important food source for *G. setosus* when nutritious diatoms are no longer available.

The main findings from the dietary analysis suggest that *G. setosus* inhabiting Adventfjorden is supported by a detrital “food bank” in the sediments (Legeżyńska et al., 2012; Mincks et al., 2008), where they utilise different carbon sources depending on the season. Diatom dominating phytodetritus predominates the diet during and shortly after the spring bloom, whereas detritus material composing of macroalgae, terrestrial material, microbes and faecal pellets may be important food sources when high-quality food is unavailable.

Trophic status and starvation

Surprisingly, $\delta^{15}\text{N}$ values in *G. setosus* decrease seasonally. However, several studies, in accordance with the present study, have found a seasonal $\delta^{15}\text{N}$ decrease in invertebrates (e.g.

Nordström et al., 2009; Woodland et al., 2012). Change in $\delta^{15}\text{N}$ values is usually attributed to a change in trophic status since $\delta^{15}\text{N}$ typically enriches with 3-4‰ from diet to consumer (Peterson & Fry, 1987). Nevertheless, this seasonal isotopic depletion is most likely a result of changing baseline values within the system, as seen in previous temporal isotopic studies (e.g. Gu, 2009; Nordström et al., 2009; Syväranta et al., 2006), rather than a shift in diet causing a decline in trophic status. Indeed, sediment POM $\delta^{15}\text{N}$ values from the present study (albeit a minimal temporal change) and pelagic POM $\delta^{15}\text{N}$ values in Svalbard's estuarine systems (McGovern et al., in prep) show a general seasonal decrease. Furthermore, varying seasonal $\delta^{15}\text{N}$ values are also seen in macroalgae from the present study. Processes responsible for temporal variation in $\delta^{15}\text{N}$ values are not well understood, but some studies have indicated that nitrogen fixation, primary productivity and isotope composition of ambient nutrient pools are important processes controlling temporal nitrogen fractionation (Gu, 2009). While a change in baseline nitrogen through the season may be responsible for the decrease in $\delta^{15}\text{N}$ in the amphipods from the current study, there could also be physiological processes happening within the amphipods themselves that would also lead to the enriched nitrogen values we see in April, such as starvation.

Starvation has been known to enrich $\delta^{15}\text{N}$ values because isotopically light nitrogen compounds are preferentially excreted during metabolism of body tissues (Gannes et al., 1997; Hobson et al., 1993; Kaufman et al., 2008). Due to the expectation of available food sources all year round (e.g. Kędra et al., 2011; Legeżyńska et al., 2012, 2014), starvation was not expected in the present study, and indeed, from FA analysis, *G. setosus* does appear to rely on a detrital-based food web outside of the phytoplankton spring bloom. However, the non-living organic matter in the sediment is derived from a variety of sources of different nutritional value (Tenore, 1988). As the nutritious phytoplankton detritus becomes utilised, the detrital pool may become deficient in essential fatty acids and decrease in nutritional value (Tenore, 1988). Furthermore, since most sediments typically consist only of a few percentages of organic matter (e.g. present study and Koziorowska et al. (2016)), it may be a poor-quality food source. This may result in *G. setosus* relying on a poor-quality food source during off-bloom periods and in effect, experience some starvation during these times, which could lead to higher $\delta^{15}\text{N}$ values. Seasonal change in lipid content may provide further support for this starvation hypothesis. When nutritious and high-quality fresh phytodetritus

(Arts et al., 2009; Tenore, 1988) are exploited by *G. setosus*, lipid content increases. Although the increase is not large, a distinct pattern is present. Therefore, starvation and changing baseline values could both be reasonable explanations for the seasonal decrease in $\delta^{15}\text{N}$ values in amphipods.

Food supplies

Lipid content in *G. setosus* from the current study is similar to values found in polar amphipods with continued food supplies (Legeżyńska et al., 2012) and other benthic organisms (Evenset et al., 2016; Graeve et al., 1997). Furthermore, the slight increase in lipid content during summer months observed in the present study has previously been observed in other polar benthos from Kongsfjorden (Evenset et al., 2016). Despite this slight increase in lipid content in May, June and July, the overall lipid concentration in *G. setosus* is low in contrast to amphipods relying on temporal food sources, such as sympagic *Onisimus* spp. (35.4–38.6% d.w.) (Scott et al., 1999) or deep-sea lysianassids (23.0–43.0% d.w.) (Bühring & Christiansen, 2001). Thus, overall, lipid results support the hypothesis that *G. setosus* has sufficient food supplies throughout the year, and does not need to accumulate reserves.

4.1.4 Turnover times

As discussed above, dietary descriptors, such as SI and FA analysis, indicate seasonal changes in the diet of *G. setosus*. However, it is typically difficult to pinpoint precisely when these shifts in feeding took place. The results from the present study suggest a quite rapid change in isotopic signatures, based on the phytoplankton signal in the pelagic POM, collected less than a week before the amphipods. Similar to Richoux et al. (2005) and Nygård et al. (2012), seasonal changes in diet-derived FAs are found in the current study. In fact, monthly distinctions are noticeable, suggesting that shifts in diet could result in FA signature change within a month. This is in line with other estimates of isotopic and diet-derived FA turnover times in amphipods (Kaufman et al., 2008; Richoux et al., 2005), suggesting a change in signatures could be apparent within weeks after a shift in diet.

4.2 Sediment contamination

4.2.1 Persistent organic pollutants

Comparing with other studies

No prior studies on seasonal PCB or chlorobenzene concentrations in Arctic marine sediments have been published, limiting the possibility to compare seasonal results. The Σ_7 PCB and chlorobenzenes concentrations from the present study are within or below previous measurements in Adventfjorden (Evenset et al., 2009; Holte et al., 1996; Pouch et al., 2017, 2018) and background concentrations from eastern Svalbard (Green et al., 2010).

Spring flux

Measurements of POP concentrations of suspended particulate matter (SPM) from Adventelva in August (2018) show that the river is a source of contaminants (Johansen, 2019). Generally, less chlorinated/hydrophobic congeners, identified as cluster 2⁶ congeners, display higher concentrations during spring/summer (highest in May) as expected due to their physiochemical properties (Meyer & Wania, 2011). Thus, these contaminants appear to enter the estuary from re-emissions of stored contaminants by spring thaw run-off (Nellier et al., 2015). Another potential source of POPs to the sediment, that could help explain higher concentrations in May and June, are the settling of phytodetritus during the spring bloom. Positive correlations have been found between phytoplankton blooming events and PCB concentrations in the sediments (Everaert et al., 2015; Söderström et al., 2000), as phytoplankton can sequester dissolved POPs in seawater (e.g. Söderström et al., 2000) before sinking to the seafloor. Seemingly, spring thaw and settling of organic particles could result in a spring/summer peak of cluster 2 congeners in sediments.

Seasonal decrease

Surprisingly, the less chlorinated cluster 2 congeners show similar or lower concentrations in August relative to April. This seasonal concentration pattern in sediments might mirror a seasonal decline in contamination in riverine run-off itself (Quémerais et al., 1994). River water can function as a dilution vector, desorbing contaminants from the sediments, and therefore explaining why there is no seasonal accumulation in the sediments. However, Johansen (2019) suggests that the ambient water in the inner parts of Adventfjorden might not

⁶ Including: HCB, PCB-28, -31, -52 and -118.

be “cleaner” nor prone to sorption from surface sediments. Alternatively, if contaminants via riverine run-off decrease seasonally, sediments might likewise experience a decrease in concentration because of high sedimentation rates (Wiedmann et al., 2016; Zajączkowski et al., 2010; Zajączkowski & Włodarska-Kowalczyk, 2007) of less contaminated riverine material (Barber & Writer, 1998). This sedimentation could dilute or bury the sediments and effectively dilute the concentration of POPs as the season progresses (Barber & Writer, 1998). Indeed, the POP congener composition in estuarine sediments are similar to that of SPM from Adventelva and SPM had slightly lower concentrations (Johansen, 2019), suggesting that the main source is riverine run-off and that sedimenting SPM could cause dilution of the sediments.

Grain size distribution and local contamination

POP concentrations in sediments have been observed to increase with organic matter content (Hung et al., 2010; Razak et al., 1996; Sapota et al., 2009). However, sediment organic matter does not explain the observed variation in the present study (Nellier et al., 2015; Pouch et al., 2017). Rather, grain size distributions might account for part of the variation in PeCB and higher chlorinated PCBs, identified as cluster 1⁷ congeners between the stations (Karickhoff et al., 1979; Pierard et al., 1996). The larger fraction of very fine particles at the City station found when influenced by run-off, can cause enhancement in POP adsorption, particularly for higher chlorinated congeners (Pierard et al., 1996). This enhancement may explain the pattern of seasonally higher concentrations of higher chlorinated congeners at the City station compared to the North station, which has coarser grains (Pierard et al., 1996). Thus, the seasonal increase of cluster 1 congeners at the City station may be a result of larger surface-to-volume ratio of the estuarine sediments. Although, from the multivariate hypothesis testing, grain size distribution explained very little of the variation in the contaminant dataset, thus other factors, not measured in the study, might be more influential.

Alternatively, or in concert with sediment properties, the seasonal decrease of cluster 1 congeners at the North station may be a result of high depositing rates from less contaminated riverine material, as suggested for cluster 2 congeners. Indeed, riverine run-off appears to influence this station, as the overall POP congener composition is similar to that of SPM from Adventelva (Bright et al., 1995; Johansen, 2019). This riverine compositional profile is not

⁷ Including: PeCB, PCB-101, -153, -138 and -180.

equally apparent at the City station, suggesting another contaminant source in addition to riverine run-off. This additional source could be a local contamination source from Longyearbyen affecting the City station but not the North station (Evenset et al., 2009; Evenset et al., 2006; Hop et al., 2001). Hop et al. (2001) found elevated POP contamination in macro-benthos closer to Longyearbyen compared to stations further out in the fjord (approximately separate by 2.5-3 km), suggesting highly localised contamination from the settlement. The composition of PCBs in soil, paint, concrete etc. from Longyearbyen is dominated by higher chlorinated PCBs (Jartun et al., 2009), reflecting the composition in sediments from the City station. Altogether, the contaminant results suggest that concentrations of POP congeners in estuarine sediments are likely influenced by riverine run-off, both in regards to amounts of contaminants that the river discharge brings and sediment burial of river material. Additionally, grain size distribution, settling of phytoplankton, and local contamination may influence POP contamination in estuarine sediments in Adventfjorden.

4.2.2 Total mercury

Comparing with other studies

No prior studies on seasonal totHg concentrations in Arctic surficial marine sediments have been conducted/published, limiting the possibility to compare seasonal results. Prior studies on sedimentary Hg from Svalbard fjords varied between 8-86 ng/g d.w. (Beldowski et al., 2015; Liu et al., 2015; Lu et al., 2013). Thus, the totHg concentrations from the present study are within previous findings from Svalbard fjords.

Riverine run-off and TOC%

Longyearelva and particularly Adventelva, appear to be sources of totHg to Adventfjorden (Carrasco, 2019). Surprisingly, there is no apparent peak of contaminants in rivers between May to August in 2018 (Carrasco, 2019). This could be explained by the fact that Adventelva, although receiving meltwater from glaciers, runs through Adventdalen for 35 km before reaching Adventfjorden (Wesławski et al., 1999). It therefore brings Hg from eroding permafrost, which contains both natural and anthropogenic long-range transported Hg (Schuster et al., 2018). Indeed, Hg in surficial sediments in Adventfjorden has been suggested to mainly derive from weathering and not from local anthropogenic sources (Beldowski et al., 2015). A recent study from Kongsfjorden (Liu et al., 2015) suggests that sedimentary Hg at inner fjord stations, in close vicinity to glaciers, are mostly affected by (glacial) meltwater.

Therefore, the Hg load at the City and North station, which are positioned close the river outlets, may be derived from run-off containing weathered and ice-cap remobilised Hg.

Sedimentary totHg do not increase seasonally as expected, and in August, at both stations, concentrations are similar or slightly lower to those measured in April. Organic matter binds strongly to Hg (Fitzgerald & Lamborg, 2007) and several studies have indicated the importance of Hg scavenged by organic-rich particles as a sink in aquatic environments to the sediments (Fitzgerald et al., 2007; Jiang et al., 2011). In the present study, the seasonal concentrations of totHg are positively correlated with organic carbon in sediments. Thus, this indicates that totHg in estuarine sediments from Adventfjorden are primarily controlled by organic matter, which is in accordance with several other studies (e.g. Chételat et al., 2008; Liu et al., 2015; Outridge et al., 2007). The main findings from the Hg results suggest that riverine run-off is the main source of Hg, but the concentrations in sediments are driven by TOC%.

4.3 Amphipod contamination

Providing that diet is the main exposure route for POPs and MeHg (Boese et al., 1990; Kaag et al., 1997; Lawrence & Mason, 2001; Tsui & Wang, 2004), and that dietary descriptors from the current study suggest a diet based on a detrital “food bank” in the sediments (Legeżyńska et al., 2012, 2014), the concentrations of sediment-adsorbed POPs and MeHg are expected to reflect concentrations in *G. setosus*. Unfortunately, MeHg was not measured in sediments, and thus, MeHg is expected to correlate with totHg in sediments instead. As seen in the previous section, there is both a seasonal increase and decrease of sedimentary POPs and totHg, suggesting that *G. setosus* would reflect similar patterns of change depending on contaminant and station. Experimental data suggest that diet and partitioning from the ambient habitat can be entry points for inorganic Hg in invertebrates (Lawrence & Mason, 2001; Tsui & Wang, 2004). Therefore, *G. setosus* is expected to reflect similar patterns of change as sedimentary totHg.

Additionally, as POPs partition into lipids, lipid content is an important physiological trait to investigate (Borgå et al., 2004). However, as suggested in the present study and prior studies, *G. setosus* do not appear to rely on lipid reserves to survive the winter (Legeżyńska et al., 2012), and there is only a small seasonal change in the lipid content in the present study.

Thus, lipid content is not expected to impact the POP concentrations. Furthermore, as *G. setosus* occupies a low trophic status, POP and Hg concentrations are expected to be low.

4.3.1 Persistent organic pollutants

Comparing with other studies

The overall Σ POP concentrations in *G. setosus* from the present study ranged between 97 to 1120 pg/g w.w. depending on sampling month. These concentrations are below or within values measured in other Arctic benthic invertebrates (Evenset et al., 2009; Evenset et al., 2016; Hop et al., 2001; Muir et al., 2003) and are below other organism groups such as fish or birds from the Arctic (Evenset et al., 2016; Letcher et al., 2010 and references therein). Thus, POP concentrations in *G. setosus* can be considered low, as expected based on the trophic status. Furthermore, when investigating the result, lipid content does not explain the variation in the contaminant dataset, and lipid normalised data show the same trends, as expected.

With only one published study on seasonal (May, July, October) POP accumulation in benthic invertebrates from the Arctic, however not in the littoral zone (Evenset et al., 2016), it limits the possibility to compare seasonal results. In this seasonal study, benthic invertebrates, collected in Kongsfjorden, exhibit the highest concentrations of HCB in October while PCBs dominate in July (Evenset et al., 2016). In contrast, the current study shows a general seasonal decrease of POPs from April to August, however less chlorinated POPs, called group 1⁸ congeners, are higher in May/June, coinciding with the onset of riverine run-off and spring bloom.

Spring peak and phytodetritus

In the present study, group 1 congeners in *G. setosus* correlate with dietary markers for diatoms, copepod faecal pellets, and PCB-52 concentrations in sediments (which was a proxy for cluster 2 congeners found in sediments), as expected. This suggests that contaminants adsorbed to sediments that presumably contain what the amphipods feed on, can explain some of the seasonal variations among these congeners. However, PeCB and PCB-101 decrease seasonally in sediments. This slight miss-match between PeCB and PCB-101 could be because these amphipods are not always bulk deposit-feeders, but are sometimes selective deposit-feeders, resulting in sediments being less representative. Indeed, selective feeding is

⁸ Including: PCB-118, -101, -52, -28, HCB and PeCB

common among invertebrates (Boon & Duineveld, 2011; Grahame, 1983). Therefore, by analysing bulk sediment samples, the food item's specific POP concentrations and patterns become “diluted” by other materials in the sediment. In fact, when investigating correlations between each specific compound, only PCB-52 and PCB-118 are correlated between amphipods and sediments. Thus, as selective feeders, investigations of the specific carbon sources might enhance interpretation of the seasonal contaminant pattern in *G. setosus*.

Results from multivariate statistics indicate that feeding on phytodetritus coincide with peak concentrations of group 1 congeners in May/June, and as the diet shifts towards faecal pellets, the concentrations decrease. This seasonal decrease could suggest that faecal pellets contain less contamination, possibly because of lower concentrations of dissolved POPs after the spring/ summer pulses from run-off, and/or that zooplankton have a limited ability to eliminate POPs through faecal excretion. Indeed, settling phytoplankton have been shown to be an important vertical flux of POPs to the benthic zone due to high uptake rates (Everaert et al., 2015; Knickmeyer & Steinhart, 1988; Söderström et al., 2000), while off-bloom situations seem to contribute less contamination to benthic habitats (Everaert et al., 2015). Thus, the results suggest that POPs are predominantly taken-up by diet, which is in accordance with experimental studies and field data (Boese et al., 1990; Borgå et al., 2002; Josefsson et al., 2011) and that diatom dominating phytodetritus may be their most contaminated food source.

Mismatch between contaminant loads in sediment and amphipods

Despite difficulties in distinguishing which sources caused a particular contamination load in biological compartments (Hutzinger et al., 1974), studies have successfully compared congener profiles between compartments to distinguish original sources (Bright et al., 1995; Hargrave et al., 2000; Morgan et al., 2010), illustrating that comparisons can be useful. When comparing compositional profiles of POPs between *G. setosus*, passive samples (deployed at F1 station (Figure 1) from May/June-August, 2018; Johansen (2019)), SPM from Adventelva (Johansen, 2019) and estuarine sediments from the City and North station, there is not a perfect match between any of the compartments. However, the closest “profile match” is with the dissolved fraction, thus a “pelagic signal” is found in *G. setosus*, which could indicate utilisation of phytoplankton that presumably adsorbs the dissolved fraction (Söderström et al., 2000). Again, these results lend support to the hypothesis that bulk sediment (if the precise food source is not collected) samples might not be the proper matrix to help interpret the

seasonal variation in *G. setosus*, despite the fact that these organisms are benthic deposit-feeding organisms.

Growth dilution

Higher chlorinated compounds, identified as group 2⁹ congeners in *G. setosus*, do not exhibit the same high concentrations in May and June as group 1 congeners but decrease seasonally. In contrast to the expectations, group 2 congeners are decoupled from the seasonal change in sediments as indicated by the multivariate analysis. Two processes working together are suggested to explain the seasonal decrease found in amphipods. Measurements from Adventfjorden show very low concentrations of the dissolved fraction of group 2 congeners in Adventfjorden (Johansen, 2019), which could result in low concentrations in phytoplankton as well. Experimental studies suggest that growth dilution due to increased lipid content might cause decreasing POP concentrations in deposit-feeding invertebrates (Granberg et al., 2008; Josefsson et al., 2011). Thus, utilisation of low contaminated food sources together with high growth rates, as *G. setosus* feed on nutritious food sources during the spring/summer, may result in growth dilution (e.g. Larsson et al., 1992). This, in turn, may cause seasonally lower concentrations of contaminants, as seen for both high and low chlorinated compounds in *G. setosus*.

Decreased bioavailability due to organic matter

Another factor that can result in a seasonal decline in POP concentrations is a reduction in the bioavailability of lipophilic compounds by binding to humic compounds (Carlberg et al., 1986; Larsson et al., 1992; McCarthy, 1983). Humic compounds originate from broken-down organic materials (Adey & Loveland, 2007), and riverine run-off can subsidise coastal ecosystems with allochthonous terrestrial humic compounds. Inputs of these substances and other inorganic material, contribute to the “browning” of water bodies, as seen in lakes and coastal areas (e.g. Aksnes et al., 2009; Finstad et al., 2016). Therefore with increasing riverine run-off, the bioavailability of POPs might decrease (Ripszam et al., 2015), and result in less uptake by diet and by direct partitioning (Black & McCarthy, 1988; Larsson et al., 1992), leading to a seasonal decrease of POP contamination in amphipods from the present study.

⁹ Including: PCB-180, -153 and -138

Riverine transport

Diet, especially diatoms, appear to be important source for the contamination peak of group 1 congeners in May and June in *G. setosus*. This overlaps with the hypothesised spring peak of less hydrophobic contaminants from snowmelt (Meyer & Wania, 2011), and thus, suggests that river transport might cause this contamination. Diatoms can grow in all of Adventfjorden but can become light-limited by the plume from river run-off. However, when the rivers start running, they first comprise of snowmelt from the precipitation of the previous winter, which has lower SPM load and dissolved organic matter than later in the season (McGovern et al., in prep). Indeed, Secchi depth (a proxy for water transparency) at station F1 in Adventfjorden (Figure 1) in May (when the river started running) is similar to the marine stations, and larger compared to later in the season (McGovern et al., in prep). Thus, phytoplankton close to the river outlets in May might be polluted with dissolved contaminants from snowmelt, and vertically transporting this to the benthic community. In fact, in alpine lakes, spring peaks of PCBs have been found in fish and the water column (Nellier et al., 2015; Perga et al., 2017). However, one cannot exclude the likely event that oceanic contaminants contributed to the contamination as these phytoplankton might be affected by both water masses. Thus, the timing of the spring bloom and riverine run-off appear to be important, since if these processes overlap, phytoplankton might function as a transport of terrestrial pollution to *G. setosus* and other benthic herbivores.

Measurements from Adventelva in August suggest that contaminants are coming in with glacial-fed rivers, however, the concentrations are generally low (Johansen, 2019). In regards to *G. setosus*, re-emissions of historically stored POPs in ice caps via riverine run-off, also hypothesised as “glacier hypothesis” or “delayed release hypothesis” by Bogdal et al. (2009), do not appear to increase concentrations in the amphipods during the study period. Nevertheless, they could still have contributed to a slower decline of POPs (Carlsson et al., 2018), but without earlier measurements, this is difficult to conclude. Moreover, how much and what layer of ice caps are melting that particular year might result in different amounts entering the coastal system, thus there might be significant inter-annual variations. However, as Adventelva and Longyearelva started running in May as a result of snowmelt, contaminants deposited on seasonal snow covered areas during the past winter of 2017/2018 entered the coastal system and likely resulted in a seasonal increase in less chlorinated POPs in *G. setosus*.

4.3.2 Mercury

Comparing with other studies

MeHg and totHg concentrations in *G. setosus* from the current study are within and below that of *Gammarus* amphipods from the littoral zone in the Canadian Arctic and sub-Arctic (Van Der Velden et al., 2012). The average fraction of MeHg relative to TotHg is 39%, which is similar to other invertebrates that are primary consumers (Morel et al., 1998). In addition, MeHg concentrations are in-between concentrations in various plankton and fish (cod and capelin) from the pelagic system in Kongsfjorden (Ruus et al., 2015), indicating low concentrations in amphipods, as expected based on trophic status. No seasonal studies of Hg concentrations in Arctic benthic invertebrates have been conducted/published, providing limited possibilities for seasonal comparisons among Arctic biota. Although there have been studies conducted in the Arctic pelagic system (e.g. Ruus et al., 2015), where, in contrast to *G. setosus*, plankton display highest Hg concentrations in July.

Decoupling

Studies on the biogeochemistry of Hg in estuarine ecosystems and experiments often show reduced accumulation of MeHg in biota with increased organic content in sediments, due to the tendency for Hg to bind to organic matter, which reduces bioavailability and partitioning (Buckman et al., 2019; Chen et al., 2009; Hammerschmidt et al., 2008; Muhaya et al., 1997; Taylor et al., 2012). MeHg concentrations in *G. setosus* in the present study are negatively correlated with TOC% in sediments, suggesting reduced accumulation with elevated organic carbon in sediments. Hammerschmidt et al. (2008) found that allochthonous-derived matter, such as terrestrial material, might have a higher affinity for MeHg, resulting in less bioavailable MeHg and a smaller flux of MeHg to the overlying water. Organic matter in Adventfjorden's estuarine sediments has a high proportion of terrestrially-derived material (82-83%) (Koziorowska et al., 2016), which could explain the observed seasonal decrease in MeHg concentrations as the season progress with more terrestrial run-off. However, the correlation between TOC% and MeHg is weak, and therefore, other variables, not measured in the current study, are more likely to influence the concentration to a greater extent. This could especially be true as *G. setosus* may be a selective deposit-feeder, and thus, the concentration of TOC nor Hg in bulk sediment samples might be adequate predictors. Indeed, in contrast to expectations, bulk sediment samples do not predict totHg nor MeHg concentrations in *G. setosus*. Decoupling between Hg concentrations in sediments and biota have also been found in other studies (Jędruch et al., 2019), especially for MeHg (Buckman et

al., 2017; Buckman et al., 2019; Chen et al., 2009; Taylor et al., 2019). Indeed, totHg concentrations in *G. setosus* appear to be primarily controlled by variations in MeHg concentrations and diatoms in diet. The importance of diet in controlling totHg concentrations have likewise been seen for various macrozoobenthos and zooplankton in temperate coastal zones (Beldowska & Mudrak-Cegiołka, 2017; Jędruch et al., 2019).

Bioavailability and terrestrial organic matter

Recent research has shown that MeHg and dissolved organic carbon concentrations in the water column influence MeHg concentrations in fish and certain invertebrates (Taylor et al., 2019). This suggests that the water column might be a more suitable matrix to sample for predicting concentrations in *G. setosus*, this may be particularly true in the current study since they feed on organic matter settled from the pelagic system. In fact, phytoplankton can bioconcentrate MeHg by about 10^5 times relative to seawater (Lee & Fisher, 2017; Schartup et al., 2017), and may provide an important contamination source (Lawrence & Mason, 2001). However, differences in the composition of dissolved organic matter can influence phytoplankton uptake of MeHg (Lee & Fisher, 2017; Schartup et al., 2015). Both experimental and field data suggest that terrestrial-derived dissolved organic matter can lower the bioavailability of MeHg, possibly by forming large complexes with MeHg that hinder uptake by cell membranes (Schartup et al., 2015). This lowering of bioavailability can result in a decreased uptake by bacteria and phytoplankton (Schartup et al., 2015). Thus, enhancement of terrestrial dissolved organic matter in Adventfjorden due to riverine run-off may explain the seasonal decrease in MeHg in *G. setosus*.

In lake sediments, enhancement of MeHg production has been detected in fresh chlorophyll, proteins and phytoplankton-derived cell wall lipids due to bacterial activity (Andrea et al., 2017). Thus, the slight increase in MeHg in June/July, which is later than the peak of less chlorinated POPs, could have resulted from *G. setosus* feeding on bacterial reworked phytodetritus.

Seasonal decrease and riverine run-off

Despite the fact that that Adventelva and Longyearelva appear to be important sources of Hg to Adventfjorden (Carrasco, 2019), Hg in *G. setosus* decreased seasonally. Although it is questionable if riverine-derived MeHg in fact is a large source, since just totHg was measured in these rivers, several studies suggest substantial MeHg contributions coming in with river

run-off (Graydon et al., 2009; Leitch et al., 2007; Loseto et al., 2004). High growth rates as a result of increased consumption of high-quality food may cause low metal concentrations in aquatic organisms (Karimi et al., 2010), as seen in zooplankton (Karimi et al., 2007) or fish (Wang & Wang, 2012). Reasonably, lowering of bioavailable Hg due to terrestrial dissolved organic matter and growth dilution due to intake of nutritious phytodetritus may act in concert, resulting in a seasonal decrease of totHg and MeHg concentrations in *G. setosus* inhabiting Adventfjorden.

4.3.3 Seasonality

Generally, all contaminants in *G. setosus* have lower concentrations in August compared to April. Without data for the whole year, one can only speculate if this seasonal decrease continues or not during the winter. However, it is likely that there are processes causing elevation during the winter time. This is because the decrease between April and August (on average) among the POP congeners and Hg is 64% and 50%, respectively, which is considerably higher than annual decreasing trends previously reported from the Arctic (AMAP, 2011; Rigét et al., 2019), and would have resulted in rapidly low concentrations. A study from the late 1990s on other primary consumer benthic invertebrates from Adventfjorden found higher POP concentrations than in the present study (Hop et al., 2001), which is in line with the long-term general decrease of POPs in the Arctic (Rigét et al., 2019). Mercury is poorly investigated in benthic invertebrates from the Arctic and no prior measurements in Adventfjorden have been conducted, thus no conclusion can be suggested for long-term trends of Hg in Adventfjorden.

Today, the Arctic is in rapid transition caused by climate change (IPCC, 2014), which has both direct and indirect effects on the Arctic environment. Direct effects include increased temperatures and changes in precipitation patterns, while indirect effects include melting icecaps, thawing permafrost, increased erosion, increased river discharge and melt season duration (Macdonald et al., 2005). Thus, climate change-induced increases in riverine run-off could alter contaminant exposure in receiving water bodies (Bogdal et al., 2010; Bogdal et al., 2009; Kallenborn et al., 2012a; Ripszam et al., 2015). Based on the results from the current study, increased riverine run-off might result in lower accumulation of contaminants in coastal biota. However, how climate change mediated effects might influence contamination in benthic organisms is complicated to predict and depends on many physiochemical and ecological factors.

5 Conclusions

The results from dietary descriptors reveal that pelagic primary and secondary production, bacteria, terrestrial- and macroalgae- derived material may contribute to the detrital “food bank” for *G. setosus*. Still, distinct seasonal signals are detected in *G. setosus*, where a clear “phytoplankton spring-bloom” and “off-bloom” diet is apparent. Together with lipid content data, dietary descriptors suggest utilisation of food sources that are available all year, although the results pointed towards some starvation.

Riverine run-off appears to affect both POPs and totHg contamination in Adventfjorden estuarine sediments, with a possible localised anthropogenic contamination of higher chlorinated POPs from Longyearbyen. However, the driver behind the seasonal changes in contamination differs between Hg and POPs. While totHg concentrations seem to be controlled by organic matter in the sediments, seasonal POP concentrations in sediments most likely reflect changes in seasonal concentrations of SPM from the river, deposition rates, grain size distributions and the sinking of pelagic production.

G. setosus appears to feed selectively in sediments, thus contaminant concentrations in bulk sediment samples and amphipods may be decoupled. Results suggest that settling of phytoplankton from the pelagic system might function as a vertical transport of terrestrial pollution to *G. setosus*, if the timing of the spring bloom and the spring pulse of less chlorinated POPs from riverine run-off overlap. The overall seasonal decrease in contaminant concentrations in *G. setosus* may be a combined result of growth dilution and lowered bioavailability due to terrestrial organic matter from riverine run-off. In regards to *G. setosus*, re-emissions of historically stored POPs in ice caps via riverine run-off do not appear to increase concentrations during the study period. However, as Adventelva and Longyearlva started running as a result of snowmelt, contaminants deposited on the snow during the previous winter entered the costal system and likely resulted in a spring increase of less chlorinated POPs in *G. setosus*. Global warming and further exploitation of land might increase the concentrations of long-range transported contaminants settling onto seasonal snow covered areas in the Arctic, which can enhance concentrations in the water column during the spring thaw with implications for the coastal ecosystem.

6 Future studies

The main aim of the present study was to investigate how seasonality and terrestrial run-off affect contamination concentrations in *G. setosus* from spring to autumn. However, it was challenging to determine how environmental conditions might influence contamination due to lack of proper compartment samples for pollutant analysis, no reference site (although not for lack of searching), and few water chemistry parameters investigated. Despite these challenges, other factors such as lipids, diet, and trophic status were thoroughly investigated. Nonetheless, in order to fully understand contaminant variation in benthic amphipods inhabiting a dynamic system like an estuary, parameters such as concentration and composition of dissolved organic matter, chlorophyll a, turbidity, river discharge, etc., should be included in future studies.

There is a vast knowledge gap regarding seasonal contaminant dynamics in the Arctic. The present study demonstrates that intra-annual processes are taking place in diet, physiological processes, environmental conditions and contamination dynamics, and studies that sample few time-points might overlook important differences. The present study merely covers five months, and completely exclude the winter season, which is a disadvantage. Future studies focusing on seasonality should consider high seasonal resolution sampling (similar to the current study), but over a whole year to broaden our understating.

Riverine run-off is predicted to increase in the future, and results from the current study suggest that this flux might function as a source of contaminants, but might also inhibit uptake. Future studies should consider investigating the influence of riverine run-off by measuring more water chemistry parameters and sampling several environmental compartments for contaminant analysis to connect this to biota.

Lastly, despite several monitoring programmes in the Arctic (e.g. AMAP), benthic invertebrates have received little attention, and more effort has been allocated to research on higher trophic level concentrations in the pelagic and the terrestrial ecosystem. Thus, in order to fully understand how contaminants flow through the Arctic system and given that benthic invertebrates are important food sources for some seabirds, marine mammals and fish, benthic invertebrates need more research.

References

- AAVSO. (2017). *Julian date (JD) calculator and calendars*. Retrieved 2019-03-05 from <https://www.aavso.org/jd-calculator>
- ACIA. (2005). *Arctic climate impact assessment. ACIA overview report*. Cambridge University Press, New York, NY, USA.
- Adey, W., & Loveland, K. (2007). *Dynamic aquaria: Building and restoring living ecosystems* (3rd ed.). London, UK: Academic Press.
- Aksnes, D. L., Dupont, N., Staby, A., Fiksen, Ø., Kaartvedt, S., & Aure, J. (2009). Coastal water darkening and implications for mesopelagic regime shifts in Norwegian fjords. *Marine Ecology Progress Series*, 387, 39-49.
- AMAP. (1998). *AMAP assessment report: Arctic pollution issues*. Arctic Monitoring and Assessment Programme (AMAP), Oslo, Norway.
- AMAP. (2004). *AMAP assessment 2002: Persistent organic pollutants in the Arctic*. Arctic Monitoring and Assessment Programme (AMAP), Oslo, Norway.
- AMAP. (2005). *AMAP assessment 2002: Heavy metals in the Arctic*. Arctic Monitoring and Assessment Programme (AMAP), Oslo, Norway.
- AMAP. (2011). *AMAP assessment 2011: Mercury in the Arctic*. Arctic Monitoring and Assessment Programme (AMAP), Oslo, Norway.
- AMAP. (2016). *AMAP assessment 2015: Temporal trends in persistent organic pollutants in the Arctic*. Arctic Monitoring and Assessment Programme (AMAP), Oslo, Norway.
- Amos, H. M., Jacob, D. J., Streets, D. G., & Sunderland, E. M. (2013). Legacy impacts of all-time anthropogenic emissions on the global mercury cycle. *Global Biogeochemical Cycles*, 27(2), 410-421.
- Andrea, G. B., Sylvain, B., Julie, T., Erik, B., Alejandro, M., & Stefan, B. (2017). Molecular composition of organic matter controls methylmercury formation in boreal lakes. *Nature Communications*, 8, 1-9.
- Arts, M. T., Brett, M. T., & Kainz, M. J. (2009). *Lipids in aquatic ecosystems*. New York, NY, USA: Springer.
- Baccarelli, A., Pfeiffer, R., Consonni, D., Pesatori, A. C., Bonzini, M., Patterson, D. G., . . . Landi, M. T. (2005). Handling of dioxin measurement data in the presence of non-detectable values: Overview of available methods and their application in the Seveso chloracne study. *Chemosphere*, 60(7), 898-906.
- Baeyens, W., Meuleman, C., Muhaya, B., & Leermakers, M. (1997). Behaviour and speciation of mercury in the Scheldt estuary (water, sediments and benthic organisms). *Hydrobiologia*, 366(1), 63-79.
- Barber, L. B., & Writer, J. H. (1998). Impact of the 1993 flood on the distribution of organic contaminants in bed sediments of the upper Mississippi River. *Environmental Science and Technology*, 32(14), 2077-2083.
- Beldowska, M., & Mudrak-Cegiołka, S. (2017). Mercury concentration variability in the zooplankton of the southern Baltic coastal zone. *Progress in Oceanography*, 159, 73-85.

- Beldowski, J., Miotk, M., Zaborska, A., & Pempkowiak, J. (2015). Distribution of sedimentary mercury off Svalbard, European Arctic. *Chemosphere*, 122, 190-198.
- Berge, J., Cottier, F., Last, K. S., Varpe, Ø., Leu, E., Søreide, J. E., . . . Brierley, A. S. (2009). Diel vertical migration of Arctic zooplankton during the polar night. *Biology Letters*, 5(1), 69-72.
- Berge, J., Renaud, P. E., Darnis, G., Cottier, F., Last, K., Gabrielsen, T. M., . . . Falk-Petersen, S. (2015). In the dark: A review of ecosystem processes during the Arctic polar night. *Progress in Oceanography*, 139, 258-271.
- Black, M. C., & McCarthy, J. F. (1988). Dissolved organic macromolecules reduce the uptake of hydrophobic organic contaminants by the gills of rainbow trout (*Salmo gairdneri*). *Environmental Toxicology and Chemistry*, 7(7), 593-600.
- Blais, J. M., Schindler, D. W., Muir, D. C. G., Sharp, M., Donald, D., Lafrenière, M., . . . Strachan, W. M. J. (2001). Melting glaciers: A major source of persistent organochlorines to subalpine Bow Lake in Banff National Park, Canada. *Ambio*, 30(7), 410-415.
- Boese, B. L., Lee Ii, H., Specht, D. T., Randall, R. C., & Winsor, M. H. (1990). Comparison of aqueous and solid-phase uptake for hexachlorobenzene in the tellinid clam *Macoma nasuta* (conrad): A mass balance approach. *Environmental Toxicology and Chemistry*, 9(2), 221-231.
- Bogdal, C., Nikolic, D., Lüthi, M. P., Schenker, U., Scheringer, M., & Hungerbühler, K. (2010). Release of legacy pollutants from melting glaciers: Model evidence and conceptual understanding. *Environmental Science & Technology*, 44(11), 4063-4069.
- Bogdal, C., Schmid, P., Zennegg, M., Anselmetti, F. S., Scheringer, M., & Hungerbühler, K. (2009). Blast from the past: Melting glaciers as a relevant source for persistent organic pollutants. *Environmental Science & Technology*, 43(21), 8173-8177.
- Boon, A. R., & Duineveld, G. C. A. (2011). Phytopigments and fatty acids in the gut of the deposit-feeding heart urchin *Echinocardium cordatum* in the southern North Sea: Selective feeding and its contribution to the benthic carbon budget. *Journal of Sea Research*, 67(1), 77-84.
- Borgå, K., Fisk, A. T., Hoekstra, P. F., & Muir, D. C. G. (2004). Biological and chemical factors of importance in the bioaccumulation and trophic transfer of persistent organochlorine contaminants in arctic marine food webs. *Environmental Toxicology and Chemistry*, 23(10), 2367-2385.
- Borgå, K., Gabrielsen, G. W., & Skaare, J. U. (2001). Biomagnification of organochlorines along a Barents Sea food chain. *Environmental Pollution*, 113(2), 187-198.
- Borgå, K., Poltermann, M., Polder, A., Pavlova, O., Gulliksen, B., Gabrielsen, G. W., & Skaare, J. U. (2002). Influence of diet and sea ice drift on organochlorine bioaccumulation in Arctic ice-associated amphipods. *Environmental Pollution*, 117(1), 47-60.
- Braaten, H. F. V., Harman, C., Øverjordet, I. B., & Larssen, T. (2014). Effects of sample preparation on methylmercury concentrations in Arctic organisms. *International Journal of Environmental Analytical Chemistry*, 94(9), 1-11.
- Breivik, K., Alcock, R., Li, Y. F., Bailey, R. E., Fiedler, H., & Pacyna, J. M. (2004). Primary sources of selected POPs: Regional and global scale emission inventories. *Environmental Pollution*, 128(1), 3-16.

- Bright, D. A., Dushenko, W. T., Grundy, S. L., & Reimer, K. J. (1995). Effects of local and distant contaminant sources: Polychlorinated biphenyls and other organochlorines in bottom-dwelling animals from an Arctic estuary. *Science of the Total Environment*, 160-161, 265-283.
- Bring, A., Fedorova, I. V., Dibike, Y. B., Hinzman, L., Mård, J., Mernild, J. S. H., . . . Woo, M. (2016). Arctic terrestrial hydrology: A synthesis of processes, regional effects, and research challenges. *Journal of Geophysical Research - Biogeosciences*, 121(3), 621-649.
- Bro, R., & Smilde, A. K. (2014). Principal component analysis. *Analytical Methods*, 6(9), 2812-2831.
- Buckman, K., Taylor, V., Broadley, H., Hocking, D., Balcom, P., Mason, R., . . . Chen, C. (2017). Methylmercury bioaccumulation in an urban estuary: Delaware River, USA. *Estuaries and Coasts*, 40(5), 1358-1370.
- Buckman, K. L., Seelen, E. A., Mason, R. P., Balcom, P., Taylor, V. F., Ward, J. E., & Chen, C. Y. (2019). Sediment organic carbon and temperature effects on methylmercury concentration: A mesocosm experiment. *Science of the Total Environment*, 666, 1316-1326.
- Budge, S. M., Iverson, S. J., & Koopman, H. N. (2006). Studying trophic ecology in marine ecosystems using fatty acids: A primer on analysis and interpretation. *Marine Mammal Science*, 22(4), 759-801.
- Budge, S. M., & Parrish, C. C. (1998). Lipid biogeochemistry of plankton, settling matter and sediments in Trinity Bay, Newfoundland. II. Fatty acids. *Organic Geochemistry*, 29(5-7), 1547-1559.
- Burkow, I. C., & Kallenborn, R. (2000). Sources and transport of persistent pollutants to the Arctic. *Toxicology Letters*, 112-113, 87-92.
- Bühning, S. I., & Christiansen, B. (2001). Lipids in selected abyssal benthopelagic animals: Links to the epipelagic zone? *Progress in Oceanography*, 50(1), 369-382.
- Carabel, S., Godínez-Domínguez, E., Verísimo, P., Fernández, L., & Freire, J. (2006). An assessment of sample processing methods for stable isotope analyses of marine food webs. *Journal of Experimental Marine Biology and Ecology*, 336(2), 254-261.
- Carlberg, G., Martinsen, K., Kringstad, A., Gjessing, E., Grande, M., Källqvist, T., & Skåre, J. (1986). Influence of aquatic humus on the bioavailability of chlorinated micropollutants in Atlantic salmon. *Archives of Environmental Contamination and Toxicology*, 15(5), 543-548.
- Carlsson, P., Breivik, K., Brorström-Lundén, E., Cousins, I., Christensen, J., Grimalt, J., . . . Wöhrnschimmel, H. (2018). Polychlorinated biphenyls (PCBs) as sentinels for the elucidation of Arctic environmental change processes: A comprehensive review combined with ArcRisk project results. *Environmental Science and Pollution Research*, 25(23), 22499-22528.
- Carlsson, P., Cornelissen, G., Bøggild, C. E., Rysgaard, S., Mortensen, J., & Kallenborn, R. (2012). Hydrology-linked spatial distribution of pesticides in a fjord system in Greenland. *Journal of Environmental Monitoring*, 14(5), 1437-1443.
- Carrasco, N. (2019). *Seasonality in mercury bioaccumulation in particulate organic matter and zooplankton in a river-influenced Arctic fjord (Adventfjord, Svalbard)* (Master's thesis). Tromsø: Department of Arctic and Marine Biology, University of Tromsø.

- Carrizo, D., Gustafsson, Ö., & Carrizo, D. (2011). Pan-arctic river fluxes of polychlorinated biphenyls. *Environmental Science & Technology*, 45(19), 8377-8384.
- Cazes, J. (2004). *Encyclopedia of chromatography*. New York, NY, USA: Marcel Dekker.
- Chan, H. M., Scheuhammer, A. M., Ferran, A., Loupelle, C., Holloway, J., & Weech, S. (2003). Impacts of mercury on freshwater fish-eating wildlife and humans. *Human and Ecological Risk Assessment: An International Journal*, 9(4), 867-883.
- Chen, C. Y., Borsuk, M. E., Bugge, D. M., Hollweg, T., Balcom, P. H., Ward, D. M., . . . Mason, R. P. (2014). Benthic and pelagic pathways of methylmercury bioaccumulation in estuarine food webs of the northeast United States. *PLoS ONE*, 9(2), 1-11.
- Chen, C. Y., Dionne, M., Mayes, B. M., Ward, D. M., Sturup, S., & Jackson, B. P. (2009). Mercury bioavailability and bioaccumulation in estuarine food webs in the Gulf of Maine. *Environmental Science & Technology*, 43(6), 1804-1810.
- Chételat, J., Amyot, M., Cloutier, L., Poulain, A., & Chételat, J. (2008). Metamorphosis in chironomids, more than mercury supply, controls methylmercury transfer to fish in high Arctic lakes. *Environmental Science & Technology*, 42(24), 9110-9115.
- Chouvelon, T., Cresson, P., Bouchoucha, M., Brach-Papa, C., Bustamante, P., Crochet, S., . . . Knoery, J. (2018). Oligotrophy as a major driver of mercury bioaccumulation in medium-to high-trophic level consumers: A marine ecosystem-comparative study. *Environmental Pollution*, 233, 844-854.
- Compeau, G. C., & Bartha, R. (1985). Sulfate-reducing bacteria: Principal methylators of mercury in anoxic estuarine sediment. *Applied and Environmental Microbiology*, 50(2), 498-502.
- Crossland, C. J., Kremer, H. H., Lindeboom, H. J., Marshall Crossland, J. I., & Tissier, M. D. A. (Eds.). (2005). *Coastal fluxes in the Anthropocene: The land-ocean interactions in the coastal zone project of the international geosphere-biosphere programme*. Berlin, Germany: Springer.
- Dalsgaard, J., St. John, M., Kattner, G., Müller-Navarra, D., & Hagen, W. (2003). Fatty acid trophic markers in the pelagic marine environment. *Advances in Marine Biology*, 46, 225-340.
- De Souza Machado, A. A., Spencer, K., Kloas, W., Toffolon, M., & Zarfl, C. (2016). Metal fate and effects in estuaries: A review and conceptual model for better understanding of toxicity. *Science of the Total Environment*, 541, 268-281.
- DeNiro, M. J., & Epstein, S. (1977). Mechanism of carbon isotope fractionation associated with lipid synthesis. *Science*, 197(4300), 261-263.
- Dietz, R., Outridge, P. M., & Hobson, K. A. (2009). Anthropogenic contributions to mercury levels in present-day Arctic animals-A review. *Science of the Total Environment*, 407(24), 6120-6131.
- Doi, H., Akamatsu, F., & González, A. L. (2017). Correction to ‘Starvation effects on nitrogen and carbon stable isotopes of animals: an insight from meta-analysis of fasting experiments’. *Royal Society Open Science*, 4(11), 1-10.
- Dommergue, A., Larose, C., Faïn, X., Clarisse, O., Foucher, D., Hintelmann, H., . . . Ferrari, C. P. (2010). Deposition of mercury species in the Ny-Ålesund area (79°N) and their transfer during snowmelt. *Environmental Science & Technology*, 44(3), 901-907.

- Drevnick, P. E., Yang, H., Lamborg, C. H., & Rose, N. L. (2012). Net atmospheric mercury deposition to Svalbard: Estimates from lacustrine sediments. *Atmospheric Environment*, 59, 509-513.
- Dunton, K. H., Schonberg, S., & Cooper, L. (2012). Food web structure of the Alaskan nearshore shelf and estuarine lagoons of the Beaufort Sea. *Estuaries and Coasts*, 35(2), 416-435.
- Dunton, K. H., Weingartner, T., & Carmack, E. C. (2006). The nearshore western Beaufort Sea ecosystem: Circulation and importance of terrestrial carbon in Arctic coastal food webs. *Progress in Oceanography*, 71(2), 362-378.
- Eilertsen, H. C., & Frantzen, S. (2007). Phytoplankton from two sub-Arctic fjords in northern Norway 2002–2004: I. Seasonal variations in chlorophyll a and bloom dynamics. *Marine Biology Research*, 3(5), 319-332.
- Evenset, A., Christensen, G. N., & Palerud, R. (2009). *Miljøgifter i marine sedimenter i Isfjorden, Svalbard 2009. Undersøkelser utenfor Longyearbyen, Barentsburg, Pyramiden og Colesbukta* [In norwegian]. Akvaplan-niva rapport- 4707-1.
- Evenset, A., Christensen, G. N., & Palerud, R. (2006). *Miljøgifter i marine sedimenter, Isfjorden, Svalbard 2005* [In norwegian]. Akvaplan-niva rapport- 414.3341.
- Evenset, A., Hallanger, I. G., Tessmann, M., Warner, N., Ruus, A., Borgå, K., . . . Renaud, P. E. (2016). Seasonal variation in accumulation of persistent organic pollutants in an Arctic marine benthic food web. *Science of the Total Environment*, 542, 108-120.
- Everaert, G., De Laender, F., Goethals, P. L. M., & Janssen, C. R. (2015). Multidecadal field data support intimate links between phytoplankton dynamics and PCB concentrations in marine sediments and biota. *Environmental Science & Technology*, 49(14), 8704-8711.
- Evers, D. C., Keane, S. E., Basu, N., & Buck, D. (2016). Evaluating the effectiveness of the Minamata Convention on Mercury: Principles and recommendations for next steps. *Science of the Total Environment*, 569-570, 888-903.
- Falk-Petersen, S., Sargent, J. R., Henderson, J., Hegseth, E. N., Hop, H., & Okolodkov, Y. B. (1998). Lipids and fatty acids in ice algae and phytoplankton from the marginal ice zone in the Barents Sea. *Polar Biology*, 20(1), 41-47.
- Findlay, R. H., Trexler, M. B., Guckert, J. B., & White, D. C. (1990). Laboratory study of disturbance in marine sediments: Response of a microbial community. *Marine Ecology Progress Series*, 62, 121-133.
- Finstad, A. G., Andersen, T., Larsen, S., Tominaga, K., Blumentrath, S., de Wit, H., . . . Hessen, D. O. (2016). From greening to browning: Catchment vegetation development and reduced S-deposition promote organic carbon load on decadal time scales in Nordic lakes. *Science reports*, 6, 1-8.
- Fitzgerald, W. F., & Lamborg, C. H. (2007). Geochemistry of mercury in the environment. In H. D. Holland & K. K. Turekian (Eds.), *Treatise on Geochemistry*. Oxford, UK: Pergamon.
- Fitzgerald, W. F., Lamborg, C. H., & Hammerschmidt, C. R. (2007). Marine biogeochemical cycling of mercury. *Chemical review*, 107(2), 641-662.
- Folch, J., Lees, M., & Sloane Stanley, G. H. (1957). A simple method for the isolation and purification of total lipides from animal tissues. *The Journal of Biological Chemistry*, 226(1), 497-509.

- Forbes, T. L., Hansen, R., & Kure, L. K. (1998). Relative role of pore water versus ingested sediment in bioavailability of organic contaminants in marine sediments. *Environmental Toxicology and Chemistry*, 17(12), 2453-2462.
- Forest, A., Galindo, V., Darnis, G., Pineault, S., Lalande, C., Tremblay, J., & Fortier, L. (2011). Carbon biomass, elemental ratios (C:N) and stable isotopic composition ($\delta^{13}\text{C}$, $\delta^{15}\text{N}$) of dominant calanoid copepods during the winter-to-summer transition in the Amundsen Gulf (Arctic Ocean). *Journal of Plankton Research*, 33(1), 161-178.
- Fox, A. L., Hughes, E. A., Trocine, R. P., Trefry, J. H., Schonberg, S. V., McTigue, N. D., . . . Cooper, L. W. (2014). Mercury in the northeastern Chukchi Sea: Distribution patterns in seawater and sediments and biomagnification in the benthic food web. *Deep-Sea Research Part II*, 102, 56-67.
- Fry, B. (2006). *Stable isotope ecology*. New York, NY, USA: Springer.
- Fry, B., & Sherr, E. B. (1989). $\delta^{13}\text{C}$ Measurements as indicators of carbon flow in marine and freshwater ecosystems. In P. W. Rundel, J. R. Ehleringer & K. A. Nagy (Eds.), *Stable isotopes in ecological research*. New York, NY, USA: Springer.
- Gannes, L., O'Brien, D., & Del Rio, C. (1997). Stable isotopes in animal ecology: Assumptions, caveats, and a call for more laboratory experiments. *Ecology*, 78(4), 1271-1276.
- Garmash, O., Hermanson, M. H., Isaksson, E., Schwikowski, M., Divine, D., Teixeira, C., . . . Garmash, O. (2013). Deposition history of polychlorinated biphenyls to the Lomonosovfonna Glacier, Svalbard: A 209 congener analysis. *Environmental Science & Technology*, 47(21), 12064-12072.
- Gjærevoll, O., Rønning, O. I., & Binns, R. (1999). *Flowers of Svalbard* (2nd ed.) [In norwegian]. Trondheim, Norway: Tapir.
- Graeve, M., Dauby, P., & Scailteur, Y. (2001). Combined lipid, fatty acid and digestive tract content analyses: A penetrating approach to estimate feeding modes of Antarctic amphipods. *Polar Biology*, 24(11), 853-862.
- Graeve, M., Kattner, G., & Piepenburg, D. (1997). Lipids in Arctic benthos: Does the fatty acid and alcohol composition reflect feeding and trophic interactions? *Polar Biology*, 18(1), 53-61.
- Grahame, J. (1983). Adaptive aspects of feeding mechanisms. In D. Bliss, F. J. Vernberg & W. B. Vernberg (Eds.), *The Biology of crustacea: Environmental adaptations*. New York, NY, USA: Academic Press.
- Granberg, M. E., Gunnarsson, J. S., Hedman, J. E., Rosenberg, R., Jonsson, P., & Granberg, M. E. (2008). Bioturbation-driven release of organic contaminants from Baltic Sea sediments mediated by the invading polychaete *Marenzelleria neglecta*. *Environmental Science & Technology*, 42(4), 1058-1065.
- Graydon, J. A., Emmerton, C. A., Lesack, L. F. W., & Kelly, E. N. (2009). Mercury in the Mackenzie river delta and estuary: Concentrations and fluxes during open-water conditions. *Science of the Total Environment*, 407(8), 2980-2988.
- Grebmeier, J., Mcroy, C., & Feder, H. (1988). Pelagic-benthic coupling on the shelf of the northern Bering and Chukchi Seas. I. Food supply source and benthic biomass. *Marine Ecology Progress Series*, 48, 57-67.

- Green, N., Molvær, J., Kaste, Ø., Schrum, C., Yakushev, E., Sørensen, K., . . . Brungot, A. L. (2010). *Pollution monitoring programme 2009. Monitoring of supply of contaminants and environmental conditions in the Barents Sea and Lofoten area*. Climate and Pollution Agency (Klif), Report TA- 2660/2010, NIVA report- 5980-2010.
- Greenacre, M., & Primicerio, R. (2013). *Multivariate analysis of ecological data*. Bilbao, Spain: Fundación BBVA.
- Gu, B. (2009). Variations and controls of nitrogen stable isotopes in particulate organic matter of lakes. *Oecologia*, 160(3), 421-431.
- Guckert, J. B., Antworth, C. P., Nichols, P. D., & White, D. C. (1985). Phospholipid, ester-linked fatty acid profiles as reproducible assays for changes in prokaryotic community structure of estuarine sediments. *FEMS Microbiology Letters*, 31(3), 147-158.
- Hagen, W., & Auel, H. (2001). Seasonal adaptations and the role of lipids in oceanic zooplankton. *Zoology*, 104(3-4), 313-326.
- Hallanger, I. G., Ruus, A., Herzke, D., Warner, N. A., Evenset, A., Heimstad, E. S., . . . Borgå, K. (2011a). Influence of season, location, and feeding strategy on bioaccumulation of halogenated organic contaminants in Arctic marine zooplankton. *Environmental Toxicology and Chemistry*, 30(1), 77-87.
- Hallanger, I. G., Warner, N., Ruus, A., Evenset, A., Christensen, G., Herzke, D., . . . Borgå, K. (2011b). Seasonality in contaminant accumulation in Arctic marine pelagic food webs using trophic magnification factor as a measure of bioaccumulation. *Environmental Toxicology and Chemistry*, 30(5), 1026-1035.
- Hammerschmidt, C. R., Fitzgerald, W. F., Balcom, P. H., & Visscher, P. T. (2008). Organic matter and sulfide inhibit methylmercury production in sediments of New York/New Jersey harbor. *Marine Chemistry*, 109(1-2), 165-182.
- Hammerschmidt, C. R., Fitzgerald, W. F., & Hammerschmidt, C. R. (2004). Geochemical controls on the production and distribution of methylmercury in near-shore marine sediments. *Environmental Science & Technology*, 38(5), 1487-1495.
- Hare, A., Stern, G. A., Macdonald, R. W., Kuzyk, Z. Z., & Wang, F. (2008). Contemporary and preindustrial mass budgets of mercury in the Hudson Bay marine system: The role of sediment recycling. *Science of the Total Environment*, 406(1), 190-204.
- Hargrave, B. T., Phillips, G. A., Vass, W. P., Bruecker, P., Welch, H. E., & Siferd, T. D. (2000). Seasonality in bioaccumulation of organochlorines in lower trophic level arctic marine biota. *Environmental Science & Technology*, 34(6), 980-987.
- Harris, C. M., McTigue, N. D., McClelland, J. W., & Dunton, K. H. (2018). Do high Arctic coastal food webs rely on a terrestrial carbon subsidy? *Food Webs*, 15, 1-14.
- Harris, D., Horwath, W., & Van Kessel, C. (2001). Acid fumigation of soils to remove carbonates prior to total organic carbon or carbon-13 isotopic analysis. *Soil Science Society of America Journal*, 65(6), 1853-1856.
- Hegseth, E. N. (1998). Primary production of the northern Barents Sea. *Polar Research*, 17(2), 113-123.
- Helsel, D. (2010). Much ado about next to nothing: Incorporating nondetects in science. *Annals of Occupational Hygiene*, 54(3), 257-262.

- Hermanson, M. H., Isaksson, E., Teixeira, C., Muir, D. C. G., Compher, K. M., Li, Y. F., . . . Hermanson, M. H. (2005). Current-use and legacy pesticide history in the Austfonna Ice Cap, Svalbard, Norway. *Environmental Science & Technology*, 39(21), 8163-8169.
- Hintelmann, H., & Nguyen, H. (2005). Extraction of methylmercury from tissue and plant samples by acid leaching. *Analytical and Bioanalytical Chemistry*, 381(2), 360-365.
- Hisdal, V. (1985). *Geography of Svalbard* (2nd ed.). Oslo, Norway: Norsk Polarinstitut.
- Hobson, K. A., Alisauskas, R. T., & Clark, R. G. (1993). Stable-nitrogen isotope enrichment in avian tissues due to fasting and nutritional stress: Implications for isotopic analyses of diet. *The Condor*, 95(2), 388-394.
- Hobson, K. A., Ambrose, W. G., & Renaud, P. E. (1995). Sources of primary production, benthic-pelagic coupling, and trophic relationships within the Northeast Water Polynya: Insights from $\delta^{13}\text{C}$ and $\delta^{15}\text{N}$ analysis. *Marine Ecology Progress Series*, 128(1-3), 1-10.
- Holden, A. V., & Marsden, K. (1967). Organochlorine pesticides in seals and porpoises. *Nature*, 216(5122), 1274-1276.
- Holte, B., Dahle, S., Gulliksen, B., & Næs, K. (1996). Some macrofaunal effects of local pollution and glacier-induced sedimentation, with indicative chemical analyses, in the sediments of two Arctic fjords. *Polar Biology*, 16(8), 549-557.
- Hop, H., Borgå, K., Gabrielsen, G., Kleivane, L., & Skaare, J. (2002). Food web magnification of persistent organic pollutants in poikilotherms and homeotherms from the Barents Sea. *Environmental Science & Technology*, 36(12), 2589-2597.
- Hop, H., Sagerup, K., Schlabach, M., & Gabrielsen, G. W. (2001). *Persistent organic pollutants in marine macro-benthos near urban settlements in Svalbard: Longyearbyen, Pyramiden, Barentsburg, and Ny-Ålesund*. Norsk Polarinstitut internrapport- nr. 8.
- Hummel, H., Bogaards, R. H., Nieuwenhuize, J., De Wolf, L., & Van Liere, J. M. (1990). Spatial and seasonal differences in the PCB content of the mussel *Mytilus edulis*. *Science of the Total Environment*, 92, 155-163.
- Hung, C., Gong, G., Ko, F., Chen, H., Hsu, M., Wu, J., . . . Santschi, P. H. (2010). Relationships between persistent organic pollutants and carbonaceous materials in aquatic sediments of Taiwan. *Marine Pollution Bulletin*, 60(7), 1010-1017.
- Hung, H., Katsoyiannis, A. A., Brorström-Lundén, E., Olafsdottir, K., Aas, W., Breivik, K., . . . Wilson, S. (2016). Temporal trends of persistent organic pollutants (POPs) in arctic air: 20 years of monitoring under the Arctic monitoring and assessment programme (AMAP). *Environmental Pollution*, 217, 52-61.
- Hutzinger, O., Safe, S., & Zitko, V. (1974). *The chemistry of PCB's*. Boca Raton, Fla, USA: CRC Press.
- Iken, K., Bluhm, B., & Dunton, K. (2010). Benthic food-web structure under differing water mass properties in the southern Chukchi Sea. *Deep-Sea Research Part II*, 57(1), 71-85.
- IPCC. (2014). *Climate change 2014: Synthesis report. Contribution of working groups I, II and III to the fifth assessment report of the intergovernmental panel on climate change [core writing team, R.K. Pachauri and L.A. Meyer (eds.)]*. IPCC, Geneva, Switzerland.
- Jartun, M., Ottesen, R. T., Volden, T., & Lundkvist, Q. (2009). Local Sources of polychlorinated biphenyls (PCB) in russian and norwegian settlements on Spitsbergen Island, Norway. *Journal of Toxicology and Environmental Health, Part A*, 72(3-4), 284-294.

- Jiang, S., Liu, X., & Chen, Q. (2011). Distribution of total mercury and methylmercury in lake sediments in Arctic Ny-Ålesund. *Chemosphere*, 83(8), 1108-1116.
- Johansen, S. F. (2019). *Riverine inputs of polychlorinated biphenyls (PCBs) and chlorobenzenes to Isfjorden, Svalbard; Implications for spatial distribution and bioavailability* (Master's thesis). Ås: Department of Chemistry, Biotechnology and Food Science, Norwegian University of Life Science.
- Jonsson, S., Skjellberg, U., Nilsson, M. B., Lundberg, E., Andersson, A., & Björn, E. (2014). Differentiated availability of geochemical mercury pools controls methylmercury levels in estuarine sediment and biota. *Nature Communications*, 5(1), 1-10.
- Josefsson, S., Leonardsson, K., Gunnarsson, J. S., & Wiberg, K. (2011). Influence of contaminant burial depth on the bioaccumulation of PCBs and PBDEs by two benthic invertebrates (*Monoporeia affinis* and *Marenzelleria* spp.). *Chemosphere*, 85(9), 1444-1451.
- Jędruch, A., Beldowska, M., & Ziolkowska, M. (2019). The role of benthic macrofauna in the trophic transfer of mercury in a low-diversity temperate coastal ecosystem (Puck Lagoon, southern Baltic Sea). *Environmental Monitoring and Assessment*, 191(3), 1-25.
- Kaag, N. H. B. M., Foekema, E. M., & Scholten, M. C. T. (1997). Comparison of contaminant accumulation in three species of marine invertebrates with different feeding habits. *Environmental Toxicology and Chemistry*, 16(5), 837-842.
- Kaiser, J., Enserink, M., & Kaiser, J. (2000). Environmental toxicology. Treaty takes a POP at the dirty dozen. *Science*, 290(5499), 2053.
- Kallenborn, R., Halsall, C., Dellong, M., & Carlsson, P. (2012a). The influence of climate change on the global distribution and fate processes of anthropogenic persistent organic pollutants. *Journal of Environmental Monitoring*, 14(11), 2854-2869.
- Kallenborn, R., Ottesen, R. T., Gabrielsen, G. W., Schrum, C., Evenset, A., Ruus, A., . . . Lundkvist, Q. (2012b). *PCB på Svalbard: Rapport 2011* [In norwegian]. Sysselmannen på Svalbard rapport- 2011.
- Karickhoff, S. W., Brown, D. S., & Scott, T. A. (1979). Sorption of hydrophobic pollutants on natural sediments. *Water Research*, 13(3), 241-248.
- Karimi, R., Chenen, C. Y., Pickhardt, P. C., Fisher, N. S., & Folt, C. L. (2007). Stoichiometric controls of mercury dilution by growth. *Proceedings of the National Academy of Sciences*, 104(18), 7477-7482.
- Karimi, R., Fisher, N. S., & Folt, C. L. (2010). Multielement stoichiometry in aquatic invertebrates: When growth dilution matters. *The American Naturalist*, 176(6), 699-709.
- Kaufman, M., Gradinger, R., Bluhm, B., & O'Brien, D. (2008). Using stable isotopes to assess carbon and nitrogen turnover in the Arctic sympagic amphipod *Onisimus litoralis*. *Oecologia*, 158(1), 11-22.
- Kelly, J. R., & Scheibling, R. E. (2012). Fatty acids as dietary tracers in benthic food webs. *Marine Ecology Progress Series*, 446, 1-22.
- Kharlamenko, V. I., Kiyashko, S. I., Imbs, A. B., & Vyshkvartzev, D. I. (2001). Identification of food sources of invertebrates from the seagrass *Zostera marina* community using carbon and sulfur stable isotope ratio and fatty acid analyses. *Marine Ecology Progress Series*, 220, 103-117.

- Kidd, K. A., Muir, D. C. G., Evans, M. S., Wang, X., Whittle, M., Swanson, H. K., . . . Guildford, S. (2012). Biomagnification of mercury through lake trout (*Salvelinus namaycush*) food webs of lakes with different physical, chemical and biological characteristics. *Science of the Total Environment*, 438, 135-143.
- Kim, E., Kim, H., Shin, K. H., Kim, M. S., Kundu, S. R., Lee, B. G., & Han, S. (2012). Biomagnification of mercury through the benthic food webs of a temperate estuary: Masan Bay, Korea. *Environmental Toxicology and Chemistry*, 31(6), 1254-1263.
- Kirk, J. L., Lehnherr, I., Andersson, M., Braune, B. M., Chan, L., Dastoor, A. P., . . . St. Louis, V. L. (2012). Mercury in Arctic marine ecosystems: Sources, pathways, and exposure. *Environmental Research*, 119, 64-87.
- Knickmeyer, R., & Steinhart, H. (1988). Cyclic organochlorines in the hermit crabs *Pagurus bernhardus* and *P. pubescens* from the North Sea. A comparison between winter and early summer situation. *Netherlands Journal of Sea Research*, 22(3), 237-251.
- Koziorowska, K., Kuliński, K., & Pempkowiak, J. (2016). Sedimentary organic matter in two Spitsbergen fjords: Terrestrial and marine contributions based on carbon and nitrogen contents and stable isotopes composition. *Continental Shelf Research*, 113, 38-46.
- Kędra, M., Legeżyńska, J., & Walkusz, W. (2011). Shallow winter and summer macrofauna in a high Arctic fjord (79° N, Spitsbergen). *Marine Biodiversity*, 41(3), 425-439.
- Larsson, P., Collvin, L., Okla, L., & Meyer, G. (1992). Lake productivity and water chemistry as governors of the uptake of persistent pollutants in fish. *Environmental Science & Technology*, 26(2), 346-352.
- Lavoie, R. A., Jardine, T. D., Chumchal, M. M., Kidd, K. A., & Campbell, L. M. (2013). Biomagnification of mercury in aquatic food webs: a worldwide meta-analysis. *Environmental Science & Technology*, 47(23), 13385-13394.
- Lawrence, A. L., & Mason, R. P. (2001). Factors controlling the bioaccumulation of mercury and methylmercury by the estuarine amphipod *Leptocheirus plumulosus*. *Environmental Pollution*, 111(2), 217-231.
- Lee, C., & Fisher, N. S. (2017). Bioaccumulation of methylmercury in a marine diatom and the influence of dissolved organic matter. *Marine Chemistry*, 197, 70-79.
- Legeżyńska, J., Kędra, M., & Walkusz, W. (2012). When season does not matter: Summer and winter trophic ecology of Arctic amphipods. *Hydrobiologia*, 684(1), 189-214.
- Legeżyńska, J., Kędra, M., & Walkusz, W. (2014). Identifying trophic relationships within the high Arctic benthic community: How much can fatty acids tell? *Marine Biology Research*, 161(4), 821-836.
- Lehnherr, I., St Louis, V. L., Hintelmann, H., & Kirk, J. L. (2011). Methylation of inorganic mercury in polar marine waters. *Nature Geoscience*, 4(5), 298-302.
- Leitch, D. R., Carrie, J., Lean, D., Macdonald, R. W., Stern, G. A., & Wang, F. (2007). The delivery of mercury to the Beaufort Sea of the Arctic Ocean by the Mackenzie River. *Science of the Total Environment*, 373(1), 178-195.
- Letcher, R. J., Bustnes, J. O., Dietz, R., Jenssen, B. M., Jørgensen, E. H., Sonne, C., . . . Gabrielsen, G. W. (2010). Exposure and effects assessment of persistent organohalogen contaminants in arctic wildlife and fish. *Science of the Total Environment*, 408(15), 2995-3043.

- Leu, E., Søreide, J. E., Hessen, D. O., Falk-Petersen, S., & Berge, J. (2011). Consequences of changing sea-ice cover for primary and secondary producers in the European Arctic shelf seas: Timing, quantity, and quality. *Progress in Oceanography*, 90(1), 18-32.
- Liu, Y., Chai, X., Hao, Y., Gao, X., Lu, Z., Zhao, Y., . . . Cai, M. (2015). Total mercury and methylmercury distributions in surface sediments from Kongsfjorden, Svalbard, Norwegian Arctic. *Environmental Science and Pollution Research*, 22(11), 8603-8610.
- Loseto, L. L., Lean, D. R. S., & Siciliano, S. D. (2004). Snowmelt sources of methylmercury to high Arctic ecosystems. *Environmental Science & Technology*, 38(11), 3004-3010.
- Lu, Z., Cai, M., Wang, J., Yin, Z., & Yang, H. (2013). Levels and distribution of trace metals in surface sediments from Kongsfjorden, Svalbard, Norwegian Arctic. *Environmental Geochemistry and Health*, 35(2), 257-269.
- Macdonald, R. W., Barrie, L. A., Bidleman, T. F., Diamond, M. L., Gregor, D. J., Semkin, R. G., . . . Yunker, M. B. (2000). Contaminants in the Canadian Arctic: 5 years of progress in understanding sources, occurrence and pathways. *Science of The Total Environment*, 254(2-3), 93-234.
- Macdonald, R. W., Harner, T., & Fyfe, J. (2005). Recent climate change in the Arctic and its impact on contaminant pathways and interpretation of temporal trend data. *Science of the Total Environment*, 342(1), 5-86.
- Macko, S. A., Fogel, M. L., Hare, P. E., & Hoering, T. C. (1987). Isotopic fractionation of nitrogen and carbon in the synthesis of amino acids by microorganisms. *Chemical Geology: Isotope Geoscience Section*, 65(1), 79-92.
- Mayzaud, P., Boutoute, M., Noyon, M., Narcy, F., & Gasparini, S. (2013). Lipid and fatty acids in naturally occurring particulate matter during spring and summer in a high Arctic fjord (Kongsfjorden, Svalbard). *Marine Biology Research*, 160(2), 383-398.
- Mayzaud, P., Laureillard, J., Merien, D., Brinis, A., Godard, C., Razouls, S., & Labat, J. P. (2007). Zooplankton nutrition, storage and fecal lipid composition in different water masses associated with the Agulhas and Subtropical Fronts. *Marine Chemistry*, 107(2), 202-213.
- McCarthy, J. F. (1983). Role of particulate organic matter in decreasing accumulation of polynuclear aromatic hydrocarbons by *Daphnia magna*. *Archives of Environmental Contamination and Toxicology*, 12(5), 559-568.
- McClelland, J., Holmes, R., Dunton, K., & Macdonald, R. (2012). The Arctic Ocean Estuary. *Estuaries and Coasts*, 35(2), 353-368.
- McGovern, M., Søreide, J. E., Leu, E., & Poste, A. (in prep). Physicochemical response to terrestrial inputs in an Arctic fjord system.
- McTigue, N. D., Bucolo, P., Liu, Z., & Dunton, K. H. (2015). Pelagic-benthic coupling, food webs, and organic matter degradation in the Chukchi Sea: Insights from sedimentary pigments and stable carbon isotopes. *Limnology and Oceanography*, 60(2), 429-445.
- McTigue, N. D., & Dunton, K. H. (2014). Trophodynamics and organic matter assimilation pathways in the northeast Chukchi Sea, Alaska. *Deep-Sea Research Part II*, 102, 84-96.
- Meyer, T., & Wania, F. (2011). Modeling the elution of organic chemicals from a melting homogeneous snow pack. *Water Research*, 45(12), 3627-3637.
- Michener, R. H., & Lajtha, K. (Eds.). (2007). *Stable isotopes in ecology and environmental science* (2nd ed.). Malden, MA, USA: Blackwell Publishing.

- Mincks, S. L., Smith, C. R., Jeffreys, R. M., & Sumida, P. Y. G. (2008). Trophic structure on the West Antarctic Peninsula shelf: Detritivory and benthic inertia revealed by $\delta^{13}\text{C}$ and $\delta^{15}\text{N}$ analysis. *Deep-Sea Research Part II*, 55(22), 2502-2514.
- Moder, K. (2010). Alternatives to F-test in one way ANOVA in case of heterogeneity of variances (a simulation study). *Psychological Test and Assessment Modeling*, 54(4), 343-353.
- Moore, J. C., Berlow, E. L., Coleman, D. C., Ruiter, P. C., Dong, Q., Hastings, A., . . . Wall, D. H. (2004). Detritus, trophic dynamics and biodiversity. *Ecology Letters*, 7(7), 584-600.
- Morel, F. M. M., Kraepiel, A. M. L., & Amyot, M. (1998). The chemical cycle and bioaccumulation of mercury. *Annual Review of Ecology and Systematics*, 29, 543-566.
- Morgan, E. J., Lohmann, R., & Morgan, E. J. (2010). Dietary uptake from historically contaminated sediments as a source of PCBs to migratory fish and invertebrates in an urban estuary. *Environmental Science & Technology*, 44(14), 5444-5449.
- Muhaya, B., Leermakers, M., & Baeyens, W. (1997). Total mercury and methylmercury in sediments and in the polychaete *Nereis diversicolor* at Groot Buitenschoor (Scheldt estuary, Belgium). *An International Journal of Environmental Pollution*, 94(1), 109-123.
- Muir, D., Savinova, T., Savinov, V., Alexeeva, L., Potelov, V., & Svetochev, V. (2003). Bioaccumulation of PCBs and chlorinated pesticides in seals, fishes and invertebrates from the White Sea, Russia. *Science of the Total Environment*, 306(1), 111-131.
- Nellier, Y., Perga, M., Cottin, N., Fanget, P., Malet, E., & Naffrechoux, E. (2015). Mass budget in two high altitude lakes reveals their role as atmospheric PCB sinks. *Science of the Total Environment*, 511, 203-213.
- Nelson, M. M., Mooney, B. D., Nichols, P. D., & Phleger, C. F. (2001). Lipids of Antarctic Ocean amphipods: Food chain interactions and the occurrence of novel biomarkers. *Marine Chemistry*, 73(1), 53-64.
- Nordström, M., Aarnio, K., & Bonsdorff, E. (2009). Temporal variability of a benthic food web: Patterns and processes in a low-diversity system. *Marine Ecology Progress Series*, 378, 13-26.
- Norwegian Meteorological Institute. (n.d.). *Norwegian Ice Service - MET Norway*. Retrieved 2018-08-10 from <http://polarview.met.no>
- Nygård, H., Berge, J., Søreide, J., Vihtakari, M., & Falk-Petersen, S. (2012). The amphipod scavenging guild in two Arctic fjords: Seasonal variations, abundance and trophic interactions. *Aquatic Biology*, 14(3), 247-264.
- Nyssen, F., Brey, T., Dauby, P., & Graeve, M. (2005). Trophic position of Antarctic amphipods- enhanced analysis by a 2-dimensional biomarker assay. *Marine Ecology Progress Series*, 300, 135-145.
- Oksanen, J., Blanchet, F. G., Friendly, M., Kindt, R., Legendre, P., McGlinn, D., . . . Wagner, H. (2017). R package 'vegan'. Community Ecology Package.
- Olenycz, M., Sokołowski, A., Niewińska, A., Wołowicz, M., Namieśnik, J., Hummel, H., & Jansen, J. (2015). Comparison of PCBs and PAHs levels in European coastal waters using mussels from the *Mytilus edulis* complex as biomonitors. *Oceanologia*, 57(2), 196-211.

- Outridge, P. M., Macdonald, R. W., Wang, F., Stern, G. A., & Dastoor, A. P. (2008). A mass balance inventory of mercury in the Arctic Ocean. *Environmental Chemistry*, 5(2), 89-111.
- Outridge, P. M., Sanei, L. H., Stern, G. A., Hamilton, P. B., & Goodarzi, F. (2007). Evidence for control of mercury accumulation rates in Canadian high Arctic lake sediments by variations of aquatic primary productivity. *Environmental Science & Technology*, 41(15), 5259-5265.
- Palmer, M. W., McGlenn, D. J., Westerberg, L., & Milberg, P. (2008). Indices for detecting differences in species composition: Some simplifications of RDA and CCA. *Ecology*, 89(6), 1769-1771.
- Perga, M., Nellier, Y., Cottin, N., Fanget, P., & Naffrechoux, E. (2017). Bioconcentration may be favoured over biomagnification for fish PCB contamination in high altitude lakes. *Inland Waters*, 7(1), 14-26.
- Peters, J., Renz, J., Beusekom, J., Boersma, M., & Hagen, W. (2006). Trophodynamics and seasonal cycle of the copepod *Pseudocalanus acuspes* in the central Baltic Sea (Bornholm Basin): Evidence from lipid composition. *Marine Biology Research*, 149(6), 1417-1429.
- Peterson, B. J., & Fry, B. (1987). Stable isotopes in ecosystem studies. *Annual Review of Ecology and Systematics*, 18(1), 293-320.
- Pierard, C., Budzinski, H., & Garrigues, P. (1996). Grain-size distribution of polychlorobiphenyls in coastal sediments. *Environmental Science & Technology*, 30(9), 2776-2783.
- Pirrone, N., Cinnirella, S., Feng, X., Finkelman, R., Friedli, H., Leaner, J., . . . Telmer, K. (2010). Global mercury emissions to the atmosphere from anthropogenic and natural sources. *Atmospheric Chemistry and Physics*, 10(13), 5951-5964.
- Post, D., Layman, C., Arrington, D., Takimoto, G., Quattrochi, J., & Montaña, C. (2007). Getting to the fat of the matter: Models, methods and assumptions for dealing with lipids in stable isotope analyses. *Oecologia*, 152(1), 179-189.
- Pouch, A., Zaborska, A., & Pazdro, K. (2017). Concentrations and origin of polychlorinated biphenyls (PCBs) and polycyclic aromatic hydrocarbons (PAHs) in sediments of western Spitsbergen fjords (Kongsfjorden, Hornsund, and Adventfjorden). *Environmental Monitoring and Assessment*, 189(4), 1-20.
- Pouch, A., Zaborska, A., & Pazdro, K. (2018). The history of hexachlorobenzene accumulation in Svalbard fjords. *Environmental Monitoring and Assessment*, 190(6), 1-14.
- Quémérais, B., Lemieux, C., & Lum, K. R. (1994). Temporal variation of PCB concentrations in the St. Lawrence river (Canada) and four of its tributaries. *Chemosphere*, 28(5), 947-959.
- Razak, I. A. A., Li, A., & Christensen, E. R. (1996). Association of PAHs, PCBs, 137Cs, and 210Pb with clay, silt, and organic carbon in sediments. *Water Science and Technology*, 34(7-8), 29-35.
- Renaud, P. E., Løkken, T. S., Jørgensen, L. L., Berge, J., & Johnson, B. J. (2015). Macroalgal detritus and food-web subsidies along an Arctic fjord depth-gradient. *Frontiers in Marine Science*, 2(31), 1-15.

- Renaud, P. E., Tessmann, M., Evenset, A., & Christensen, G. (2011). Benthic food-web structure of an Arctic fjord (Kongsfjorden, Svalbard). *Marine Biology Research*, 7(1), 13-26.
- Reuss, N., & Poulsen, L. (2002). Evaluation of fatty acids as biomarkers for a natural plankton community. A field study of a spring bloom and a post-bloom period off West Greenland. *Marine Biology Research*, 141(3), 423-434.
- Richoux, N. B., Deibel, D., Thompson, R. J., & Parrish, C. C. (2005). Seasonal and developmental variation in the fatty acid composition of *Mysis mixta* (Mysidacea) and *Acanthostepheia malmgreni* (Amphipoda) from the hyperbenthos of a cold-ocean environment (Conception Bay, Newfoundland). *Journal of Plankton Research*, 27(8), 719-733.
- Rigét, F., Bignert, A., Braune, B., Dam, M., Dietz, R., Evans, M., . . . Wilson, S. (2019). Temporal trends of persistent organic pollutants in Arctic marine and freshwater biota. *Science of the Total Environment*, 649, 99-110.
- Ripszam, M., Paczkowska, J., Figueira, J., Veenaas, C., & Haglund, P. (2015). Dissolved organic carbon quality and sorption of organic pollutants in the Baltic Sea in light of future climate change. *Environmental Science & Technology*, 49(3), 1445-1452.
- Ruus, A., Øverjordet, I. B., Braaten, H. F. V., Evenset, A., Christensen, G., Heimstad, E. S., . . . Borgå, K. (2015). Methylmercury biomagnification in an Arctic pelagic food web. *Environmental Toxicology and Chemistry*, 34(11), 2636-2643.
- Sapota, G., Wajtasik, B., Burska, D., & Nowiński, K. (2009). Persistent organic pollutants (POPs) and polycyclic aromatic hydrocarbons (PAHs) in surface sediments from selected fjords, tidal plains and lakes of the North Spitsbergen. *Polish Polar Research*, 30(1), 59-76.
- Sargent, J., & Falk-Petersen, S. (1981). Ecological investigations on the zooplankton community in Balsfjorden, northern Norway: Lipids and fatty acids in *Meganctiphanes norvegica*, *Thysanoessa raschi* and *T. inermis* during mid-winter. *Marine Biology*, 62(2), 131-137.
- Sargent, J., & Falk-Petersen, S. (1988). The lipid biochemistry of calanoid copepods. *Hydrobiologia*, 167(1), 101-114.
- Schartup, A. T., Ndu, U., Balcom, P. H., Mason, R. P., & Sunderland, E. M. (2015). Contrasting effects of marine and terrestrially derived dissolved organic matter on mercury speciation and bioavailability in seawater. *Environmental Science & Technology*, 49(10), 5965-5972.
- Schartup, A. T., Qureshi, A., Dassuncao, C., Thackray, C. P., Harding, G., & Sunderland, E. M. (2017). A model for methylmercury uptake and trophic transfer by marine plankton. *Environmental Science & Technology*, 52(2), 654-662.
- Schell, D. M. (1983). Carbon-13 and carbon-14 [isotopes] abundances in Alaskan aquatic organisms: Delayed production from peat in Arctic food webs. *Science*, 219(4588), 1068-1071.
- Scheuhammer, A. M., Meyer, M. W., Sandheinrich, M. B., & Murray, M. W. (2007). Effects of environmental methylmercury on the health of wild birds, mammals, and fish. *Ambio*, 36(1), 12-19.

- Schuster, P. F., Schaefer, K. M., Aiken, G. R., Antweiler, R. C., Dewild, J. F., Gryziec, J. D., . . . Zhang, T. (2018). Permafrost stores a globally significant amount of mercury. *Geophysical Research Letters*, 45(3), 1463-1471.
- Schuster, P. F., Striegl, R. G., Aiken, G. R., Krabbenhoft, D. P., Dewild, J. F., Butler, K., . . . Schuster, P. F. (2011). Mercury export from the Yukon River basin and potential response to a changing climate. *Environmental Science & Technology*, 45(21), 9262-9267.
- Scott, C. L., Falk-Petersen, S., Sargent, J. R., Hop, H., Lønne, O. J., & Poltermann, M. (1999). Lipids and trophic interactions of ice fauna and pelagic zooplankton in the marginal ice zone of the Barents Sea. *Polar Biology*, 21(2), 65-70.
- Shaw, G. R., & Connell, D. W. (1987). Comparative kinetics for bioaccumulation of polychlorinated biphenyls by the polychaete (*Capitella capitata*) and fish (*Mugil cephalus*). *Ecotoxicology and Environmental Safety*, 13(1), 84-91.
- Sparks, T. H., Scott, W. A., & Clarke, R. T. (1999). Traditional multivariate techniques: Potential for use in ecotoxicology. *Environmental Toxicology and Chemistry*, 18(2), 128-137.
- St Louis, V. L., Sharp, M. J., Steffen, A., May, A., Barker, J., Kirk, J. L., . . . Smol, J. P. (2005). Some sources and sinks of monomethyl and inorganic mercury on Ellesmere Island in the Canadian high Arctic. *Environmental Science & Technology*, 39(8), 2686-2701.
- Starek-Świechowicz, B., Budziszewska, B., & Starek, A. (2017). Hexachlorobenzene as a persistent organic pollutant: Toxicity and molecular mechanism of action. *Pharmacological Reports*, 69(6), 1232-1239.
- Steele, J. H., Thorpe, S. A., & Turekian, K. K. (2008). *Encyclopedia of ocean sciences* (2nd ed.). Amsterdam, Netherlands: Academic Press.
- Sunderland, E. M., & Mason, R. P. (2007). Human impacts on open ocean mercury concentrations. *Global Biogeochemical Cycles*, 21(4), 1-15.
- Syvitski, J. P. M., Asprey, K. W., Clattenburg, D. A., & Hodge, G. D. (1985). The prodelta environment of a fjord: Suspended particle dynamics. *Sedimentology*, 32(1), 83-107.
- Syväranta, J., Hämäläinen, H., & Jones, R. I. (2006). Within-lake variability in carbon and nitrogen stable isotope signatures. *Freshwater Biology*, 51(6), 1090-1102.
- Söderström, M., Nylund, K., Järnberg, U., Lithner, G., Rosén, G., & Kylin, H. (2000). Seasonal variations of DDT compounds and PCB in a eutrophic and an oligotrophic lake in relation to algal biomass. *Ambio*, 29(4/5), 230-237.
- Søreide, J. E., Falk-Petersen, S., Hegseth, E. N., Hop, H., Carroll, M. L., Hobson, K. A., & Blachowiak-Samolyk, K. (2008). Seasonal feeding strategies of *Calanus* in the high-Arctic Svalbard region. *Deep-Sea Research Part II*, 55(20-21), 2225-2244.
- Søreide, J. E., Hop, H., Carroll, M. L., Falk-Petersen, S., & Hegseth, E. N. (2006a). Seasonal food web structures and sympagic–pelagic coupling in the European Arctic revealed by stable isotopes and a two-source food web model. *Progress in Oceanography*, 71(1), 59-87.
- Søreide, J. E., & Nygård, H. (2012). Challenges using stable isotopes for estimating trophic levels in marine amphipods. *Polar Biology*, 35(3), 447-453.

- Søreide, J. E., Tamelander, T., Hop, H., Hobson, K., & Johansen, I. (2006b). Sample preparation effects on stable C and N isotope values: A comparison of methods in Arctic marine food web studies. *Marine Ecology Progress Series*, 328, 17-28.
- Taylor, D. L., Linehan, J. C., Murray, D. W., & Prell, W. L. (2012). Indicators of sediment and biotic mercury contamination in a southern New England estuary. *Marine Pollution Bulletin*, 64(4), 807-819.
- Taylor, V. F., Buckman, K. L., Seelen, E. A., Mazrui, N. M., Balcom, P. H., Mason, R. P., & Chen, C. Y. (2019). Organic carbon content drives methylmercury levels in the water column and in estuarine food webs across latitudes in the Northeast United States. *Environmental Pollution*, 246, 639-649.
- Tenore, K. R. (1988). Nitrogen in benthic food chains. In T. H. Blackburn & J. Sørensen (Eds.), *Nitrogen cycling in coastal marine environments*. New York, NY, USA: John Wiley.
- Thomann, R. V., Connolly, J. P., & Parkerton, T. F. (1992). An equilibrium model of organic chemical accumulation in aquatic food webs with sediment interaction. *Environmental Toxicology and Chemistry*, 11(5), 615-629.
- Thompson, R. J., Deibel, D., Redden, A. M., & McKenzie, C. H. (2008). Vertical flux and fate of particulate matter in a Newfoundland fjord at sub-zero water temperatures during spring. *Marine Ecology Progress Series*, 357, 33-49.
- Tsui, M. T. K., & Wang, W. (2004). Uptake and elimination routes of inorganic mercury and methylmercury in *Daphnia magna*. *Environmental Science & Technology*, 38(3), 808-816.
- Tzvetkova, N. L. (1972). Taxonomy of the genus *Gammarus* Fabr. with the description of some new species of gammarids (Amphipoda, Gammaridae) from the north-western part of the Pacific Ocean. *Akademiia Nauk SSSR*, 52, 201-222.
- USEPA. (1998). Method 1630 methylmercury in water by distillation, aqueous ethylation, purge and trap, and cold vapor atomic fluorescence spectrometry. USEPA, Office of water.
- USEPA. (2007). Method 7473 mercury in solids and solutions by thermal decomposition, amalgamation, and atomic absorption spectrophotometry. USEPA, Office of water.
- Van Der Velden, S., Dempson, J. B., Evans, M. S., Muir, D. C. G., & Power, M. (2012). Basal mercury concentrations and biomagnification rates in freshwater and marine food webs: Effects on Arctic charr (*Salvelinus alpinus*) from eastern Canada. *Science of the Total Environment*, 444, 531-542.
- Varpe, Ø. (2017). Life history adaptations to seasonality. *Integrative and comparative biology*, 57(5), 943-960.
- Väinölä, R., Witt, J. D. S., Grabowski, M., Bradbury, J. H., Jazdzewski, K., & Sket, B. (2008). Global diversity of amphipods (Amphipoda; Crustacea) in freshwater. *Hydrobiologia*, 595(1), 241-255.
- Wang, R., & Wang, W. (2012). Contrasting mercury accumulation patterns in tilapia (*Oreochromis niloticus*) and implications on somatic growth dilution. *Aquatic Toxicology*, 114-115, 23-30.

- Wania, F., & Daly, G. L. (2002). Estimating the contribution of degradation in air and deposition to the deep sea to the global loss of PCBs. *Atmospheric Environment*, 36(36), 5581-5593.
- Webster, L., Roose, P., Bersuder, B., Kotterman, M., Haarich, M. & Vorkamp, K. (2013). *Determination of polychlorinated biphenyls (PCBs) in sediment and biota*. Copenhagen, Denmark: International Council for the Exploration of the Sea.
- Welch, B. L. (1938). The significance of the difference between two means when the population variances are unequal. *Biometrika*, 29, 350-362.
- Welch, B. L. (1947). The generalization of 'student's' problem when several different population variances are Involved. *Biometrika*, 34, 28-35.
- Wesławski, J. M. (1990). Distribution and ecology of south Spitsbergen coastal marine Amphipoda (Crustacea). *Polskie archiwum hydrobiologii*, 37(4), 503-519.
- Wesławski, J. M. (1994). Gammarus (Crustacea, Amphipoda) from Svalbard and Franz Josef Land. Distribution and density. *Sarsia*, 79, 145-150.
- Wesławski, J. M. (2011). *Adventfjorden: Arctic sea in the backyard*. Sopot, Poland: Institute of Oceanology, Polish Academy of Sciences.
- Wesławski, J. M., & Legeżyńska, J. (2002). Life cycles of some Arctic amphipods. *Polish Polar Research*, 23(3-4), 253-264.
- Wesławski, J. M., Szymelfenig, M., Zajączkowski, M., & Keck, A. (1999). Influence of salinity and suspended matter on benthos of an Arctic tidal flat. *ICES Journal of Marine Science*, 56, 194-202.
- Wesławski, J. M., Wiktor, J., & Kotwicki, L. (2010). Increase in biodiversity in the Arctic rocky littoral, Sorkapland, Svalbard, after 20 years of climate warming. *Marine Biodiversity*, 40, 123-130.
- Wesławski, J. M., Wiktor, J., Zajączkowski, M., & Swerpel, S. (1993). Intertidal zone of Svalbard. *Polar Biology*, 13(2), 73-79.
- Wesławski, J. M., Zajączkowski, M., Wiktor, J., & Szymelfenig, M. (1997). Intertidal zone of Svalbard 3. Littoral of a subarctic, oceanic island: Bjørnøya. *Polar Biology*, 18(1), 45-52.
- Whitlock, M. C., & Schluter, D. (2015). *The analysis of biological data* (2nd ed.). New York, NY, USA: Macmillan education.
- Wiedmann, I., Reigstad, M., Marquardt, M., Vader, A., & Gabrielsen, T. M. (2016). Seasonality of vertical flux and sinking particle characteristics in an ice-free high Arctic fjord-Different from subarctic fjords? *Journal of Marine Systems*, 154, 192-205.
- Wiktor, J. (1999). Early spring microplankton development under fast ice covered fjords of Svalbard, Arctic. *Oceanologia*, 41(1), 51-72
- Woodland, R., Magnan, P., Glémet, H., Rodríguez, M., & Cabana, G. (2012). Variability and directionality of temporal changes in $\delta^{13}\text{C}$ and $\delta^{15}\text{N}$ of aquatic invertebrate primary consumers. *Oecologia*, 169(1), 199-209.
- Zajączkowski, M., Nygård, H., Hegseth, E., & Berge, J. (2010). Vertical flux of particulate matter in an Arctic fjord: The case of lack of the sea-ice cover in Adventfjorden 2006–2007. *Polar Biology*, 33(2), 223-239.

- Zajączkowski, M., & Włodarska-Kowalczyk, M. (2007). Dynamic sedimentary environments of an Arctic glacier-fed river estuary (Adventfjorden, Svalbard). I. Flux, deposition, and sediment dynamics. *Estuarine, Coastal and Shelf Science*, 74(1), 285-296.
- Zdanowicz, C., Lean, D., & Clark, I. (2009). Atmospheric deposition and release of methylmercury in glacially-fed catchments of Auyuittuq National Park, Baffin Island. In S. Smith, J. Stow & J. Edwards (Eds.), *Synopsis of research conducted under the 2008-2009 northern contaminants program*. Ottawa, Canada: Ministry of Indian and Northern Development.
- Zhang, Y., Jacob, D. J., Dutkiewicz, S., Amos, H. M., Long, M. S., & Sunderland, E. M. (2015). Biogeochemical drivers of the fate of riverine mercury discharged to the global and Arctic oceans. *Global Biogeochemical Cycles*, 29(6), 854-864.
- Zheng, J., Fisher, D., Koerner, R., Zdanowicz, C., Bourgeois, C., Hall, G., . . . Ke, F. (2009). Temporal studies of atmospheric Hg deposition with ice cores and snow in the Canadian high Arctic. In S. Smith, J. Stow & J. Edwards (Eds.), *Synopsis of research conducted under the 2008-2009 northern contaminants program*. Ottawa, Canada: Ministry of Indian and Northern Development.

Appendices

Appendix A: Protocols

Terrestrial taxa

Terrestrial plants collected south of Isdammen (N78°12.1, E15°45.1): Two sorts of graminoids, *Cerastium arcticum*, *Salix polaris*, *Bistorta viviparum*, *Cassiope tetragona*, *Dryas octopetala*, *Oxyria digyna* and Mosses.

Stable isotope analysis

Instrumental analysis

The relative abundance for the heavier and the lighter isotopes of carbon and nitrogen in samples were analysed by an elemental analyser interfaced with an isotope ratio mass spectrometer with dual nitrogen and carbon measurements. Shortly described, the samples were first combusted to denominator gases in the elemental analyser. Afterwards the gases were conveyed to the isotope ratio mass spectrometer, where the gases became ionized, passed through an magnetic field that separated the isotopes according to their mass to charge ratio (m/z ratio), and became detected and measured by collectors. Via collectors connected to computers, the relative abundance of the isotopes in the samples were determined (Fry, 2008). The instrument used at UC Davis Stable isotope facility for analysing amphipods, plant material and detritus was a PDZ Europa ANCA-GSL elemental analyser interfaced to a PDZ Europa 20-20 isotope ratio mass spectrometer (Sercon Ltd., Cheshire, UK). While for filters and sediments, an Elementar Vario EL Cube or Micro Cube elemental analyser (Elementar Analysensysteme GmbH, Hanau, Germany) interfaced to a PDZ Europa 20-20 isotope ratio mass spectrometer (Sercon Ltd., Cheshire, UK) was used.

Analytic quantification and quality assurance

At the UC Davis stable isotope facility, standard reference gases were analysed with the samples (Vienna PeeDee Belemite (VPDB) for carbon and atmospheric nitrogen for nitrogen). The measured isotopic ratios in the samples were expressed relative to these reference gases when quantified, as shown in equation A.1 below.

$$\delta X = \left[(R_{\text{sample}}/R_{\text{standard}}) - 1 \right] \times 10^3 \quad (\text{Equation A.1})$$

X= ¹³C or ¹⁵N

R=corresponding ratio ¹³C/¹²C, ¹⁵N/¹⁴N

Sample= corresponding ratio in the unknown sample

Standard=corresponding ratio in the standard reference gas

The final delta (δ) values of ¹³C or ¹⁵N are in units of per mil (‰) and is a relative, not an absolute, value (Peterson and Fry, 1987).

A quality assurance method to study precision was employed by splitting every 10th sample into two replicates when packing the samples for analysis. The long term standard deviation reported from UC Davis Stable Isotope Facility at the University of California is ± 0.2 ‰ for ¹³C and ± 0.3 ‰ for ¹⁵N.

Fatty acid analysis

Extraction

Extraction of lipids followed the method described by Folch et al. (1957). Shortly, prior to extraction, amphipods were weighed (Mettler Toledo® Scale, model: MS303TS) and lyophilised (Labconco Freezone 2.5) and weighed again to determine dry weight. Extraction began by adding chloroform: methanol (2:1) mixture to the samples and then vortexing (Vortex Genie 2, Model: G-560) the samples. Afterwards, aqueous 0.88% Potassium chloride (KCl) solution was added to remove methanol and water-soluble components from the extracts. Next, 18 ug of Tricosanoic acid (23:0) was added to each tube as an internal standard (23:0) for determining methylation efficiency, and again vortexed and centrifuged (Thermo Scientific Multifuge X3R). The organic phase was collected into new containers. Samples were altogether extracted three times (once with 2:1 chloroform: methanol and twice with 86:14:1 chloroform: methanol: MilliQ water). The collected extracts were gently vaporised to dryness with a stream of nitrogen.

Lipid determination

Hexane was added to the extracts, and two subsamples were taken out and placed in pre-weighed tin-cups, vaporised to dryness and was weighed (gravimetric estimates) using a microbalance (Sartorius, Model X with one µg precision).

Derivatization

To derivatise the extracted FAs to FA methyl esters (FAMES), which makes the FAs more amenable for gas chromatograph (GC) analysis, sulphuric acid (catalyst) in methanol (1% v/v) was added to the remaining extracts (Christie 1989). The samples were vortexed and gently vaporised with a stream of nitrogen to remove reactive oxygen. Samples were then heated to 90°C for 90 min, to aid esterification between hydroxyl groups of the methanol and carboxyl groups of the FAs. After cooling, distilled water (MilliQ water) and hexane were added, after which they were vortexed, centrifuged and the organic phase was collected to new tubes. This was done altogether three times and next, evaporated under a stream of nitrogen gas and transferred into 2 mL VWR® Auto-sampler gas chromatography (GC) vials and stored at 4°C until analysis.

Instrumental analysis

Extracts were analysed and quantified with a GC (A Shimadzu GC-2010 plus, with an AOC-20i/s autosampler and twin auto-injectors) connected to a detector (flame ioniser detector) using a “splitless” or “split” approach (for detailed information regarding operational setting see Appendix B, Table B2). In the GC the mobile phase is a carrier gas that carries the sample, and the stationary phase consists of a column, that separates the sample. The separation is based on the notion that different compounds interact differently with the column, thus the stronger the interaction, the more time it will take to travel through it. In the flame ionisation-detector, the sample becomes burnt in a flame, which produces ions and electrons. These charged particles are located between electrodes, which result in a measurable current. This current is directly proportional to the amount of ions, hence sample, in the detector.

Analytic quantification and quality assurance

FAs were identified and quantified by referencing their retention times with those obtained from standard mixtures with known compositions (GLC 463, GLC 68E, and 23:0, NuChek Prep., Waterville, MN, USA). Tricosanoic acid was added as an internal standard for determining methylation efficiency.

Persistent organic pollutant analysis

Instrumental analyses

Instrumental analysis on sediment and amphipod samples was conducted using gas chromatography (GC) (Agilent 7890 gas chromatograph), that separates vaporized substances in the sample, equipped with a triple quadrupole mass spectrometer (MS) detector (Agilent 7010B GC/MS-EI Triple Quad that provides detection limits in Electron Ionization (EI) mode) that scans and distinguishes the masses continuously throughout the separation. Shortly described, from the GC, the separated substances travelled to the MS, where the substances became ionised by an electron-impact source. Next, the newly produced ions passed through a quadrupole mass filter, where only a certain molecular mass-to-charge ratio (m/z) could pass through. Next, the substances became further fragmented as they interacted with an inert gas in a collision cell. The fragments passed through yet another quadrupole mass filter, where, again, only a certain m/z ratio could pass through, and after which the fragments finally reach the detector and became quantified. Detailed information regarding GC-MS triple quadrupole operational settings can be found in Appendix B, Table B5.

Analytic quantification and quality assurance

Quantification of the target analytes (HCB, PeCB, PCB-28, -52, -101, -118, -138, -153, -180) was accomplished by using an internal standard (ISTD). The ISTD contained three POPs congeners with low, intermediate and high chlorination, covering the chlorination spectrum of the target analytes (for detailed information about the congeners in the internal standard see Appendix B, Table B3). Thus, these ISTD congeners were assumed to behave comparable to the target analytes throughout the extraction and clean-up procedure. Target analytes, during the quantification process, were associated with one of these three ISTD congeners based on highest similarity in physicochemical properties (e.g. molecular weight, volatility, polarity, functional groups). The ISTD congeners are not commonly found in the environment and are readily distinguishable from the target analytes during quantification. First during quantification, an eight point calibration curve was made for each target analyte by linear regression. The calibration curve was made by using ratios from the concentrations of the target analyte, whose concentration covers the range of concentrations expected in the samples, with the concentration of the associating congener in the internal standard on the x-axis. On the y-axis, corresponding ratios of these calibration solutions' peak areas calculated from the chromatograms following analysis were plotted. The unknown concentrations of the analyte in samples were thus quantified by analysing samples together with a defined amount

of internal standard, calculating the ratios between peak areas from the chromatograms and determine the corresponding ratios of analyte concentration to ISTD concentration from the calibration curve. The final concentrations were found by multiplying the ratios of analyte concentration to ISTD concentration discovered from the calibration curve with the concentration of internal standard in the sample.

Quality assurance techniques, such as blanks and certified reference material (CRM-1944; National standard of Standards and Technology for sediments and CRM-2974a; National standard of Standards and Technology for amphipods), were used during every batch-run. To investigate the accuracy of the work performed in the laboratory, certified reference materials (n=2 with every sample batch), with known concentration values, were prepared together with the samples. Hence, by comparing known concentration values with concentrations detected from the analytic measurements (recovery calculations), one can investigate how close the outcome of the analytic procedure was to the true concentration. Method validation/procedural blanks (n=1-2 with every sample batch) were used in the procedure alongside the samples to disclosure contamination from interfering compounds that could cause errors in quantification and to establish the LOD (Webster, 2013).

Methyl mercury analysis

Analytic quantification and quality assurance

Quantification of the analytes was accomplished by using an external standard (Methyl mercury (II) chloride, standard solution in H₂O, Alfa Aesar™, Fisher Scientific®) to construct a six point calibration curve with linear regression. The calibration curve was produced by plotting increasing levels of known concentrations of the external standard against the corresponding peak areas calculated from the light absorbance measurements during cold-vapour atomic absorption spectrophotometry. Analyte concentrations were determined by comparing the peak areas calculated from the samples against the calibration curve.

Quality assurance measures, such as instrumental blanks (n=3) and method blanks (n=3), to discover contamination, and certified reference materials (CRM-DORM-4; National Research Council Canada and TORT-2; National Research Council Canada) (n=6), sample duplicates

(n=3-4) and matrix spikes (n=3), to study precision and recovery, were included for every batch-run.

Appendix B: Tables

Table B1. Overview of the number of amphipods allocated to each analysis and the overall weight. Letter corresponds to: SI; stable isotope analysis, FA; fatty acid analysis, POP; POP analysis, totHg and MeHg; total and methyl mercury analysis, Nr; numbers of amphipods, We.; overall weight in grams of the sample and NA; not available.

Month	Station	SI/totHg/MeHg		FA		POP	
		Nr.	We.	Nr.	We.	Nr.	We.
City	April						
	A	3	0.3	NA	NA	NA	NA
	B	3	0.3	3	0.3	23	2.3
	C	3	0.3	3	0.3	25	2.5
	D	3	0.3	3	0.3	37	3.7
	May						
	A	15	3.7	5	1.3	60	11.3
	B	20	3.9	5	1.1	60	11.3
	C	10	1.4	NA	NA	NA	NA
	D	12	2.6	5	1.3	60	12.3
	June						
	A	27	4.3	5	1.1	60	10.6
	B	10	1.9	4	0.8	43	9.3
	C	5	8.6	NA	NA	NA	NA
	D	27	6.3	5	1.0	70	14.3
	July						
	A	3	0.8	NA	NA	NA	NA
	B	8	1.9	5	1.2	54	14.3
	C	8	2.2	5	1.1	41	12.1
	D	11	3.6	5	1.2	55	11.4
	August						
	A	12	1.3	NA	NA	NA	NA
	B	10	3	4	0.6	70	10
	C	4	1.4	4	0.8	34	7.3
	D	5	0.6	3	0.9	34	5.1
North	April						
	A	2	0.2	2	0.2	31	3.1
	B	2	0.2	2	0.2	49	4.9
	C	2	0.2	NA	NA	NA	NA
	D	2	0.2	2	0.2	31	3.1
	June						
	A	5	1.1	NA	NA	NA	NA
	B	10	2.2	NA	NA	NA	NA
	C	3	0.9	NA	NA	NA	NA
	D	14	2.2	NA	NA	NA	NA
	July						
	B	2	7	2	0.5	29	6
	D	2	0.5	2	0.2	12	1.9
	August						
	A	9	1.3	6	0.7	47	5.3
	B	5	0.5	NA	NA	NA	NA
	C	7	0.8	5	0.5	46	5.2
	D	8	0.7	4	0.4	69	6.9

Table B2. Overview of operational settings on the Shimadzu GC-2010 plus, with an AOC-20i/s auto sampler.

Parameter	Settings
Column	2x (100 m X 0.25 mm ID X 0.20µm). Supelco SP-2560
Split Restek Topaz inlet liners	Split ratio of 50
Injector temperature	250 °C
Carrier gas	Helium
Flow rate	60.1 mL/min
Temperature programme	140 °C (held for 5 min) before increasing to 240 °C at a rate of 2 °C/min for 50 min. then holding at 240°C for a final 10 min
Total run time	65min/sample

Table B3. Overview of the three PCB congeners used in the internal standard.

Group	Abbreviation	Analyte
PCBs	PCB 30	2,4,6-Trichlorobiphenyl
	PCB 53	2,2',5,6'-Tetrachlorobiphenyl
	PCB 204	2,2',3,4,4',5,6,6'-Octachlorobiphenyl

Table B4. Overview of the operational settings on the Agilent Technologies, 1260 infinity II.

Parameter	Settings
Mobil phase	80% ethyl acetate and 20% cyclohexane.
Column temperature	50°C
Flow	2ml/min
Injection volume	100µl (x2)
Fraction window	4.6-11.0 min
GPS/SEC Columns	PLgel 10um Guard 50 x 7.5 mm; PLgel 10um 100A. 7.5 x 300 mm
Detector	UV-detector. 254nm

Table B5. Overview of the parameter settings on the Agilent 7890 gas chromatograph equipped with a Agilent 7010B GC/MS-EI Triple Quad.

Parameter	Settings
Column	2x (15m x 250µm x 0.25µm). Agilent HP-5ms
Split less injection	1 uL injection
Injector temperature	280 °C
Carrier gas	Helium
Flow rate	1.02 mL/min in the first column and 1.23 mL/min in the second column
Temperature programme	60 °C (held for 1 min) before increasing to 120 °C at a rate of 40 °C/min followed by an increase to 280 °C at a rate of 5 °C/min
Collision gas	Nitrogen

Table B6. Overview of the operational settings on the DMA-80 direct mercury analyser.

Parameter	Settings
Drying	200°C. 90s
Decomposition Ramp	650°C. 120s
Decomposition Hold	650°C. 90s
Catalysis Temp	600°C
Purge time	60s
Amalgam	900°C. 12s
Carrier gas	Oxygen
Inlet pressure	4 bar
Flow rate	120mL/min
Light source	Low pressure mercury lamp
Wavelength	253.7nm

Table B7. Overview of the operational settings on the 2700 Methyl Mercury Auto-Analysis System.

Parameter	Settings
Run duration	5 min
Heating duration	9.9 s
Cooling duration	3 min
Purge duration	6 min
Flow rate	60.1 mL/min

Table B8. Overview of totHg and MeHg concentrations (ng/g w.w.) in amphipods.

Station	Month and replicate	totHg ng/g w.w.	MeHg ng/g w.w.
City	April		
	A	6,66	4,6
	B	4,71	5,0
	C	4,97	2,6
	D	NA	3,2
	May		
	A	4,16	1,5
	B	4,74	1,1
	C	4,57	0,5
	D	4,99	0,9
	June		
	A	5,71	3,7
	B	5,08	0,2
	C	5,05	0,8
	D	5,18	1,4
	July		
	A	4,66	1,0
	B	6,12	0,7
	C	4,82	2,2
	D	4,71	0,4
	August		
	A	3,81	0,5
	B	4,34	2,1
	C	4,46	0,6
	D	4,00	0,5
North	April		
	A	6,28	5,3
	B	6,27	5,2
	C	6,61	8,6
	D	5,50	5,0
	June		
	A	5,40	0,9
	B	5,85	2,2
	C	6,72	1,5
	D	5,17	3,9
	July		
	B	5,68	2,7
	D	7,13	4,0
	August		
	A	3,95	0,7
	B	3,40	1,1
	C	4,49	0,7
	D	3,36	0,3

Table B9. Overview of LODs of POP concentrations (ng/g w.w.) in amphipods. Numbers in column "Sample" indicate station. 1=City and 2=North.

Sample	HCB ng/g ww	PCB-52 ng/g ww
July2D		<0.04
August1B	<0.01	
August2C		<0.01

Table B10. Overview of average and sd of FA composition and summation metrics as the percent of total fatty acid in amphipod samples. Number of replicates are indicated in parentheses.

of total fatty acid in unimpounded samples. Number of replicates are indicated in parentheses.								
	April		May	June	July	August		
Fatty acids/ summation metrics	City (3) % average ±sd	North (3) % average ±sd	City (3) % average ±sd	City (3) % average ±sd	City (3) % average ±sd	North (2) % average ±sd	City (3) % average ±sd	North (3) % average ±sd
14:0	2.1 ± 0.2	2.4 ± 0.3	3.3 ± 0.2	3.6 ± 0.2	3.6 ± 0.1	3.7 ± 0.6	3.2 ± 0.3	3.3 ± 0.3
14:1n-5	0.1 ± 0.1	0.2 ± 0.05	0.2 ± 0.03	0.17 ± 0.02	0.2 ± 0.01	0.2 ± 0.06	0.2 ± 0.03	0.2 ± 0.02
15:0	0.4 ± 0.01	0.4 ± 0.02	0.4 ± 0.02	0.3 ± 0.01	0.3 ± 0.04	0.3 ± 0.01	0.3 ± 0.02	0.4 ± 0.01
16:0	14.2 ± 0.32	14.5 ± 1.3	15.0 ± 0.2	15.9 ± 0.3	15.5 ± 0.4	15.6 ± 0.3	15.7 ± 0.4	16.5 ± 0.4
16:1n-7c	8.9 ± 0.7	8.1 ± 2.02	11.0 ± 0.4	13.4 ± 0.3	11.7 ± 1.3	12.1 ± 1.7	8.3 ± 0.8	7.5 ± 0.8
16:1n-7t	0.2 ± 0.02	0.3 ± 0.03	0.17 ± 0.01	0.1 ± 0.01	0.1 ± 0.01	0.2 ± 0.01	0.2 ± 0.01	0.3 ± 0.02
17:0	0.3 ± 0.03	0.3 ± 0.04	0.2 ± 0.01	0.18 ± 0.03	0.2 ± 0.03	0.2 ± 0.03	0.2 ± 0.01	0.3 ± 0.01
17:1n-7	0.2 ± 0.2	0.3 ± 0.2	0.2 ± 0.1	0.2 ± 0.08	0.2 ± 0.05	0.2 ± 0.04	0.2 ± 0.04	0.3 ± 0.01
18:0	0.8 ± 0.01	0.8 ± 0.1	1.0 ± 0.1	1.5 ± 0.2	1.3 ± 0.08	1.2 ± 0.2	1.1 ± 0.2	1.2 ± 0.05
18:1n-7c	3.3 ± 0.1	3.7 ± 0.6	3.7 ± 0.2	4.3 ± 0.1	4.4 ± 0.3	4.5 ± 0.2	3.8 ± 0.2	3.7 ± 0.4
18:1n-7t	0.0 ± 0.0	0.0 ± 0.0	0.0 ± 0.0	0.0 ± 0.0	0.03 ± 0.03	0.02 ± 0.03	0.0 ± 0.0	0.0 ± 0.0
18:1n-9c	22.2 ± 1.0	24.5 ± 0.06	20.5 ± 0.2	20.0 ± 0.9	20.3 ± 0.5	21.4 ± 0.9	22.4 ± 1.9	24.2 ± 2.0
18:1n-9t	0.2 ± 0.01	0.3 ± 0.05	0.1 ± 0.01	0.1 ± 0.02	0.1 ± 0.01	0.2 ± 0.1	0.1 ± 0.02	0.2 ± 0.02
18:1n-12c	1.3 ± 0.05	1.0 ± 0.07	1.4 ± 0.2	1.0 ± 0.1	0.9 ± 0.1	0.9 ± 0.2	0.8 ± 0.1	0.8 ± 0.05
18:2n-6c	2.8 ± 0.1	3.3 ± 1.1	1.9 ± 0.2	1.9 ± 0.2	2.3 ± 0.3	1.8 ± 0.1	2.7 ± 0.2	2.6 ± 0.1
18:3n-3	2.0 ± 0.01	1.9 ± 0.1	1.7 ± 0.1	1.8 ± 0.1	2.2 ± 0.2	1.9 ± 0.01	2.6 ± 0.5	2.2 ± 0.1
18:3n-6	0.2 ± 0.01	0.1 ± 0.02	0.5 ± 0.1	1.2 ± 0.3	1.1 ± 0.5	0.6 ± 0.2	0.4 ± 0.04	0.2 ± 0.1
18:4n-3	1.8 ± 0.08	0.9 ± 0.05	2.2 ± 0.1	2.9 ± 0.2	3.4 ± 0.6	3.6 ± 0.3	3.3 ± 0.4	2.6 ± 0.3
19:0	0.1 ± 0.02	0.1 ± 0.02	0.1 ± 0.01	0.1 ± 0.01	0.1 ± 0.02	0.1 ± 0.02	0.1 ± 0.02	0.1 ± 0.01
20:0	0.02 ± 0.03	0.06 ± 0.05	0.02 ± 0.04	0.08 ± 0.04	0.1 ± 0.01	0.1 ± 0.01	0.07 ± 0.03	0.07 ± 0.01
20:1	0.8 ± 0.03	0.7 ± 0.4	0.7 ± 0.1	0.4 ± 0.1	0.4 ± 0.1	0.4 ± 0.2	0.7 ± 0.04	0.7 ± 0.4
20:1n-9	4.9 ± 0.4	5.6 ± 2.0	4.1 ± 0.5	2.2 ± 0.1	3.0 ± 0.7	3.3 ± 0.1	4.4 ± 0.08	4.4 ± 0.5
20:1n-15	0.0 ± 0.0	0.1 ± 0.1	0.0 ± 0.0	0.0 ± 0.0	0.0 ± 0.0	0.1 ± 0.0	0.0 ± 0.0	0.1 ± 0.02
20:2n-6	0.5 ± 0.04	0.5 ± 0.1	0.4 ± 0.01	0.3 ± 0.01	0.3 ± 0.03	0.3 ± 0.08	0.4 ± 0.1	0.4 ± 0.02
20:3n-3	0.3 ± 0.01	0.3 ± 0.01	0.3 ± 0.01	0.31 ± 0.01	0.3 ± 0.1	0.3 ± 0.04	0.4 ± 0.1	0.3 ± 0.04
20:3n-6	0.1 ± 0.01	0.2 ± 0.02	0.2 ± 0.04	0.2 ± 0.05	0.3 ± 0.1	0.2 ± 0.02	0.2 ± 0.1	0.13 ± 0.01
20:4n-6	1.5 ± 0.04	1.6 ± 0.3	1.1 ± 0.2	0.8 ± 0.1	0.9 ± 0.1	0.8 ± 0.2	1.0 ± 0.2	1.1 ± 0.1
20:5n-3	16.2 ± 0.2	13.8 ± 1.7	17.1 ± 1.1	17.5 ± 0.6	16.2 ± 1.1	14.9 ± 1.2	13.6 ± 1.5	12.8 ± 0.2
22:0	0.0 ± 0.0	0.02 ± 0.04	0.02 ± 0.03	0.04 ± 0.03	0.04 ± 0.1	0.2 ± 0.09	0.1 ± 0.1	0.1 ± 0.1
22:1n-9	0.6 ± 0.01	0.6 ± 0.2	0.5 ± 0.05	0.3 ± 0.01	0.4 ± 0.05	0.5 ± 0.05	0.6 ± 0.1	0.6 ± 0.08
22:3n-3	0.0 ± 0.0	0.0 ± 0.0	0.07 ± 0.01	0.05 ± 0.04	0.1 ± 0.03	0.0 ± 0.0	0.04 ± 0.04	0.0 ± 0.0
22:4n-6	0.0 ± 0.0	0.1 ± 0.01	0.05 ± 0.09	0.0 ± 0.0	0.0 ± 0.0	0.1 ± 0.02	0.03 ± 0.02	0.1 ± 0.01

Table B10 continued. Overview of average and sd of FA composition and summation metrics as the percent of total fatty acid in amphipod samples. Number of replicates are indicated in parentheses.

	April		May	June	July	August		
	City (3)	North (3)	City (3)	City (3)	City(3)	North (2)	City (3)	North (3)
Fatty acids/ summation metrics	% average ±sd	% average ±sd	% average ±sd	% average ±sd	% average ±sd	% average ±sd	% average ±sd	% average ±sd
22:5n-3	0.45 ± 0.01	0.5 ± 0.02	0.4 ± 0.03	0.4 ± 0.03	0.4 ± 0.01	0.5 ± 0.02	0.5 ± 0.2	0.6 ± 0.05
22:6n-3	9.3 ± 0.7	8.7 ± 1.0	8.2 ± 0.5	7.0 ± 0.3	7.8 ± 0.2	6.8 ± 1.1	8.5 ± 0.8	8.8 ± 0.9
24:1n-9	0.3 ± 0.05	0.3 ± 0.06	0.2 ± 0.03	0.2 ± 0.01	0.2 ± 0.03	0.3 ± 0.1	0.4 ± 0.03	0.3 ± 0.1
Flagellate metric	16.2 ± 0.6	14.8 ± 1.1	14.8 ± 0.6	15.1 ± 0.1	17.0 ± 0.9	14.8 ± 0.9	17.8 ± 0.5	16.4 ± 1.1
Diatom metric	25.3 ± 1.0	22.2 ± 2.6	28.2 ± 0.7	31.0 ± 0.9	28.0 ± 0.5	27.2 ± 0.5	22.0 ± 0.8	20.5 ± 1.0
Copepod metric	9.7 ± 0.9	10.6 ± 3.9	8.3 ± 1.0	4.1 ± 0.2	5.4 ± 1.4	6.4 ± 0.9	8.8 ± 0.4	8.5 ± 1.7
Macroalgae metric	1.5 ± 0.04	1.6 ± 0.3	1.1 ± 0.2	0.8 ± 0.1	0.9 ± 0.1	0.8 ± 0.2	1.0 ± 0.2	1.1 ± 0.1
Bacteria metric	0.9 ± 0.2	0.9 ± 0.2	0.8 ± 0.1	0.6 ± 0.1	0.7 ± 0.1	0.8 ± 0.1	0.7 ± 0.1	0.9 ± 0.03
Detritus metric	23.2 ± 1.0	25.6 ± 0.1	21.6 ± 0.3	21.7 ± 1.1	21.7 ± 0.5	22.8 ± 1.2	23.5 ± 1.8	25.7 ± 2.0
Terrestrial metric	0.0 ± 0.0	0.02 ± 0.04	0.02 ± 0.03	0.04 ± 0.04	0.04 ± 0.1	0.2 ± 0.1	0.1 ± 0.1	0.1 ± 0.1
18:1n-9	22.2 ± 1.0	24.5 ± 0.06	20.5 ± 0.2	20.0 ± 0.9	20.3 ± 0.5	21.4 ± 0.9	22.4 ± 1.9	24.2 ± 2.0
Terr>2.5%	4.7 ± 0.1	5.2 ± 1.0	3.7 ± 0.2	3.7 ± 0.1	4.5 ± 0.5	3.7 ± 0.1	5.3 ± 0.3	4.8 ± 0.2
Sum PUFA	35.7 ± 0.4	32.2 ± 2.2	34.4 ± 1.9	34.8 ± 0.6	35.5 ± 0.6	32.1 ± 0.2	34.0 ± 2.4	31.8 ± 0.8
Diatom ratio	1.8 ± 0.2	1.6 ± 0.1	2.1 ± 0.1	2.5 ± 0.1	2.1 ± 0.2	2.2 ± 0.5	1.6 ± 0.1	1.5 ± 0.2
Flagellat ratio	1.6 ± 0.2	1.8 ± 0.3	1.4 ± 0.04	1.2 ± 0.05	1.3 ± 0.4	1.3 ± 1.1	1.9 ± 0.2	2.1 ± 0.3

Appendix C: Figures

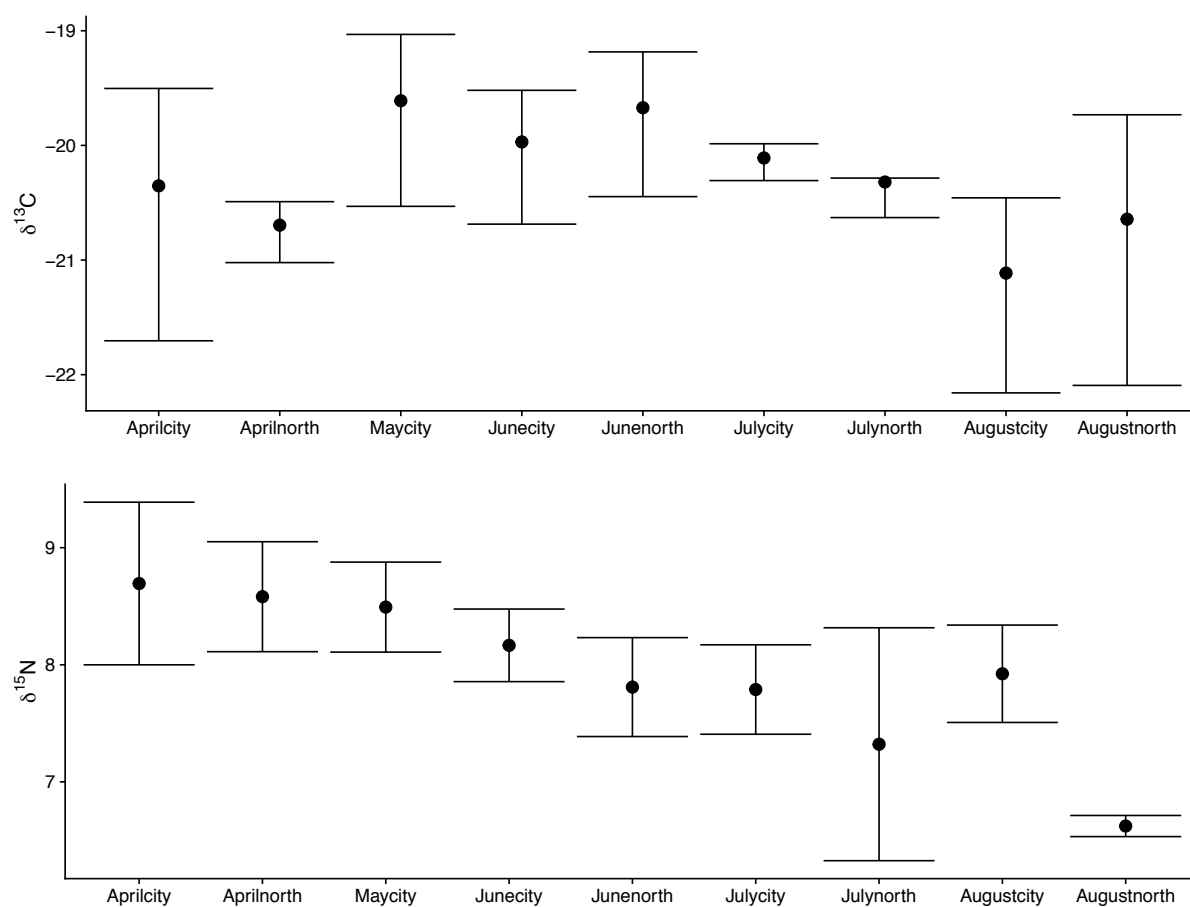


Figure C1. Above: plot of average values and confidence intervals (t-distribution) of $\delta^{13}\text{C}$ in amphipods. Below: plot of average values and confidence intervals (t-distribution) of $\delta^{15}\text{N}$ in amphipods. City/North: April/May/July/August; $n=4$, June; $n=3$. Interpretation: if the 95% confidence intervals do not overlap the null hypothesis can be rejected. If one of the confidence intervals average lays within the other 95% confidence interval the null hypothesis cannot be rejected (Whitlock & Schluter, 2015).

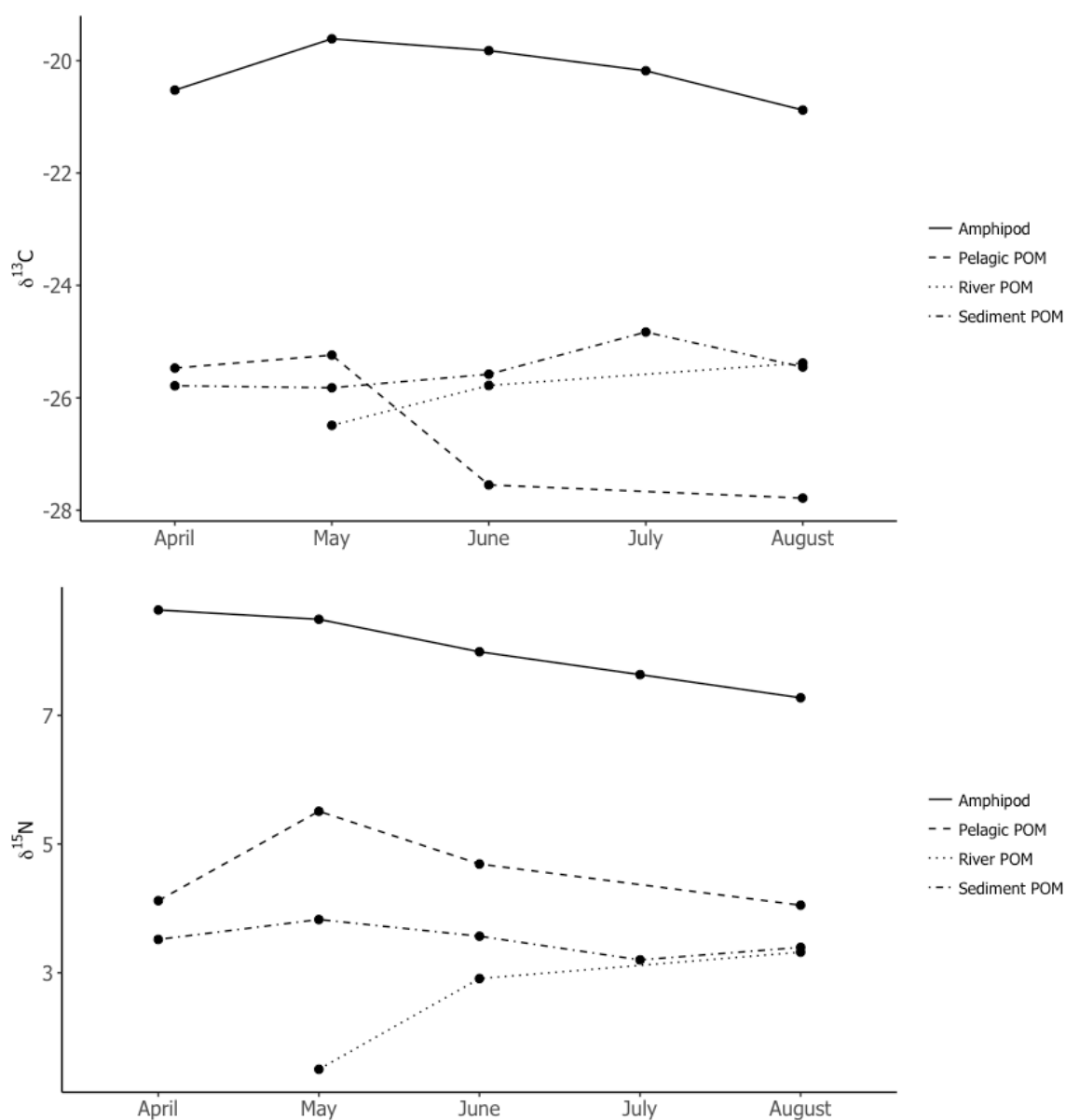


Figure C2. Above: plot of seasonal trends of the $\delta^{13}\text{C}$ values. Below: plot of seasonal trends of the $\delta^{15}\text{N}$ values. Solid line with circles represents average isotopic values in amphipod samples (pooled by station). The dashed line with circles, the two-dashed line with circles and the dotted line with circles represent pelagic, river and sediment POM samples, respectively. Amphipods: April/June/August $n=8$, July; $n=6$, May; $n=4$. Sediment POM: April/June/August; $n=2$, May/July; $n=1$. River and pelagic POM; $n=1$ (except pelagic POM in April: $n=2$).

